UNIVERSIDADE DE LISBOA
INSTITUTO SUPERIOR TÉCNICO

From Umbilical Cord Blood Hematopoietic Stem/Progenitor Cells to T Cells: a Scalable and Bioengineering Approach of the Thymic Microenvironment

Sara Ventura Bucar

Supervisor: Doctor Cláudia Alexandra Martins Lobato da Silva
Co-Supervisor: Doctor Íris Maria Ferreira Caramalho

Thesis approved in public session to obtain the PhD Degree in
Bioengineering

Jury Final Classification: **Pass with Distinction**

2024

UNIVERSIDADE DE LISBOA
INSTITUTO SUPERIOR TÉCNICO

From Umbilical Cord Blood Hematopoietic Stem/Progenitor Cells to T Cells: a Scalable and Bioengineering Approach of the Thymic Microenvironment

Sara Ventura Bucar

Supervisor: Doctor Cláudia Alexandra Martins Lobato da Silva
Co-Supervisor: Doctor Íris Maria Ferreira Caramalho

Thesis approved in public session to obtain the PhD Degree in **Bioengineering**

Jury Final Classification: **Pass with Distinction**

Jury

Chairperson: Doctor João Pedro Estrela Rodrigues Conde, Instituto Superior Técnico, Universidade de Lisboa

Members of the Committee:

Doctor Cláudia Alexandra Martins Lobato da Silva, Instituto Superior Técnico, Universidade de Lisboa

Doctor Perpétua da Conceição Pinto do Ó, i3S - Instituto de Investigação e Inovação em Saúde, Universidade do Porto

Doctor Maria Gabriela Gomes de Figueiredo Rodrigues, Faculdade de Ciências, Universidade de Lisboa

Doctor Tiago Paulo Gonçalves Pinheiro Fernandes, Instituto Superior Técnico, Universidade de Lisboa

Doctor Ricardo Neves Pires das Neves, Centro de Neurociências e Biologia Celular

Funding Institution – FCT: Fundação para a Ciência e a Tecnologia

2024

To André, my partner in ~~crime~~ life.

To Olivia, our flawless unique experiment.

♥

Em memória do meu Padrinho.

"The flower that blooms in adversity is the most rare and beautiful of all."
- The Emperor, Mulan

ABSTRACT

Umbilical cord blood (UCB) is a clinically-relevant source of hematopoietic stem/progenitor cells (HSPC) for allogeneic hematopoietic cell transplantation. However, its use is limited by the low cell number in a single unit, as well as cell immaturity. These limitations frequently result in engraftment and reconstitution delays, increased risk of opportunistic infections (OI) and, subsequently, death. Donor lymphocyte infusions after transplantation, commonly employed to enhance donor-derived immunity to treat OI, are not available. We envision using a three-dimensional (3D) acellular thymic bioscaffold, combined with Notch signaling, as a platform for T cell differentiation from UCB cells.

Here, different sources of mesenchymal stromal cells (MSC) were evaluated for the expansion/maintenance of UCB $CD34^+$-enriched cells *ex-vivo*, in a co-culture setting. Bone marrow (BM)-, umbilical cord matrix- and adipose tissue (AT)-derived MSC, expanded with/without xenogeneic components, were compared. AT showed to be a promising alternative to BM in HSPC co-culture expansion, while UCB cells expanded over MSC showed enhanced lymphoid potential.

A 3D system recently developed to differentiate T cells from HSPC, the artificial thymic organoids (ATOs) system, was also implemented. Previously expanded UCB-derived HSPC, in co-culture with MSC, were used in this ATOs system, expecting an improvement and acceleration of T cell differentiation. Remarkably, ATOs established with HSPC expanded with MSC allowed a 5-fold increase in the percentage of $CD3^+TCR\alpha\beta^+$ T cell population and in the absolute number of $CD3^+TCR\alpha\beta^+CD8^+$ T cells.

In parallel, a decellularization protocol of human thymic fragments was established and optimized. Decellularized fragments were characterized through immunohistochemistry, allowing confirmation of efficient cell removal without compromising structure and components of the native thymic extracellular matrix.

Considering the promising results in differentiating T cells using expanded UCB-derived HSPC and success in thymic decellularization, we foresee a great potential in their combination as a platform to ultimately boost and widen the clinical use of UCB cells.

Keywords: Umbilical cord blood (UCB)-derived hematopoietic stem/progenitor cells (HSPC), Mesenchymal stromal cells (MSC), *Ex-vivo* expansion, T cell differentiation, Decellularized thymus

RESUMO

O sangue do cordão umbilical (UCB) constitui uma fonte de células estaminais/progenitoras hematopoiéticas (HSPC) com relevância no contexto da transplantação alogénica de células progenitoras hematopoiéticas. Contudo, a sua utilização é dificultada pelo baixo número celular numa unidade de UCB e pela imaturidade celular. Estas limitações levam a reconstituições imunológicas tardias, aumentando o risco de infeções oportunistas (OI) e, consequentemente, morte dos pacientes. Adicionalmente, infusões de leucócitos derivadas do dador, que são comumente utilizadas após o transplante para aumentar a imunidade e tratar OI, não se encontram disponíveis. Idealizamos, assim, a utilização de uma estrutura biológica acelular, tridimensional, que, combinada com sinalização Notch, servirá como plataforma para a diferenciação de linfócitos T a partir de células do UCB.

Neste trabalho foi explorado o suporte hematopoiético de células estromais mesenquimais (MSC) da medula óssea (BM) a HSPC do UCB, num sistema de co-cultura, com especial enfoque no potencial linfoide das células expandidas *ex-vivo*. Verificado um aumento deste potencial no sistema de co-cultura face à expansão sem MSC, foi ainda explorada a utilização de outras fontes de MSC, nomeadamente, tecido adiposo e matriz do cordão umbilical, tendo a primeira mostrado ser uma alternativa promissora à BM.

Implementou-se um sistema tridimensional recentemente desenvolvido para diferenciação de linfócitos T a partir de HSPC, os organoides tímicos artificiais (ATOs). Os ATOs foram estabelecidos com HSPC previamente expandidas com MSC, sob a hipótese de que estas células potenciariam uma aceleração no processo de diferenciação em linfócitos T, a qual se verificou.

Paralelamente, estabeleceu-se e otimizou-se um protocolo de descelularização celular para fragmentos tímicos humanos. Após caracterização imunohistoquímica, verificou-se a remoção celular sem compromisso da estrutura e componentes da matriz extracelular.

Considerando os resultados promissores de diferenciação de linfócitos T (usando HSPC expandidas) e de descelularização de fragmentos tímicos, antevê-se grande potencial na sua utilização combinada como plataforma, ampliando o uso clínico de células do UCB.

Palavras-chave: Células estaminais/progenitoras hematopoiéticas (HSPC) do sangue do cordão umbilical (UCB), Células estromais mesenquimais (MSC), Expansão *ex-vivo*, Diferenciação de linfócitos T, Timo descelularizado

ACKNOWLEDGMENTS

As most of the people I would like to acknowledge are Portuguese or speak fluent Portuguese, I will acknowledge them in my mother tongue, so they can better feel my gratitude.

Em primeiro lugar, gostaria de agradecer à Fundação para a Ciência e Tecnologia (FCT), pelo apoio financeiro através das bolsas de doutoramento SFRH/BD/128379/2017 e COVID/BD/151637/2021. Foram estas bolsas que me permitiram desenvolver este trabalho e alcançar mais um marco pessoal e profissional.

Agradecer também ao Prof. Joaquim Cabral. Numa primeira instância por me ter selecionado para integrar o programa doutoral em Bioengenharia e, posteriormente, por me ter acolhido no seu grupo de investigação, onde pude desenvolver o meu trabalho ao longo dos últimos anos.

O meu profundo agradecimento à minha orientadora Prof. Cláudia Lobato da Silva que, mesmo sem saber e indiretamente, foi a responsável por eu me ter apaixonado pela área das células estaminais hematopoiéticas e me ter "desviado" da minha primeira área de interesse, muito tempo antes de iniciar o doutoramento. O bichinho acabou por ficar, crescer, e os nossos caminhos voltaram a cruzar-se. A sua motivação, dedicação e capacidade de trabalho serão sempre uma referência para mim.

Gostaria também de agradecer à Dra. Íris Caramalho, minha co-orientadora, que, apesar de ter embarcado nesta jornada apenas a meio da viagem, não mostrou menos entusiamo pelo meu projeto e esteve sempre disponível para me ouvir. Ainda que desconfiando da minha estratégia, não me colocou limites, e mesmo a pandemia e um instituto fechado não foram suficientes para nos demover!

Agradecer à Dra. Ana Fernandes Platzgummer por todo o esforço e dedicação em prol do laboratório, do grupo e dos seus investigadores. Guardo com muito carinho todos os momentos em que lhe fui bater à porta do gabinete e das três uma: ou fui pedinchar algo, reclamar de alguma coisa ou simplesmente tagarelar. Vou ter saudades!

O meu agradecimento também à Jaqueline Garcia, por ter representado uma lufada de ar fresco no grupo e ter sempre um sorriso para nos dar. O nosso trabalho ficou indubitavelmente mais facilitado com a sua chegada.

Quero também agradecer à Prof. Gabriela Rodrigues por ter possibilitado que eu desenvolvesse uma parte do meu projeto na FCUL. É sempre bom regressar à escola-mãe. Agradecer também a disponibilidade e ajuda do Pedro Santos e do Dr. Luís Marques, que

possibilitaram que eu ficasse com umas fotografias de microscopia de fluorescência mesmo giras!

Agradecer também à Dra. Carla Lilaia e ao Dr. Rui Rodrigues pelas colaborações com o nosso grupo. Mais especificamente, pelo fornecimento de amostras para o meu trabalho (sangue do cordão umbilical e timos, respetivamente), sem as quais este projeto não seria possível. I would also like to acknowledge Prof. Gay Crooks for her collaboration. By letting us have one vial of her MS5-hDLL4 cells, she allowed my work to become much more interesting. Por fim, agradecer também ao Centro de Química Estrutural (CQE, IST) e, em particular, à Prof. Teresa Duarte e à Vânia André, por me terem dado a oportunidade de experimentar o moinho de bolas e me terem ajudado com a moagem, respetivamente.

Passando àqueles com quem partilhei o meu dia-a-dia no laboratório. Como não podia deixar de ser, o meu especial agradecimento ao André Branco, com quem iniciei a minha formação no laboratório e com quem fiz equipa até ao fim desta jornada. Obrigada por teres partilhado comigo muitas das horas infindáveis no laboratório, pelas discussões de resultados, por contrariares os meus pontos de vista, pelas cantorias, mas também pelo apoio interminável nos momentos de desespero, que foram muitos. A tua disponibilidade imediata para ajudar toda a gente e resolver todos os problemas do laboratório são impagáveis, e tens toda a minha gratidão por isso.

Marília e Carina, as minhas companheiras no laboratório e fora dele. Obrigada por todo o apoio, carinho e amizade. Vocês foram fundamentais nos momentos de desânimo e desmotivação, mas também é com vocês que guardo as melhores memórias desta etapa da minha vida. É engraçado como, à partida, seria tão improvável darmo-nos bem, porque somos tão diferentes, mas acabámos por nos complementar e crescer muito umas com as outras.

Agradecer também ao Miguel, à Ana Rita, à Cláudia Miranda e à Cristiana. Não esquecendo a Sara Morini, Laura Sordini, João Cotovio, André Rodrigues e Teresa Silva. Guardo com carinho as memórias dos almoços e jantares, idas à praia e viagens. Divertimo-nos muito!

Uma palavra de agradecimento também ao Diogo Pinto, António Soure, Marta Costa e Sara Rosa. Quando cheguei ao Tagus, foram vocês os principais responsáveis pela partilha de conhecimento e também pela minha integração no grupo.

Agradecer também às minhas colegas do programa doutoral Francisca, Catarina Perdigão, Catarina Fonseca, Teresa e Alex. Juntamente com a Marília e a Ana Rita, as minhas eternas Marotinhas. Que belo grupo fizemos e que boas memórias trago comigo. Os jantares, aniversários e respetivos presentes que fizemos umas para as outras. Fico mesmo feliz por

ver que todas conseguimos completar esta missão com sucesso! Tenho muito orgulho de todas.

E aos meus amigos Sérgio, Sofia e Bruno. Metemo-nos todos na mesma "alhada" mas, ao tempo de cada um, vamos todos conseguir acabar! Estou curiosa para ver onde estaremos todos daqui a uns anos.

Um obrigada também às minhas amigas do iMM Rita, Maria, Ana Vieira, Mariana e Inês. Todas me serviram de exemplo e me inspiraram de alguma forma. Passei a ver a investigação de outra forma quando trabalhei convosco, o que me levou a arriscar e fazer um doutoramento. Agradeço também os conselhos e apoio que me deram numa fase inicial deste trabalho.

Um especial agradecimento à minha família, Mãe, Karen, Generali, Sam e Dani. Por me terem dado ânimo nos momentos tristes, por me terem apoiado e incentivado a ultrapassar os obstáculos. Por terem acreditado em mim. Mas também pelos muitos bons momentos que me proporcionaram, que guardo e coleciono com amor.

Voltar a agradecer ao André (Branco), agora numa esfera mais pessoal, porque nunca serão vezes de mais. Obrigada por estares sempre do meu lado e pelo apoio incansável. Pelos mimos e o amor com que cuidas de mim. Por me ouvires. Mas também por me obrigares a falar. Pela tranquilidade e segurança que me dás. Por seres o meu maior admirador e veres em mim aquilo que eu não consigo ver. Foste a melhor coisa que o doutoramento, e a vida, me trouxeram! Sou eternamente grata. Amo-te e amo a nossa família.

Por último, e sem dúvida não menos importante, agradecer à minha filha Olivia. Vieste pôr este trabalho em pausa, num momento de pandemia e incerteza, mas foste a minha maior motivação para conseguir terminá-lo. O meu doutoramento ficou certamente mais rico porque existes. Amo-te de paixão e és o meu maior orgulho! A mamã conseguiu!

TABLE OF CONTENTS

LIST OF FIGURES

LIST OF TABLES

LIST OF ABBREVIATIONS AND ACRONYMS

#

2D – Two-dimensional
3D – Three-dimensional

A

A/A – Antibiotic-Antimycotic
AhR – Aryl hydrocarbon receptor
APC – Antigen-presenting cells
AT – Adipose tissue
ATOs – Artificial thymic organoids

B

BFU-E – Erythroid burst-forming unit
BM – Bone marrow
BSA – Bovine serum albumin

C

CAFC – Cobblestone area-forming cells
CAR – Chimeric antigen receptor
CFU – Colony-forming unit
CFU-GM – Colony-forming unit granulocyte-monocyte
CFU-Mix – Multilineage colony-forming unit
cGMP – Current good manufacturing practices
CHAPSO – 3-[(3-Cholamidopropyl)dimethylammonio]-2- Hydroxy-1-Propanesulfonate
CLP – Common lymphoid progenitors
CMP – Common myeloid progenitors
cTEC – Cortical thymic epithelial cells

D

dGuo – Deoxyguanosine
DLI – Donor lymphocyte infusions
DLL – Delta-like
DMEM – Dulbecco's modified Eagle's medium
DP – Double positive

E

EDTA – Ethylenediamine tetraacetic acid
EMOs – Embryonic mesoderm organoids
ETP – Early thymic progenitors

F

FACS – Fluorescence-activated cell sorting
FBS – Fetal bovine serum
FI – Fold increase

FL – Feeder layer
FLT3-L – FMS-like tyrosine kinase-3 ligand
FTOC – Fetal thymic organ culture

G
G-CSF – Granulocyte colony-stimulating factor
GVL – Graft *vs* leukemia
GMP – Granulocyte/macrophage progenitors
GVHD – Graft-*vs*-host disease

H
HCT – Hematopoietic cell transplantation
hEMPs – Human embryonic mesodermal progenitors
HLA – Human leukocyte antigen
HPL – Human platelet lysate
HSC – Hematopoietic stem cells
HSPC – Hematopoietic stem/progenitor cells

I
iBB – Institute for Bioengineering and Biosciences
IFNγ – Interferon-γ
IGC – Instituto Gulbenkian de Ciência
IL – Interleukin
ISP – Immature single positive
iPSC – Induced pluripotent stem cells
ISCT – International Society for Cell & Gene Therapy
IST – Instituto Superior Técnico

L
LMPP – Lymphoid-primed multipotential progenitors
LTC-IC – Long-term culture-initiating cells
LT-HSC – Long-term reconstituting hematopoietic stem cells

M
MACS – Magnetic-activated cell sorting
MEP – Megakaryocyte/erythroid progenitors
MHC – Major histocompatibility complex
MNC – Mononuclear cells
mPB – Mobilized peripheral blood
MPP – Multipotent progenitors
MSC – Mesenchymal stromal cells
mTEC – Medullary thymic epithelial cells

N
NAM – Nicotinamide
NOG – N-octyl glucoside

O

OCT – Optimal cutting temperature

OI – Opportunistic infections

P

PB – Peripheral blood

PBS – Phosphate buffered saline

proT – Progenitor T

R

RT – Room temperature

RTOC – Reaggregate thymic organ culture

S

SCERG – Stem Cell Engineering Research Group

SCF – Stem cell factor

SDS – Sodium dodecyl sulfate

SEM – Standard error of the mean

SF – Serum-free

SP – Single positive

SR1 – StemReginin1

ST-HSC – Short-term reconstituting hematopoietic stem cells

SVF – Stromal vascular fraction

T

TCR – T cell receptor

TEC – Thymic epithelial cells

TE/RM – Tissue engineering and regenerative medicine

TNC – Total nucleated cells

TNF – Tumor necrosis factor

TPO – Thrombopoietin

Treg – Regulatory T cells

TSC – Thymic stromal cells

TSP – Thymus seeding progenitors

U

UCB – Umbilical cord blood

UCBT – Umbilical cord blood transplantation

UCM – Umbilical cord matrix

USA – United States of America

X

XF – Xenogeneic-free

I. Introduction

I.1. Hematopoiesis featuring hematopoietic stem cells

Hematopoietic stem cells (HSC) are multipotent stem cells that reside in the bone marrow (BM) and have the ability to originate all types of hematopoietic cells, in a process termed hematopoiesis. Hematopoietic cells form the solid component of the blood and are responsible for three main functions in the body: oxygen delivery, hemostasis and protection against invading pathogens and tumorigenic cells (innate and adaptive immune systems). Cells derived from HSC are classically classified as belonging to one of two lineages, myeloid or lymphoid. Myeloid lineage include the majority of hematopoietic cells, such as: erythrocytes (transport oxygen throughout the body); megakaryocytes (responsible for platelet production which are involved in blood clotting); granulocytes (neutrophils, basophils and eosinophils) and monocytes (involved in innate immunity). The lymphoid lineage include B, T and NK cells. B and T cells are involved in adaptive immunity, while NK cells are critical to the innate immune system. Dendritic cells are antigen-presenting cells (APC) and work as messengers between the innate and adaptive immune systems. Some dendritic cells belong to the myeloid lineage, while others belong to the lymphoid lineage (Fig.I.1)[1,2].

As any other stem cell, HSC are characterized by possessing two main features: self-renewal capacity and ability to differentiate into any of the previous mentioned hematopoietic cells. The existence of hematopoietic "blood-forming" stem cells was first realized in 1961, when Ernest McCulloch and James Till injected BM cells from a donor mouse into a genetically-identical lethally irradiated mice. Although isolation and characterization of HSC were not done at that time, they macroscopically verified the occurrence of clonogenic colonies of multiple hematopoietic lineages in the spleen of the recipient mice. Ultimately, those BM cells were responsible for the regeneration and reconstitution of the irradiation-ablated hematopoietic system[3].

In humans, during embryonic development, self-renewing HSC emerge in a specific region called aorta-gonad-mesonephros. Later during embryogenesis, these HSC colonize and proliferate in the fetal liver and ultimately in the BM, where they can be found in adulthood[4,5]. Hematopoiesis used to be described according to the "hematopoietic tree" model (Fig.I.1.A). In this classical model, HSC were seen as a group of homogeneous multipotential long-term reconstituting hematopoietic stem cells (LT-HSC), localized at the apex of the hematopoietic tree. These LT-HSC would then ramify to produce increasingly more differentiated cells, while losing stemness potential, culminating with the production of all mature hematopoietic cells. Also, LT-HSC would remain mainly quiescent, while short-term reconstituting HSC (ST-HSC) and downstream progenitors would assure homeostatic hematopoiesis. Foundations of this model were based on the knowledge given by cell surface markers and flow cytometry, that allowed separation and ordering of different cell populations according to their

degree of maturation[2,6,7]. However, this model has been discredited as new insights given essentially by single-cell transcriptomics emerged. Through single-cell RNA sequencing and respective computational reconstruction of the different profiles of hematopoietic cells, a "continuum model" of hematopoiesis was presented (Fig.I.1.B). In this continuum model, HSC are not perceived as a homogeneous population and differentiation to progenitors and to mature cells is defended to occur constantly, without defined phenotypic changes as in the classical model[8,9]. However, characterization of hematopoietic cells based on gene expression only may be insufficient as cell biological aspects, including cell function, are missed out. Thus, while

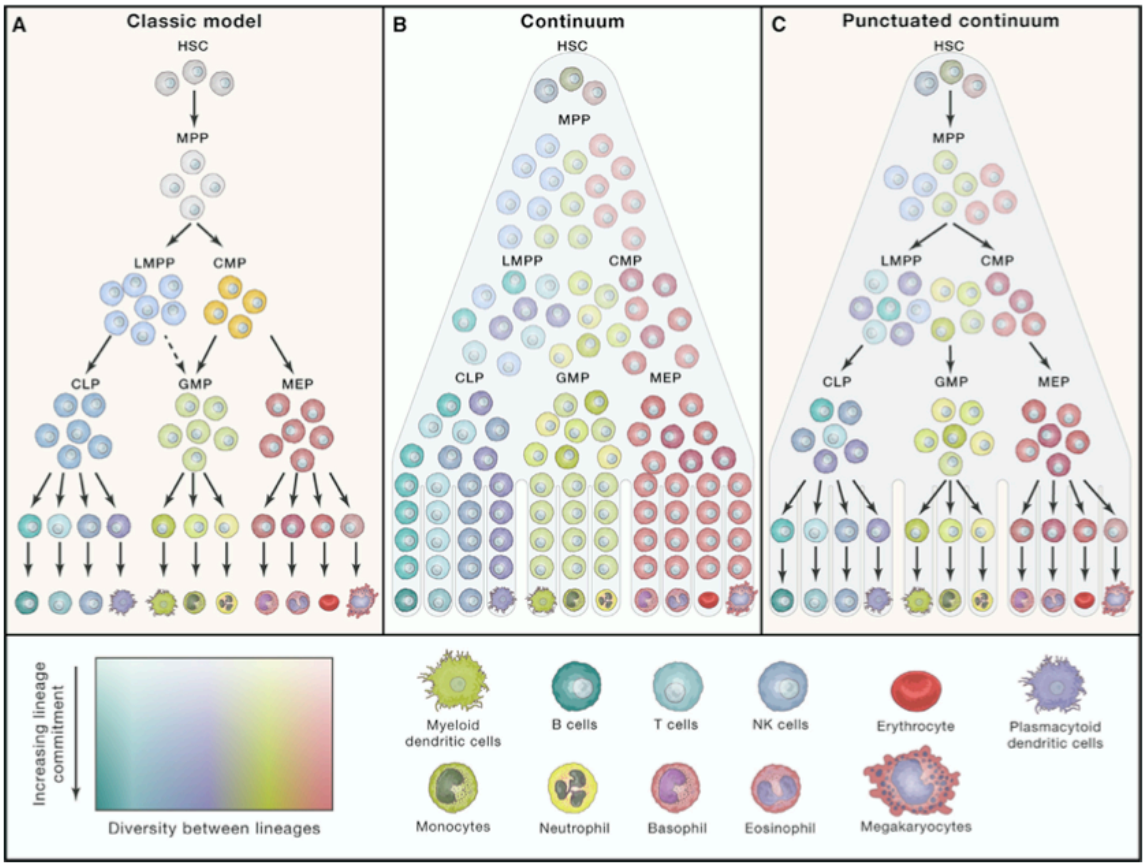

Figure I.1. *From hematopoietic stem cells to all mature hematopoietic cells they can differentiate into – a view of hematopoiesis throughout time.* ***(A)*** *Classical model: it is a ramification model, involving discrete states. Each state includes cells of uniform potential that express the same phenotype.* ***(B)*** *Continuum model: all cells are variably lineage based and punctuated transitions do not exist – differentiation occurs as a continuum process.* ***(C)*** *Punctuated continuum model: a combination of the previous two models. Hematopoiesis occur mainly as a continuum process but with occurrence of punctuated transitions that allow individualization of distinct cell populations. HSC: hematopoietic stem cells; MPP: multipotent progenitors; CMP: common myeloid progenitors; MEP: megakaryocyte/erythroid progenitors; GMP: granulocyte/macrophage progenitors; CLP: common lymphoid progenitors; LMPP: lymphoid-primed multipotential progenitors. Adapted*[2]*.*

hematopoiesis may be far more of a continuous process than what was initially thought, punctuated transitions may still occur through this landscape of continuous gene expression, allowing individualization of distinct cell populations – "punctuated continuum model" (Fig.I.1.C)[9].

In humans, phenotypic characterization using cell surface markers allowed to distinguish between LT-HSC and ST-HSC in fresh umbilical cord blood (UCB) samples[10]. Although rare, LT-HSC were found to be $CD34^+CD38^-CD45RA^-CD90^+CD49f^+$, while ST-HSC were found to be $CD34^+CD38^-CD45RA^-CD90^-CD49f^-$. However, some of these markers are no longer reliable once HSC are placed in culture. For instance, CD38 becomes strongly downregulated[11]. Also, in contradiction to what is observed in fresh samples, a high expression of CD49f in cultured cells identifies progenitor cells with limited self-renewal capacity, while a dim expression of CD49f identifies functional HSC[12]. On the other hand, endothelial protein C receptor (EPCR) was found to be a reliable surface marker for human HSC expanded *in vitro*[12]. More recently, integrin-α3 (ITGA3) was identified as a LT-HSC marker for cultured UCB cells. Specifically, ITGA3 allows to identify two functionally distinct populations within the $EPCR^+$ population: ST-HSC ($ITGA3^-$) and both ST- and LT-HSC ($ITGA3^+$)[13]. CD34 is a surface marker express in all human HSC (i.e., neonatal (UCB) and adult HSC (BM and mobilized peripheral blood (mPB)) but also in a wide range of hematopoietic progenitors, including multipotent progenitors (MPP), common myeloid progenitors (CMP), megakaryocyte/erythroid progenitors (MEP), granulocyte/macrophage progenitors (GMP), common lymphoid progenitors (CLP) and lymphoid-primed multipotential progenitors (LMPP). Therefore, CD34 is considered a universal surface marker for hematopoietic stem/progenitor cells (HSPC), whose expression is lost as cells mature into terminal effectors. At a clinical level, quantification of viable $CD34^+$ cells is used to determine the cell dose to be harvested in BM and mPB donors in the context of hematopoietic cell transplantation (HCT). For UCB donors, while total nucleated cells (TNC) is the parameter used to determine UCB graft dose, the number of viable $CD34^+$ cells is associated to better engraftment speed and UCB transplantation (UCBT) success[14].

I.1.1. Sources of hematopoietic stem/progenitor cells

BM was the first source of HSPC to be identified, following the bombings in Hiroshima and Nagasaki, in 1945. The harmful impact of radiation to the BM was recognized and drove the search for HSC[15]. Thus, in 1959, BM cells were infused into two patients suffering from advanced leukemia after supralethal doses of radiation. Hematopoietic recovery was observed, yet the patients died from their disease. A couple years later, in 1962, HSPC were identified for the first time in the peripheral blood (PB) of murine models[16]. Despite the quantity of HSPC in PB being very low, there were two major

events that led PB to be considered another HSPC source in a clinical context. The first event was the development of a continuous-flow apheresis device, a system that allows collection of blood components (e.g., leukocytes; in that case, leukapheresis) from PB while returning the remaining blood components to the donor. The second event was the discovery, in 1984, of granulocyte colony-stimulating factor (G-CSF), a growth factor that promotes HSPC mobilization from the BM into the blood. Administration of G-CSF to healthy allogeneic stem cells donors increased the yield of HSPC that could be harvested through apheresis. Thus, mPB-derived HSPC started to be used in autologous and allogeneic HCT studies[17,18]. At last, UCB was identified as the third HSPC source, following some studies conducted by the group of Edward Boyse in the 1980s[19]. In 1988, the first successful HCT using UCB-derived HSPC was conducted to treat a patient with Fanconi anemia, whose donor was his human leukocyte antigen (HLA)-identical sister[20].

Although the discovery of other sources than BM broadened HSPC donor availability, the three sources possess different characteristics concerning CD34 cell quantity and T cell quantity and maturity (Table I.1)[15]. These features, in their turn, have influence on the type of disease that can be treated (e.g., malignant or non-malignant disease). On the other hand, the donor has to surpass some hurdles depending on the HSPC source chosen and respective collection method. BM collection is the source that requires the most invasive procedure, including general anesthesia and multiple perforations along the posterior iliac crest, using 8- to 11-gauge biopsy needles. While no more than 20 mL/kg of the donor weight can be collected, up to 1.5 L is collected in a 2-3 h surgery. Usual complications associated to BM collection include bleeding, infection and localized pain. Although HSPC collection from PB is not as invasive as BM collection, it requires mobilization of HSPC from the BM through injections of G-CSF 4-5 days before apheresis. Main complications associated with this source are bone pain, insomnia and flu-like symptoms, associated with the mobilizing agents used, such as G-CSF. Fortunately, HSPC collection from UCB presents no side effects to the donor. The blood is collected from a severed umbilical cord, that otherwise would be considered medical waste.

As can be found in Table I.1, CD34 content is greatest in mPB and least in UCB. All three sources possess T cells, which means all sources are able to cause graft-*vs*-host disease (GVHD) in an allogeneic transplantation context. T cell content is also highest for mPB and least for UCB samples. Additionally, UCB-derived T cells are immunologically naïve. Due to inferior T cell content and their immature characteristics, HCT using UCB samples allow for a less restrictive HLA matching than BM or mPB and also possess lower incidence of either acute or chronic GVHD[15].

Table I.1. Sources of hematopoietic stem and progenitor cells and their features (adapted[15]).

	mPB	BM	UCB
Donor characteristics			
Transplant donor type	Haploidentical donor, MSD, MUD	Haploidentical donor, MSD, MUD	MUD
Collection risk	Apheresis related severe adverse events ~1/1000	Surgical risk (severe adverse events) ~1/100	Postdelivery Absent/none reported
Graft characteristics			
Relative CD34 content	50x	10x	1x
Relative T cell content	100x	10x	1x (naïve T cells)
Minimum cell dose for engraftment	Autologous: $2x10^6$ $CD34^+$ cells/kg Allogeneic: $4x10^6$ $CD34^+$ cells/kg	Same as for mPB grafts	Single cord: $2.5x10^7$ TNC/kg Dual cord: $1.7x10^7$ TNC/kg/unit
Collection volume, mL	~300	~1000	~100
Relative graft procurement cost	~2x	~2.3x	~1-2x
HLA matching criteria	6/6 (MSD) 7/8 (haploidentical donor) 8/8-12/12 (MUD)	Similar to mPB	4-6/6
Recipient characteristics			
Disease type	Preferred source for malignant disease	Preferred source for non-malignant disease	Used for either
Speed of engraftment	Faster	Moderate	Slower
Anti-tumor effect	Higher	Lower	Higher
Acute/chronic GVHD risk	Higher	Moderate	Lower

BM: bone marrow; GVHD: graft-vs-host disease; mPB: mobilized peripheral blood; MSD: matched sibling donor; MUD: matched unrelated donor; TNC: total nucleated cells; UCB: umbilical cord blood.

I.2. Hematopoietic cell transplantation: a life-saving procedure with many challenges

HCT is a medical procedure used to treat a wide range of diseases, being the only curative option in several cases. The procedure consists in eliminating existing unhealthy BM cells and/or immune system and replace it by healthy HSPC from a compatible donor. HCT can be classified according to the source of donated HSPC (BM, mPB and UCB) but also according to the relationship between recipient and donor (autologous or allogeneic)[21]. In autologous HCT, the donor and the recipient are the same person. HSPC are collected before BM ablation, cryopreserved, and then reinfused into the patient. In these cases, HCT has only one purpose: eliminating the tumor, with reinfused HSPC serving to recover from BM aplasia. In allogeneic HCT, HSPC derive from a different person, who is HLA-compatible. As in autologous HCT, allogeneic HCT allows recovery from BM aplasia, but can also provide an additional benefit in a hemato-oncological context: the effect of graft *vs* leukemia (GVL). GVL is mediated by donor T cells that eliminate residual tumor cells of the patient[22]. After a decrease in HCT activity in 2020 due to SARS-CoV-2 pandemic, the European Society

for Blood and Marrow Transplantation (EBMT) reported a total of 47,412 HCT performed in 694 European centers in 2021[23]. From these, 42% were allogeneic and 58% were autologous.

Most HCT are conducted to treat hematologic malignancies. Within hematologic malignancies, autologous HCT is usually indicated to treat multiple myeloma[24] and lymphoma. Acute myeloid leukemia, acute lymphoblastic leukemia, myelodysplastic syndromes, and myeloproliferative neoplasms are commonly indicated for allogeneic HCT[25]. Some solid tumors (e.g., neuroblastoma[26] and medulloblastoma[27]) and non-malignant diseases (severe aplastic anemia, inherited BM failure syndromes, sickle cell disease, transfusion-dependent thalassemia, inherited immune deficiency syndromes, and certain metabolic disorders)[28–33] can also have indication for HCT. Autologous HCT have also been employed successfully in cases of severe therapy-refractory autoimmune diseases, including multiple sclerosis[34,35].

Despite being a life-saving procedure, HCT entails many burdens to the patient, either before or after the transplant. Once a donor is found, the patient is admitted to the hospital for a period of 3-5 weeks. A conditioning regime (i.e., chemotherapy and/or radiotherapy) is employed to eliminate the existing BM and provide sufficient immunosuppression to allow donor HSPC to engraft. After the conditioning regime and the HCT are performed, prophylaxis against several infectious (bacterial, viral and fungi) and non-infectious (e.g., GVHD) diseases are administered. Time to engraftment is variable (usually between 10 and 21 days) and is defined as the first three consecutive days of neutrophil count above $0.5x10^9/L$[36].

Numerous complications associated to HCT can arise in distinct moments, including the pre-engraftment period (starting in the conditioning regimen until neutrophil recovery), the early post-engraftment (from neutrophil recovery until day 100 post-HCT) and the late post-engraftment (from day 100 and beyond) periods. Complications during the pre-engraftment period are usually toxicities caused by the conditioning regimen, but also infections associated to a common neutropenia state. Acute GVHD can emerge during the early post-engraftment period, only for allogeneic HCT. GVHD is mediated by donor immune cells present in the graft that recognize the recipient as foreign, mounting an immune response against the patient and causing disease. Acute GVHD affects the skin, the gastrointestinal system and the liver and severe manifestations of the disease are associated with poor survival. Although recovered from neutropenia, patients in the early-post engraftment period continue to be susceptible to complications due to infection. Opportunistic infections (OI) such as *P. jirovecii* and cytomegalovirus, as well as common respiratory viruses (e.g., influenza, respiratory syncytial virus and adenovirus), are very frequent. Since the treatment for GVHD relies on systemic corticosteroids that cause immunosuppression, patients are highly susceptible to invasive fungal infections and viral reactivation. GVHD can persist in the

late post-engraftment period, becoming chronic GVHD, and besides the affected organs above mentioned, lungs can also be affected. Patients suffering from chronic GVHD are thus even more susceptible to OI and have a poor quality of life.
As previously mentioned, UCB was the third of three HSC sources to be established. In what concerns GVHD, UCB possess an advantage compared to the other sources due to immaturity and low immunogenicity of T cells present in the graft. These characteristics allow for a higher degree of HLA mismatching between donor and recipient, while reducing GVHD incidence after transplant. Thus, UCB is particularly interesting for patients lacking a suitable donor, especially those of racial and ethnic minorities who are poorly represented in donor banks. However, low cell number and cell immaturity represent critical drawbacks of UCBT as patients receiving UCB grafts have delayed engraftment and immune reconstitution, which frequently results in graft failure, OI, and subsequently death. Indeed, OI are the major cause of death during the first six months after UCBT[37,38]. Unfortunately, conventional donor lymphocyte infusions (DLI), commonly employed to enhance donor-derived immunity to treat infections, but also mixed chimerism or disease relapse, are not available for UCB recipients due to ethical reasons, constituting a major obstacle to widen UCBT. Despite these limitations, UCB continues to be an attractive source and becomes crucial to find adoptive cell therapy strategies to improve recipients survival[38–40].

I.3. *Ex-vivo* expansion of umbilical cord blood-derived hematopoietic stem/progenitor cells

Given the advantages UCB offers compared to the other sources, there has been a great effort in circumvent its major drawback: the presence of a limited number of HSPC per UCB unit. This feature limits the use of UCB-derived HSPC to adult patients and high weight children. To overcome low cell numbers, the use of two UCB units combined with improved conditioning regimens has become an effective therapeutic option for heavier patients. However, this solution is not ideal, since a higher 100-day mortality and delayed reconstitution has been described compared to other sources, while also entailing higher costs[41,42]. Great effort has been put in expanding HSPC from UCB *ex-vivo*. This seems to be the ideal approach to pursue, as theoretically all UCB units could be expanded until sufficient numbers are obtained to perform HCT. If the right expansion conditions are given, meaning enhancement of HSPC number with engraftment and reconstituting potential, this solution allows UCB to become a readily available source of HSPC for a vast range of patients[43].
Initial attempts of UCB-derived HSPC expansion profoundly explored combinations of different cytokines, often resulting in proliferation with loss of HSC phenotype through

differentiation[44]. Although many different cytokines were found to induce HSPC proliferation *in vitro*, a specific combination of cytokines (i.e., stem cell factor (SCF), FMS-like tyrosine kinase-3 ligand (FLT3-L) and thrombopoietin (TPO), with or without interleukin (IL)-6) became the most common core of cytokines used[45]. Since then, other approaches have appeared, contributing to a vast range of expansion systems[44,46]. Currently, expansion strategies that have shown the most progression towards approval by regulatory agencies are associated with different small molecules[47].

Nicotinamide (NAM) is a form of vitamin B3 and an inhibitor of the sirtuin family of histone/protein deacetylases. In the presence of serum and cytokines, NAM was found to enhance the absolute number and the percentage of HSPC (defined as $CD34^+CD38^-$ cells) cultured *ex-vivo* during three weeks, compared to control conditions cultured with cytokines only[48]. In this 2012 study, grafts using HSPC treated with NAM were transplanted into mice and resulted in improved short-term engraftment at 6 weeks post-transplantation (93%), compared to grafts using HSPC expanded with cytokines only (46%) or untreated cells (33%). Of note, reconstitution of both myeloid and lymphoid lineages with human cells was observed. A phase I clinical trial to assess NAM safety was then conducted with adult patients suffering from hematological malignancies. 11 patients received two units of UCB, with one of them being unmanipulated. The manipulated unit, named NiCord, was composed of two parts: (i) $CD133^+$ cells expanded during 21 days with NAM and (ii) uncultured $CD133^-$ cells containing T cells. 10 patients successfully engrafted the donor cells. Importantly, from these 10 patients, 8 had persistent chimerism of myeloid cells derived from NiCord (41-100%) and 6 patients showed engraftment of T cells also derived from NiCord. While rates of infection and GVHD were identical to a matched historical control group, patients enrolled in this clinical trial had a significant decrease in median time to neutrophil recovery, from 25 (historical control group) to 13 days[49]. Indeed, this was the first clinical trial demonstrating that an *ex-vivo* expanded UCB product outcompeted an unmanipulated UCB graft. Following these results, a phase I/II clinical trial was conducted in 2018 to assess safety and efficacy of NiCord as a stand-alone graft. 36 patients with hematologic malignancies underwent HCT at 11 sites. In this case, not only time to neutrophil recovery, but also platelet recovery, were significantly shortened compared with standard UCBT patients[50]. Remarkably, this was the first study showing that an *ex-vivo* expanded UCB product could safely be administered as a stand-alone graft while providing a fast recovery. Indeed, it was demonstrated that this faster neutrophil recovery was associated with a decreased incidence of bacterial and fungi infections in the first 100 days post-transplant, correlating with a shortened hospitalization[49,50]. At last, a phase III clinical trial was conducted to evaluate the efficacy of Omidubicel (previously termed NiCord). 125 patients with hematologic malignancies were randomly allocated to one of two groups: one underwent Omidubicel UCBT and

the other underwent standard UCBT. Without surprise, but still remarkably, patients that underwent UCBT with Omidubicel had significantly faster hematopoietic recovery and reduced complications in comparison to patients that underwent standard UCBT[51]. Notably, this year (2023), the US Food and Drug Administration has approved Omidubicel for HCT[52]. For the first time, an *ex-vivo* expanded product derived from UCB was approved and can be used at a clinical level. Indeed, Omidubicel may be considered the new standard of care for adult patients eligible for UCBT.

In parallel to the studies developed with NAM, other small molecule has provided equally interesting results, the StemReginin1 (SR1). SR1 is a purine derivative and an antagonist of the aryl hydrocarbon receptor (AhR), which is linked to pathways regulating metabolism and hematopoiesis[53]. Initially SR1 was found to promote *ex-vivo* expansion of human mPB-derived $CD34^+$ cells[54]. Following observation that UCB-derived $CD34^+$ cells cultured for 5 weeks with cytokines and SR1 also significantly promoted their *ex-vivo* expansion, compared to cultures with cytokines only, a phase I/II was conducted to assess safety of this small molecule. Similarly to what was done with the first clinical trial using NAM, two UCB units were transplanted into 17 patients. One UCB unit was unmanipulated and the other was manipulated and divided into two parts containing (i) isolated $CD34^+$ cells expanded for 15 days with SR1 and cytokines and (ii) cells from the $CD34^-$ fraction (re-cryopreserved and administered on HCT day). A 330-fold expansion was observed in SR1-treated $CD34^+$ cells and all 17 patients successfully engrafted. As seen with NAM, time to neutrophil and platelet recovery significantly decreased compared to a historical control group[55]. Given these promising results, two phase II studies were conducted to assess safety of SR1 as a stand-alone cell product. The product, i.e., $CD34^+$ cells *ex-vivo* expanded with SR1 together with the unmanipulated $CD34^-$ cell fraction, was renamed to MGTA-456. In one study, 18 patients with high-risk hematological malignancies received and successfully engrafted MGTA-456. Patients enrolled in this study either received a myeloablative conditioning regimen or a non-myeloablative regimen. Both groups showed a decreased time to engraftment compared to historical controls, from 23 days (control) to 14 days in the case of myeloablative regimen, and from 15 days (control) to 7 days in the case of non-myeloablative regimen[56]. Importantly, the second study employed cryopreserved MGTA-456 *ex-vivo* expanded cells to also treat patients with high-risk hematological malignancies[57]. Comparable results were seen between cryopreserved and fresh MGTA-456 samples. MGTA-456 has also been employed in another phase II clinical trial to treat 12 patients with inherited metabolic disorders and preliminary results were favorable[58].

An additional small molecule candidate, UM171, a pyrimidoindole derivative, was found to promote *ex-vivo* expansion of mPB-derived $CD34^+CD45RA^-$ cells, using a continuous medium delivery system (i.e., fed-batch culture)[59]. In addition to cytokines, UM171 was

later used to expand UCB-derived $CD34^+$ cells for 15 days. This expansion was compared to expansion cultures with SR1 alone, both UM171 and SR1, or cytokines only. Interestingly, UM171 alone was the expansion condition that allowed a considerable fold expansion of HSC (defined as $CD34^+CD45RA^-$ and $CD34^+CD38^-CD90^+CD45RA^-49f^+$), while a positive combo effect between UM171 and SR1 seemed to be restricted to progenitor cell subsets[59]. Favorable pre-clinical results led to a phase I-II clinical trial with a shorter expansion phase, from 15 to 7 days. Due to the previous encouraging results in clinical trials using a single expanded UCB unit (either with NAM or SR1), the first 4 patients enrolled in this clinical trial received two UCB units (one expanded and one unmanipulated) but then the large majority (22 patients) received only a single UM171-expanded graft. As also seen with NAM and SR1 clinical trials, patients enrolled in this clinical trial received not only an UM171-expanded product, but also the $CD34^-$ fraction containing T cells. As consistently seen before, median time to neutrophil and platelet recovery was significantly reduced, and a decrease in hospital stay duration was observed (a median of 35 days, compared to 46 days in patients receiving unmanipulated UCB). A clinical benefit of using UM171-expanding cells was reported, not only due to faster engraftment with fewer infection complications, but also due to the possibility of using smaller UCB units, better matched, without compromising their engraftment potential[60]. Nonetheless, long-term clinical benefits from using these expanded cells, such as immune reconstitution, GVHD and overall survival, are now awaited[43].

Although abovementioned molecules have significantly progressed the clinical pipeline towards approval, other approaches have also shown potential to promote *ex-vivo* expansion of HSPC. Instead of using single small molecules discovered through screening, HSPC expansion has been pursued based on mimicking their native environment. Considering the residence of adult HSPC (i.e., the BM), resident non-hematopoietic cell types can be explored *in vitro* to mimic the native interactions that regulate HSPC expansion *in vivo*. Also, the complexity of the BM demonstrates that multiple signaling is required to maintain HSPC stemness, highlighting the importance of phenotype maintenance as HSPC expand. While multiple cell types exist that can be applied in co-culture with HSPC, mesenchymal stromal cells (MSC) stand out due to their rich secretome[61], their known contribution to HSPC proliferation[62] and their great compatibility with *in vitro* culture platforms[63]. Co-culture of HSPC with MSC as an *ex vivo* expansion platform for clinical purposes has a long track record. After proving, *in vitro*, the benefit of stromal support with murine cell lines[64], use of human MSC feeder layers for HSPC expansion was initially shown in the early 2000s[65–67]. At the time, co-culture expansions outperformed standard cytokine-only systems by triplicating the total nucleated cell number[65]. When pursuing novel serum-free conditions, UCB-derived $CD34^+$-enriched cells were only able to expand in the presence of supportive

mesenchymal stroma[66]. Eventually, efforts in determining the mechanisms responsible for improved HSPC expansion during co-cultures demonstrated the importance of cell-cell contact[68–70]. Unsurprisingly, *in vitro* cell contact recapitulates the natural interactions between BM MSC and HSPC in the BM niche[71].

MSC have also been used at a clinical level, in the context of UCBT. In order to avoid cell loss after HSPC enrichment from mononuclear cells (MNC), MSC have been combined with unselected MNC. This approach allowed direct expansion of progenitor populations, with a fold increase (FI) between 16 and 37[72], and was then tested at a clinical level. In a phase I clinical trial with 31 enrolled patients[73], an enhancement in neutrophil reconstitution (15 days) was shown, compared to controls that received unmanipulated UCB (24 days). Currently, this approach has been combined with fucosylation (which promotes HSPC homing to the BM after transplantation) in a phase II clinical trial (ClinicalTrials.gov Identifier: NCT03096782).

Although expansion of HSPC has improved engraftment and reconstitution of certain hematopoietic populations after UCBT, delays in complete immune reconstitution remain a relevant issue. Specifically, T cell reconstitution may take between 1-2 years, causing the patient to be more vulnerable to OI during this time period[74].

I.4. T cell development in their unique "bird nest": the thymus

T cells belong to the immune system and play a pivotal role in adaptive immunity, through responses against invading pathogens, allergens and tumors, while maintaining immune homeostasis[75]. Interestingly, although the majority of hematopoietic cells develop within the BM, T cells specifically have their maturation and differentiation process within a specialized organ, the thymus, in a process called thymopoiesis. The thymus is thus the primary lymphoid organ, whose only function is T cell production. Nevertheless, we can associate the very beginning of T cells with BM, as thymus seeding progenitors (TSP) are hematopoietic progenitors that initially reside in the BM and then migrate to the thymus.

The thymus houses a very important cell population, named thymic epithelial cells (TEC), which have an essential role in thymopoiesis. TEC provide homing signals that guide TSP towards the thymus and, through Notch signaling, promote their T cell lineage commitment, differentiation and maturation[76,77]. Thymic stroma, comprising TEC, mesenchymal cells, fibroblasts and vascular endothelial cells, present a particular three-dimensional (3D) sponge-like architecture that is essential for TEC survival and function. Therefore, recapitulation of thymic function *in vitro* is difficult to achieve as TEC cultured in a two-dimensional (2D) environment are unable to promote T cell differentiation[78]. Using a 3D approach, through engineered human thymic aggregates

(i.e., TEC, thymic mesenchymal cells and UCB-derived $CD34^+$ HSPC), T cell development was observed both *in vitro* and in immunodeficient mice[79].

Once in the thymus, TSP give rise to early thymic progenitors (ETP). Following a quiescent period, ETP are subjected to a process of differentiation that includes T-lineage specification and commitment, followed by T cell receptor (TCR) rearrangement, originating a diverse population of T cells able to recognize a wide range of antigens. After T-lineage commitment, T cell development in the thymus can be simply characterized by the acquisition (and then loss) of two coreceptors: CD4 and CD8. ETP are double negative (DN) for these coreceptors (i.e., $CD4^-CD8^-$ cells). Then, there is an initial acquisition of CD4 ($CD4^+$ immature single positive (ISP) T cells), followed by a double positive (DP) stage (i.e., $CD4^+CD8^+$ cells). At this point, DP cells already have they TCR rearranged and are subjected to a selection process, termed positive selection. During positive selection, through their TCR, DP cells will recognize major histocompatibility complex (MHC)-peptide complexes presented by APC located in the thymus cortex. The DP cells that can recognize these MHC-peptide complexes are positively selected and continue their differentiation pathway. They lose one of the markers (CD4 or CD8) and become single positive (SP) T cells, i.e., $CD4^+$ T cells or $CD8^+$ T cells. SP cells then face a new selection event, named negative selection, in the thymus medulla[80]. During this selection process, autoreactive T cells are eliminated. Following the selection events, T cells are considered mature and leave the thymus to the periphery. The population of peripheral T cells include naïve, memory and regulatory T (Treg) cells. Children predominantly have naïve T cells, which are cells able to recognize and respond to new antigens. As age increases, the naïve subtype decreases and is replaced by the memory subtype, which becomes the predominant T cell subtype. Memory T cells are the result of previous immunes responses that required antigen activation and are responsible to assure long-term immunity. Treg have an important role of keeping immune responses controlled[75].

As previously mentioned, the TCR is responsible for providing T cells their unique feature of recognizing many different antigens (i.e., peptide fragments). These peptides are generated through proteolytic degradation of foreign or self-proteins within APC expressing either MHC class I or class II molecules. CD4 T cells only recognize peptide fragments presented by MHC class II, while CD8 T cells only recognize antigens presented by MHC class I APC. Interestingly, for T cell activation to occur, a TCR-CD3 complex is needed. This complex is composed of a diverse $\alpha\beta$ TCR heterodimer noncovalently associated with the invariant CD3 dimers $CD\varepsilon\gamma$, $CD3\varepsilon\delta$ and $CD3\xi\xi$ (Fig.I.2). Thus, while TCR mediates recognition of a specific antigenic peptide, the CD3 molecules associated to TCR transduce activation signals to the T cell[81].

CD8 T cells, also known as cytotoxic T cells, mediate the killing of infected cells through many mechanisms, including the expression of cytotoxic proteins (such as granzymes

and perforin) and the secretion of cytokines (such as interferon-γ (IFNγ) and tumor necrosis factor (TNF))[82]. Upon an acute infection, T cell response is normally divided into three phases: (i) priming and expansion, (ii) resolution and contraction and (iii) memory. During phase (i), naïve CD8 T cells divide and differentiate into effector T cells, acquiring the ability to produce IFNγ, TNF and cytotoxic proteins[83]. Following viral clearance, phase (ii) takes place, culminating in the death of most effector CD8 T cells. Only ~5-10% of these cells survive and enter phase (iii), the "memory" phase. Memory T cells are maintained long term through signals such as IL-7 and IL-15[84]. CD4 T cells, also known as helper T cells, do not directly eliminate pathogens as CD8 T cells. Instead, they are essential in the formation of memory CD8 T cells following infection or immunization[82].

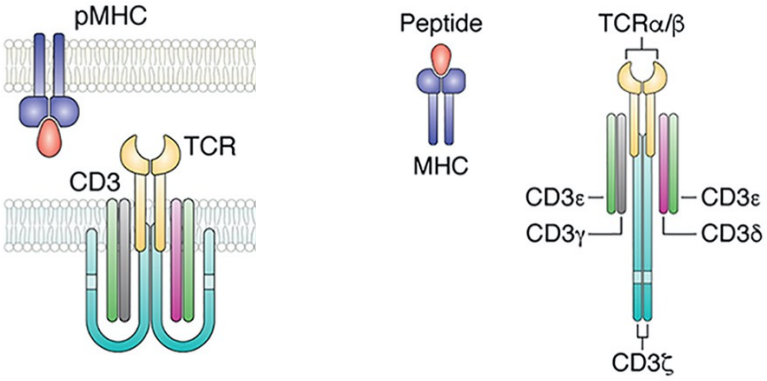

Figure I.2. *Schematic representation of a TCR-CD3 complex. MHC: major histocompatibility complex; TCR: T cell receptor. Adapted*[81].

I.5. Tissue and organ decellularization: establishing an extracellular matrix-based bioscaffold

Patients suffering from end-stage tissue or organ structural and functional disorders frequently do not have satisfactory conventional solutions to treat their conditions. In these cases, tissue or organ transplantation emerges as a last resource to improve their quality of life and survival. Despite representing the only curative solution in irreversible end-stage organ failure, transplanted patients have thereafter to face adverse life-long challenges with immunosuppression and rejection[85]. On the other hand, although efforts are being done to increase the supply pool of suitable organs for transplantation, there is still a significant gap between the number of organ donors and the number of organs recipients, not allowing each candidate eligible for organ transplantation to receive an organ. In the US, data of 2021 indicates there were 162,561 candidates for organ transplantation but only 40,046 transplants were performed (with 20,399 donors recovered)[86].

As an attempt to overcome organ donor shortage and chronic immunosuppression, there has been a quest for alternatives to allogeneic transplantation. Tissue engineering and regenerative medicine (TE/RM) have put some efforts in the last years to find the methods and techniques necessary to develop functional replacement tissues or whole organs of clinical relevance[87]. A common approach of TE/RM consists in the creation of a structural and molecular environment that mimics the natural environment (physically, biochemically and mechanically) of native tissues and organs, allowing repopulation by cells of the recipient and subsequently the creation of an autologous tissue/organ[85]. Although there have been some attempts to produce synthetic scaffolds, the constructs only partially mimic the natural vascular network. Also, synthetic scaffolds can bring toxicity to recipients, constituting a major disadvantage of these scaffolds[88].

One way of overcoming vascularization and toxicity associated with synthetic scaffolds is to create natural bioscaffolds, taking advantage of existing organs. These are highly organized due to an extracellular matrix (ECM) structure, which is a naturally occurring scaffold secreted by populating cells. Structural and functional molecules of the ECM are in a state of dynamic equilibrium with the surrounding tissue and provide the means by which cells communicate with each other and the tissue environment. The ECM contains growth factors and other bioinductive factors, which facilitate cell attachment, tissue integration, remodeling, and development. The ECM also provides organ-specific physical, biochemical and biomechanical properties. Physical properties are important to stimulate anchorage-related biological function (e.g., cell division, tissue polarity and cell migration) and cellular mechanotransduction to convert the mechanical stimulus into chemical activity, whereas the biochemical properties provide local and soluble growth factor signals[89]. To be able to isolate and use tissue ECM, a technique called decellularization was developed. This technology relies on eliminating the cells present in a tissue or organ to obtain a cell-free ECM, creating a 3D bioscaffold that preserves the native tissue architecture, including the vasculature[88].

I.5.1. Different ways to reach one end

There are several different decellularization agents available that can be used to decellularize either tissues or organs. The choice of the best agents is dependent upon many factors related with the nature of the tissue/organ, including thickness, cell density, tissue cellularity and lipid content. Irrespective of the decellularization agents elected, all of them will damage in some degree the ECM ultrastructure as well as ECM composition. Hence, the purpose of selecting the best cell removal agents is the minimization of undesirable effects[90]. Decellularization agents can be chemical, biologic or physical agents (Table I.2)[90].

Table I.2. Decellularization agents and techniques (adapted[90]).

Agent/Technique	Mode of action	Effects on ECM
Chemical Agents		
Acids and bases	Solubilizes cytoplasmic components of cells, disrupts nucleic acids, tend to denature proteins	May damage collagen, GAG, and growth factors
Hypotonic and hypertonic solutions	Cell lysis by osmotic shock, disrupt DNA-protein interactions	Effectively lyses cells, but does not effectively remove cellular residues
Non-ionic detergents	Disrupt DNA-protein interactions, disrupt lipid-lipid and lipid-protein interactions and to a lesser degree protein-protein interactions	
- Triton X-100		Mixed results with efficacy dependent on tissue, more effective cell removal from thin tissues, some disruption of ultrastructure and removal of GAG, less effective than SDS
Ionic detergents	Solubilize cell and nucleic membranes, tend to denature proteins	
- Sodium dodecyl sulfate (SDS)		Effectively removes nuclear remnants and cytoplasmic proteins from dense tissues, tends to disrupt ultrastructure, removes GAG and growth factors and damages collagen
- Sodium deoxycholate		Mixed results with efficacy dependent on tissue thickness, some disruption of ultrastructure and removal of GAG
- Triton X-200		More effectively removes cells from thin tissues but with greater disruption of ultrastructure compared to other detergents
Zwitterionic detergents	Exhibit properties of non-ionic and ionic detergents	
- CHAPS		Effectively removes cells with mild disruption of ultrastructure in thin tissues
- Sulfobetaine-10 and -16 (SB-10, SB-16)		Effectively removes cells with mild disruption of ultrastructure in thin tissues
Solvents		
- Alcohols	Cell lysis by dehydration, solubilize and remove lipids	Effectively removes cells from dense dense tissues and inactivates pyrogens, but crosslinks and precipitates proteins, including collagen
- Acetone	Cell lysis by dehydration, solubilizes and removes lipids	Effectively removes cells from dense dense tissues and inactivates pyrogens, but crosslinks and precipitates proteins, including collagen
- Tributyl phosphate (TBP)	Forms stable complexes with metals, disrupts protein-protein interactions	Mixed results with efficacy dependent on tissue, dense tissues lost collagen but impact on mechanical properties was minimal
Biologic Agents		
Enzymes		
- Nucleases	Catalyze the hydrolysis of ribonucleotide and deoxyribonucleotide chains	Difficult to remove from the tissue, could invoke an immune response
- Trypsin	Cleaves peptide bonds on the C-side of Arg and Lys	Prolonged exposure can disrupt ECM ultrastructure, removes ECM constituents such as collagen, laminin, fibronectin, elastin, and GAG, slower removal of GAG compared to detergents
- Dispase	Cleaves specific peptides, mainly fibronectin and collagen IV	Prolonged exposure can disrupt ECM ultrastructure, removes ECM components such as fibronectin and collagen IV
Chelating Agents (EDTA, EGTA)	Chelating agents bind metallic ions, thereby disrupting cell adhesion to ECM	Typically used with enzymatic methods (e.g. trypsin) but can be used with other agents, ineffective when used alone
Physical and Miscellaneous Agent		
Temperature (freezing and thawing)	Intracellular ice crystals disrupt cell membrane	Ice crystal formation can disrupt or fracture ECM
Direct application of force	Removal of tissue eliminates cells and force can burst remaining cells	Force can directly damage ECM
Pressure	Pressure can burst cells and aid in removal of cellular material	Pressure can disrupt ECM
Electroporation	Pulsed electrical fields disrupt cell membranes	Electrical field oscillation can disrupt ECM

Chemical agents include: acid and bases, hypertonic and hypotonic solutions, alcohols, ionic (e.g., sodium dodecyl sulphate (SDS)) and non-ionic (e.g., Triton X-100) detergents, and other solvents. Biological agents can be enzymes (e.g., trypsin) and non-enzymatic (e.g., ethylenediaminetetraacetic acid (EDTA)) agents, while some physical parameters such as temperature, force and pressure can be manipulated to induce cell lysis. Each one of these agents has advantages and disadvantages[85,90]. For instance, in what concerns chemical detergent agents, Triton X-100 is a better decellularization detergent for thinner tissues while SDS is better for thicker tissues. Despite being an efficient cell remover, SDS retains less ECM molecules in the decellularized scaffold compared to other detergents, such as Triton X-100. Chemical acid agents can solubilize the cytoplasmic components removing nucleic acids, but at the same time they remove collagen from the ECM. Biological agents, specifically enzymes, can promote cell detachment from the ECM by disrupting the protein-protein interaction but they also damage the collagen structure. On the other hand, non-enzymatic agents are able to disconnect cells through their metal ion separation but are unsuccessful in cellular removal. Therefore, many decellularization protocols combine non-enzymatic biological agents with detergents able to gently remove disconnected cells from the matrix. Lastly, physical strategies for decellularization comprise freeze-thawing cycles and hydrostatic-based procedures. These methods can produce cellular lysis and subsequent removal from the ECM structure, but also induce great damage to the ECM architecture.

There are also different methods of delivering the decellularization agents to the tissues, such as perfusion or agitation (Fig.I.3)[91]. The choice of the most efficient method is dependent upon tissue characteristics (such as thickness and density), agents used and clinical purpose of the decellularized tissue[85,90]. In whole organ decellularization (e.g., heart or liver), perfusion of detergents throughout the vasculature is considered the most effective method concerning cell removal and maintenance of organ microarchitecture. However, perfusion-associated pressure can disrupt and create holes within the cellular vascular network. Therefore, flow rate perfusion has a critical role in decellularization and should be controlled.

Overall, the decellularization process is essentially performed in three steps. Decellularization itself is the first step and includes removal of all native cells from the ECM framework, using decellularization agents with different timings and concentrations. This step ends with the production of an acellular ECM-based 3D scaffold that should possess the native organ-specific structure almost intact. In the second step, quality of the scaffold is assessed, namely evaluating the texture, quantifying existing growth factors and studying the biological properties of the scaffold. At last, recellularization is the third step and includes seeding the scaffold with

organ-specific cells. Ideally, these cells should be autologous to avoid immunological problems[85].

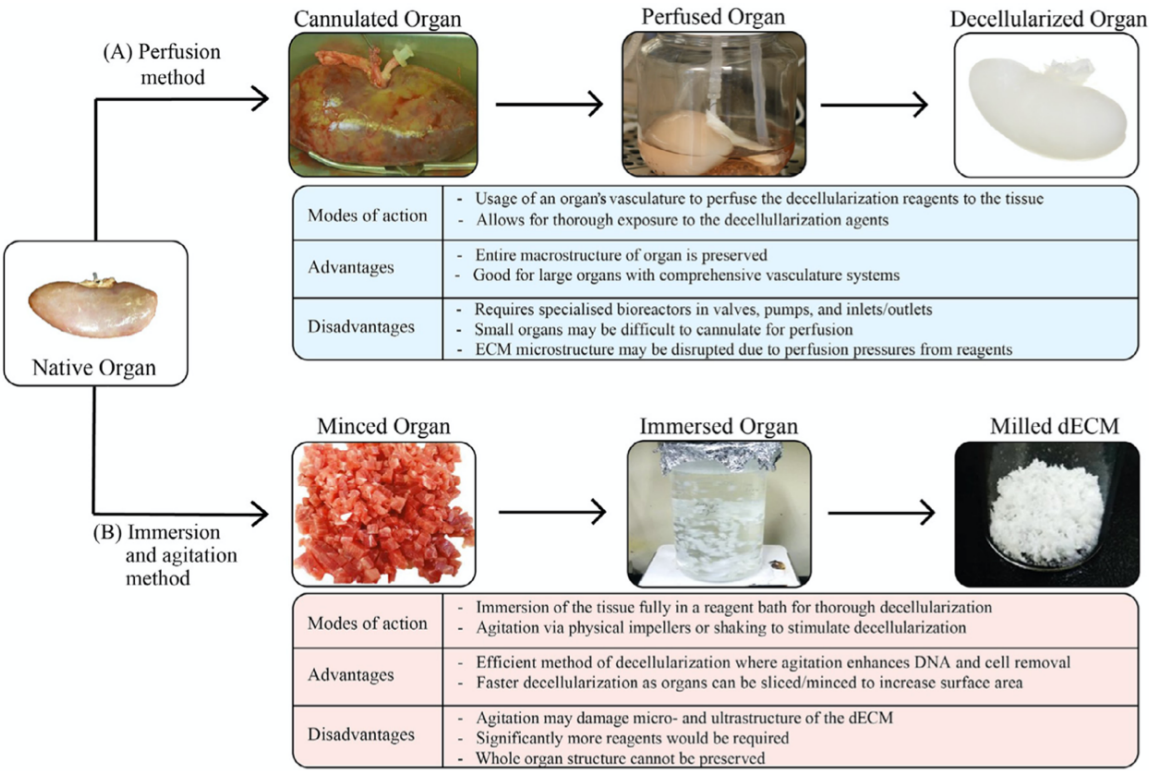

Figure I.3. *Methods of decellularization agent delivery.* ***(A)*** *Perfusion.* ***(B)*** *Immersion and agitation. dECM: decellularized extracellular matrix; ECM: extracellular matrix. Adapted*[91].

I.5.2. Decellularization and recellularization of tissues/organs

The number of decellularization studies have increased considerably in the last decades, after Badylak and colleagues first postulated the technique to decellularize a tissue. In that seminal study of 1995, the authors decellularized porcine small intestinal submucosa using chemical detergents[92]. In 2008, Ott and colleagues showed that decellularization of whole organs was possible through decellularization of a rat heart. The organ was substantially decellularized, while still preserving the interconnected vascular architecture, functional valves and ventricular integrity[93]. In 2015, the same group attempted to scale their previous success to human hearts, which are considerably bigger than rat. Obtained acellular human heart scaffolds showed preserved ECM composition, architecture and perfusable vasculature. iPSC-derived cardiomyocytes were used to repopulate the native human heart matrix, generating tissues with 3D complexity. Cardiac tissue was maintained for 120 days, demonstrating definitive sarcomeric structure, contractile force and electrical conduction[94]. Successful decellularization of porcine liver[95] and kidney[96] as whole organs were also reported.

While promising results have emerged from whole organ decellularization studies at early stages, the functional complexity associated to organs constitutes a great challenge towards evolving into clinical products.

Although decellularization seems a promising alternative and could eventually be a solution for the worrying problem of organ shortage, it also raises some ethical concerns. As a starting material, these natural scaffolds can be obtained from people (live or deceased) or animals (such as porcine, since the organ size is similar between both species). The ideal solution would always be to use organs from human donors. However, most of the organs recovered are from deceased people and oftentimes these organs are not in good conditions to be transplanted, either because they are from aged people or because they were unhealthy. This problem could be overcome using a xenograft, however we should ethically question to what extent producing porcine to obtain scaffolds is acceptable. This would also imply the creation of donor animal facilities, with great costs associated.

I.5.3. Studies of thymic decellularization

In 2015, Fan and colleagues successfully decellularized mouse thymi. The decellularization protocol included repeated cycles of freeze-thawing and incubation with detergent solutions (0.1% SDS solution followed by 1% Triton X-100 solution) using agitation[97]. The decellularized thymi were able to support TEC survival in culture. Furthermore, when transplanted to athymic nude mice, the bioengineered thymic organoids promoted homing of lymphoid progenitors and thymopoiesis. A few years later, other group compared different detergent solutions to decellularize mouse thymi, also following a diffusion approach[98]. The thymi were subjected for two days to one of four detergent solutions: 0.5% 3-[(3-Cholamidopropyl)dimethylammonio]-2- Hydroxy-1-Propanesulfonate (CHAPSO), 1% n-octyl glucoside (NOG), 0.05% SDS or 0.1% Triton X-100. In this study, the authors found CHAPSO to be the best detergent solution to decellularize mouse thymi, as it allowed best preservation of major ECM proteins in their native conformation, while allowing cell removal. CHAPSO-treated scaffolds were successfully repopulated with TEC and, following transplantation into athymic nude mice, allowed formation of an organized thymic microenvironment that was able to attract circulating lymphoid progenitors and generating naïve $TCR\beta^+$ $CD4^+$ and $CD8^+$ T cells.

In 2020, a very interesting study reported the identification of a particular population of TEC, with epithelial-mesenchymal characteristics[99]. They found that these "hybrid" cells (that can be found within both cTEC and mTEC populations) were capable of long-term expansion *in vitro* and could be identified through the express of CD49f, the α6-integrin. Remarkably, they also reported decellularization of whole rat thymi, using a 6-

day perfusion approach. The perfusion method was not the obvious choice to decellularize the thymus since this organ does not possess a main arterial supply to the whole organ. Therefore, to be able to do it, the carotid artery was left open for subsequent cannulation and perfusion of the organ, while all other arteries were closed. An anatomic phenocopy of the native thymus was reconstituted when "hybrid" TEC were combined with thymic interstitial cells and injected into the natural decellularized rat scaffolds. Importantly, this reconstituted "human" thymus proved to be functional, as it was capable of supporting mature T cell development *in vivo* after transplantation into humanized mice (i.e., immunocompromised mice engrafted with human HSC).

One year later, other group used a perfusion bioreactor to decellularize murine thymi also using a 6-day period[100]. The decellularization protocol included a combination of hypotonic stress, DNase and shear stress. Following homogenization and freeze-drying of the decellularized thymi, 3D porous thymic scaffolds were generated and subjected to a crosslinking process for improved stability and handling. These thymic scaffolds were repopulated with fetal murine thymic stromal cells and thymocytes *in vitro* and were able to generate DP cells. However, when transplanted to athymic nude mice, the majority fail to engraft and was resorbed 8 weeks after grafting. Nevertheless, one third of the mice successfully engrafted the scaffold and was able to harbor thymocytes exclusively of recipient origin. On the other hand, the study also reports that the decellularized thymic tissue was very difficult to handle and cell seeding was particularly challenging. Generation or maintenance of DP or SP thymocytes was not possible, which motivated the authors choice for the scaffold production.

More recently, the Fan's group also produced an artificial "human" thymus and engrafted them in humanized mice to study T cell immunity. The artificial human thymi were constituted by decellularized murine thymi that were injected with induced pluripotent stem cells (iPSC)-derived thymic epithelial progenitor cells (differentiated in 3D alginate capsules) together with UCB-derived $CD34^+$ cells[101,102]. Engraftment of these artificial human thymi into immunocompromised mice allowed differentiation of a diverse population of mature functional human T cells, expressing a complex TCR repertoire. A functional human T cell compartment was seen in the humanized mice through restoration of cellular and/or humoral immune responses mediated by T cells (including proinflammatory responses upon TCR engagement) and inhibition of allogeneic tumor graft growth. Importantly, morosity and difficulties associated with this approach are mentioned by the authors, as all process to generate and engraft these artificial human thymi takes at least 4 months.

I.6. Aim of studies and Thesis outline

Allogeneic HCT is considered a life-saving therapeutic procedure in different hemato-oncology settings. UCB has emerged as an alternative source of HSPC for patients eligible for HCT who lack a suitable donor. However, UCBT is limited by the low cell numbers in a single unit, as well as immaturity of the immune cells present in the UCB, which results in delays of engraftment, increased risk of OI and, subsequently, death. Another disadvantage of UCBT is the lack of DLI availability after transplantation, commonly employed to enhance donor-derived immunity to treat OI, but also mixed chimerism, or disease relapse.

In this thesis we aimed at developing a 2-stage culture protocol for the scalable *ex-vivo* generation of functional human T cells from UCB-derived HSPC, to be used as DLI in a clinical context. This 2-stage protocol comprised (i) an initial step of UCB-derived HSPC expansion to maximize the starting cell material to be used in (ii) a second stage where expanded UCB-derived HSPC are differentiated into functional T cells. Differentiation of T cells is aspired by using an innovative bioengineering approach, where the natural environment of the thymus (the primary lymphoid organ responsible for T cell lymphopoiesis) is recreated. By using a 3D acellular human thymic bioscaffold combined with Notch signaling (responsible for T cell lineage commitment, differentiation and maturation *in vivo*), ideally under serum-free (SF)/xenogeneic-free (XF) conditions, we are confident that an improved niche for T cells to differentiate and mature will be provided. Overall, we envision that the scalable *in vitro* generation of functional human T cells, derived from UCB HSPC, could potentially provide a readily available source of cells for adoptive transfer immunotherapies (namely DLI upon OI or malignancy recurrence after UCBT). In this way, we can contribute to boost and widen the clinical use of UCB cells, while giving important insights on the mechanisms of T cell development.

An overview of the five main chapters of this thesis is given:

Chapter I aims at giving context and introducing concepts about the main topics approached in the thesis. A comprehensive literature review of relevant subjects, including: the hematopoietic system; HSPC and their different sources; HCT and its limitations; expansion of UCB-derived HSPC; T cells and the thymus; as well as ECM and decellularization studies are given.

Chapter II targets the development of an optimized XF *ex-vivo* expansion protocol to attain a large number of UCB-derived HSPC. Different strategies are approached, including co-culture with a MSC feeder layer from different sources (e.g., adipose tissue

and umbilical cord matrix) and establishing MSC using medium supplemented with fibrinogen-depleted human platelet lysate (HPL) instead of fetal bovine serum (FBS), to achieve a commitment between cell yield and product features of interest.

Chapter III describes the establishment of the artificial thymic organoids (ATOs) system in our lab, a system that allows differentiation of functional T cells from HSPC *in vitro*, using MS5 ectopically expressing a delta ligand. A further improvement of the system is explored by using our expanded UCB HSPC (Chapter II).

Chapter IV aims at developing a novel decellularization protocol to be applied to human thymic tissue, envisaging its potential use as a scaffold for *in vitro* T cell differentiation and maturation. Maintenance of ECM structure and composition are evaluated to assure the best natural 3D scaffold for T cell differentiation is provided.

Finally, Chapter V summarizes the breakthroughs achieved in each chapter. Future work is also presented based on the results of this thesis.

II. Influence of mesenchymal stromal cells (and their tissue source) on the hematopoietic supportive capacity of umbilical cord blood-derived CD34$^+$-enriched cells

Part of this chapter is published as:

Bucar, S. *et al.* Influence of the mesenchymal stromal cell source on the hematopoietic supportive capacity of umbilical cord blood-derived CD34$^+$-enriched cells. *Stem Cell Research & Therapy*. **12**, 399 (2021)

II.1. Summary

Umbilical cord blood (UCB) is a clinically-relevant alternative source of hematopoietic stem/progenitor cells (HSPC). To overcome the low cell number per UCB unit, *ex-vivo* expansion of UCB HSPC in co-culture with mesenchymal stromal cells (MSC) has been established. Bone marrow (BM)-derived MSC have been the standard choice but the use of MSC from alternative sources, less invasive and discardable, could ease clinical translation of an expanded $CD34^+$ cell product. Here, we compared the capacity of BM-, umbilical cord matrix (UCM)- and adipose tissue (AT)-derived MSC, expanded with/without xenogeneic components (i.e., fetal bovine serum (FBS) or human platelet lysate (HPL), respectively) to expand/maintain UCB $CD34^+$-enriched cells *ex-vivo*. MSC from all tissue sources effectively supported UCB HSPC expansion/maintenance *ex-vivo*. Remarkably, AT-derived MSC co-culture resulted in higher total cell numbers of expanded cells with similar phenotypic profile compared to BM-derived MSC, representing a promising alternative to BM as a source of MSC for co-culture protocols to expand/maintain HSPC *ex-vivo*. On the other hand, UCM-derived MSC demonstrated inferior hematopoietic supportive capacity compared to MSC from adult tissues. Importantly, a subpopulation of more primitive cells ($CD34^+CD90^+$) was maintained in all co-cultures and the presence of a MSC feeder layer was essential to maintain and expand a subpopulation of progenitor T cells ($CD34^+CD7^+$). The use of HPL to expand MSC prior to co-culture establishment did not influence the expansion potential of UCB cells, but differences were seen in what concerns the phenotypic profile of expanded cells.

II.2. Background

Umbilical cord blood (UCB) has emerged as an alternative source of hematopoietic stem/progenitor cells (HSPC) for patients lacking a suitable donor in the context of allogeneic hematopoietic cell transplantation (HCT). Despite being a readily available source, with lower immunogenicity and lower risk of development of graft-*vs*-host disease (GVHD) compared to other sources, the low cell dose in a single UCB unit constitutes a major limitation[103]. To overcome the limitations of a low cell dose for transplantation of adult patients, two main strategies have been employed: (i) HCT using two unmanipulated UCB units (standard of care)[104] and (ii) HCT using two UCB units, one of which containing cells that were expanded *ex-vivo*[105]. Several protocols were developed to promote *ex-vivo* expansion of UCB HSPC, including the use of different media, cytokines, growth factors, and more recently the use of small molecules and chemical compounds[45,46,105]. Alongside these approaches, bone marrow (BM)

mesenchymal stromal cells (MSC) have been used in a co-culture system to support the *ex-vivo* expansion and maintenance of HSPC. This strategy emerged to recapitulate the hematopoietic niche within the BM, where MSC have a pivotal role by giving structural support for HSPC to grow but also to influence their homing, stemness and differentiation potential[45]. Over the last years, we have studied the capacity of BM MSC to support UCB HSPC *ex-vivo* in a co-culture setting[66,68,106] with a tailored cytokine cocktail recently established[107]. In a clinical context, a significant improvement in neutrophil and platelet engraftment was observed in patients with hematologic cancers who received a unit of UCB previously expanded with BM MSC in addition to an unmanipulated UCB unit, compared to patients who received two units of unmanipulated UCB[73].

Despite the majority of studies employing human MSC use BM-derived cells[108], requiring an invasive procedure that entails risks to donors, MSC can also be efficiently isolated from other tissues[109]. Overall, adipose tissue (AT) and umbilical cord matrix (UCM) display advantages over BM as a source of MSC, namely ease of collection using minimally/non-invasive procedures. For instance, AT MSC, derived from the stromal vascular fraction (SVF) of AT, can be easily obtained through enzyme-based isolation procedures from subcutaneous AT[110], which is usually discarded as medical waste and offers the possibility of resampling. Interestingly, stromal cells in the SVF share similarities with those of the BM[111] and some studies have focused on the potential of these cells to support *ex-vivo* expansion of UCB progenitors[112–114]. On the other hand, the umbilical cord tissue, specifically the Wharton's jelly or matrix (UCM), has been explored as a promising source of MSC[115]. Of notice, Wharton's jelly MSC has been recently proposed as a preferable feeder layer (FL) choice for UCB HSPC expansion *ex-vivo* considering the microenvironment of the umbilical cord and placenta, where UCB hematopoietic progenitors reside in, which differs from the adult BM niche[116]. Although these alternative sources of MSC have been compared with the standard BM-derived MSC, namely focusing on identity criteria such as immunophenotype and multilineage differentiation potential[117,118], a direct comparison among these tissue sources is still missing in what concerns their capacity to support the *ex-vivo* expansion of UCB HSPC.

Regardless of the MSC source chosen for the co-culture system, the main goal would be the development of a cost-effective, clinical-grade, co-culture system using serum-free (SF)/xenogeneic-free (XF) culture materials towards the maximization of cell yield, while increasing product consistency and maintaining product features[107]. Specifically, the translation of such system to an approved cell therapy product would certainly rely on two main parameters that are commonly evaluated in clinical trials: total nucleated cells (TNC) and percentage of $CD34^+$ cells. This is due to the fact that higher doses of TNC, as well as UCB units enriched with $CD34^+$ cells, have been positively correlated

with better clinical outcomes (namely, neutrophil engraftment) in patients receiving expanded UCB cells[105].

Consistent with previous studies from our lab[66], a first set of experiments in this chapter showed that expansion of UCB HSPC was favored by the presence of a feeder layer of BM-derived MSC (compared to feeder-free conditions), particularly in expanding a subpopulation of progenitor T cells ($CD34^+CD7^+$). To fulfill the existing gap regarding the efficacy of using alternative sources to BM-derived MSC, we designed this study whose aim is to make a comprehensive comparison of the *ex-vivo* expansion capacity of UCB $CD34^+$-enriched cells in a co-culture system using different sources of MSC, namely BM, AT and UCM. In an attempt to establish a XF co-culture system, we also tested the feasibility of establishing FL of MSC from the different sources using medium supplemented with fibrinogen-depleted human platelet lysate (HPL), instead of fetal bovine serum (FBS). Although FBS raises issues related to safety and animal welfare[119], it is still a commonly used supplement for MSC manufacturing, including at a clinical level[73].

II.3. Material and Methods

II.3.1. Human samples

Human samples were obtained from local hospitals (umbilical cord blood (UCB) and tissue: Hospital São Francisco Xavier, Centro Hospitalar de Lisboa Ocidental; bone marrow (BM): Instituto Português de Oncologia Francisco Gentil, Lisboa; adipose tissue (AT): Clínica de Todos-os-Santos, Lisboa) under collaboration agreements with Institute for Bioengineering and Biosciences, Instituto Superior Técnico (iBB-IST), after written and informed consent and according to the Directive 2004/23/EC of the European Parliament and of the Council of 31 March 2004 regarding standards of quality and safety for the donation, procurement, testing, processing, preservation, storage and distribution of human tissues and cells (Portuguese Law 22/2007, June 29), with the approval of the Ethics Committee of the respective clinical institution. All samples used in this study were obtained from human donors (the mothers, in the case of UCB and tissue) that have previously tested negative for common virus and diseases.

II.3.2. Preparation of human mesenchymal stromal cell (MSC)-feeder layers (FL)

Cells from a single donor of each tissue source (BM, AT and umbilical cord matrix (UCM)) were used to establish FL, mimicking an allogeneic universal donor for each source, as recently proposed by our group[107]. Human MSC were obtained from the Stem Cell Engineering Research Group (SCERG) cell bank, at iBB-IST, Lisboa, Portugal. These cells were previously isolated and expanded under normoxia conditions (i.e., 21% O_2) using

fetal bovine serum (FBS)-supplemented medium, characterized and cryopreserved by our group according to established protocols[120]. Cells from all tissue sources used in this study have been previously shown to comply with International Society for Cell & Gene Therapy (ISCT) criteria in what concerns identity and characterization of MSC (i.e., expression of CD73, CD90 and CD105; lack of expression of CD34, CD45, CD80, CD14 and HLA-DR and confirmation of tri-lineage differentiation potential)[121,122]. Firstly, MSC were thawed and seeded using low glucose Dulbecco's Modified Eagle's Medium (DMEM) (Cat. #31600-091, Thermo Fisher Scientific, United States of America (USA)) supplemented with 10% (v/v) MSC-qualified FBS (Cat. #12662-029, Thermo Fisher Scientific) (i.e., specially tested to support the expansion and clonal enumeration (MSC CFU-F assay) of MSC) and 1% (v/v) Antibiotic-Antimycotic (A/A) (Cat. #15240-062, Gibco, USA). Then, in order to establish MSC-based FL under xenogeneic-free (XF) conditions, i.e., MSC expanded without FBS-containing medium, half of the cells were subjected to two adaptive passages with low glucose DMEM supplemented with 5% (v/v) fibrinogen-depleted human platelet lysate (HPL) (UltraGRO™-PURE; Cat. #HPCHXCRL50, kindly provided by AventaCell Biomedical Corp., USA) (Certificate of Analysis (CoA) provided), while the other half continued to be expanded in low glucose DMEM with 10% MSC-qualified FBS (both supplemented with 1% (v/v) A/A). MSC were seeded at 3000 cells/cm^2 into cell culture flasks and medium was changed every 3 days until 80-90% confluence was reached. After the two adaptive passages, MSC were seeded (in P5 or P6) onto wells of a 12-well plate using the appropriate medium. Once confluence was reached, MSC growth was arrested by using medium supplemented with 0.5 μg/mL (BM and AT MSC)[123] or 5 μg/mL (UCM MSC)[33] Mitomycin-C (Cat. #M4287-2MG, Sigma-Aldrich, USA) for 2.5-3h at 37°C and 5% CO_2. A higher concentration of Mitomycin-C was used for UCM MSC due to their higher *in vitro* proliferative capacity compared to their adult counterparts[115]. Mitomycin-C treated FL were carefully washed twice and kept with the respective medium at 37°C and 5% CO_2 for no more than 72 hours until further co-culture with hematopoietic stem/progenitor cells (HSPC).

II.3.3. Isolation of UCB mononuclear cells (MNC)

MNC were isolated from fresh UCB samples through a Ficoll (Cat. #17544203, GE Healthcare, USA) density gradient centrifugation. After washing with 2 mM ethylenediamine tetraacetic acid (EDTA) (Cat. #03690-100mL, Sigma-Aldrich) in phosphate buffered saline (PBS) (Cat. #21600-044, Sigma-Aldrich) and upon treatment with ammonium chloride (155 mM) (Cat. #254134-25G, Sigma-Aldrich) for 10 min at 4°C to eliminate residual erythrocytes, MNC were cryopreserved using Recovery Cell Culture Freezing Medium (Cat. #12648-010, Gibco) and stored in a liquid/vapor phase nitrogen tank.

II.3.4. Enrichment for CD34$^+$ cells

Cryopreserved MNC from three UCB samples were individually thawed in DMEM + 20% (v/v) FBS and washed with magnetic-activated cell sorting (MACS) buffer. CD34$^+$ HSPC were then isolated using the CD34 MicroBead Kit UltraPure (Cat. #130-100-453, Miltenyi Biotec, Germany) through MACS, according to the manufacturer's instructions. In order to attain a highly pure CD34$^+$ cell population (i.e., >98%), cells from the positive fraction were subjected to a second LS MACS column.

II.3.5. *Ex-vivo* expansion of CD34$^+$-enriched cells

CD34$^+$-enriched cells from UCB (30 000/mL) were resuspended in StemSpan SFEM II medium (Cat. #09655, STEMCELL Technologies, Canada) supplemented with 1% (v/v) A/A and defined concentrations of SCF, TPO, FLT3-L and bFGF cytokines (Cat. #AF-HHSC3 and #AF-100-18B, PeproTech, USA). In the first set of studies, testing the impact of the presence of a FL *vs* feeder-free conditions, 60, 50, 55 and 5 ng/mL, respectively, were used for cultures with and without a MSC FL (Fig. II.1). Upon optimization of the cytokine concentrations for these culture systems by our group[107], tailored concentrations were used in the experiment using MSC from different tissue sources. SCF, TPO, FLT3-L and bFGF cytokines were used in the following concentrations: 90, 77, 82 and 5 ng/mL, respectively, for co-cultures with a MSC FL; and 64, 80, 61 and 5 ng/mL, respectively, for cultures without a MSC FL. 2 mL of cell suspension were deposited in each well of a 12-well plate containing a MSC FL previously prepared as mentioned above (or under stroma-free conditions, i.e., no feeder layer (NO FL)) and expanded for 7 days at 37ºC and 5% CO_2 in a humidified atmosphere (Fig. II.5). At the end of the experiment, UCB total nucleated cell (TNC) count and viability were determined through the Trypan Blue (Cat. #15250-061, Gibco) exclusion method.

II.3.6. Immunophenotypic characterization

HSPC before and after expansion (days 0 and 7, respectively) were firstly incubated with Far Red LIVE/DEAD Fixable Dead Cell Stain Kit (Cat. #L34974, Thermo Fisher Scientific) to assess cell viability and then surface stained with the following anti-human antibodies: CD34 (8G12) PerCP-Cy5.5, CD41α (HIP8) PE (Cat. #347222 and #555467, BD Pharmingen, USA); CD90 (5E10) PE, CD7 (CD7-6B7) FITC, CD14 (M5E2) FITC, CD15 (HI98) PE and CD33 (WM53) PE (Cat. #328110, #343103, #301806, #301904, #303404, respectively, BioLegend, USA). Cells were acquired on a FACSCalibur flow cytometer (BD Biosciences, USA) and data was analyzed using FlowJo v10 software (FlowJo LLC, USA).

II.3.7. *In vitro* clonogenic assays

The ability of expanded and non-expanded hematopoietic progenitors to proliferate and differentiate was assessed through the colony-forming unit (CFU) assay. Briefly,

1000 (day 0) or 2500 (day 7) cells were resuspended in MethoCult H4434 Classic (Cat. #04434, STEMCELL Technologies) and seeded onto wells of a 24-well plate. After 14 days of incubation at 37°C and 5% CO_2, formed colonies were counted using a bright-field microscope (Olympus CK40-F200, Japan) and classified as erythroid burst-forming unit (BFU-E), colony forming unit granulocyte-monocyte (CFU-GM) or multilineage colony forming unit (CFU-Mix). Colony number was normalized by the number of seeded cells and multiplied by the TNC number. Fold increase (FI) of CFU was calculated dividing the number of colonies on day 7 by the number of colonies on day 0.

Primitiveness of expanded and non-expanded cells was also assessed through the cobblestone area-forming cells (CAFC) assay. 2000 cells were resuspended in MyeloCult™ medium (Cat. #05150, STEMCELL Technologies) supplemented with 350 ng/mL of hydrocortisone (Cat. #07904, STEMCELL Technologies), seeded on top of a growth-arrested FL of MS5 cells on a 24 well-plate, in duplicates, and incubated for 14 days at 37°C and 5% CO_2. CAFC were visualized using a phase-contrast microscope (Leica DMI3000 B, Germany) and registered if at least 5 cells with cobblestone-like morphology were able to migrate beneath the murine FL[125]. FI of CAFC was calculated dividing the number of CAFC on day 7 by the number of CAFC on day 0.

II.3.8. Statistical analysis

Statistical analysis was performed using SPSS Statistics v26 software (IBM, USA). Results are presented as mean ± standard error of the mean (SEM). The Shapiro-Wilk test was carried out to assess normal distribution. Paired sample t-tests were conducted to compare differences between conditions. A p-value <0.05 was considered statistically significant for all tests.

II.4. Results

II.4.1. Impact of using bone marrow (BM)-derived mesenchymal stromal cells (MSC) to expand umbilical cord blood (UCB)-derived $CD34^+$-enriched cells – preliminary study

To evaluate the impact of using MSC in the expansion of UCB hematopoietic stem/progenitor cells (HSPC), a preliminary study using three donors of UCB was done. UCB HSPC were expanded for 7 days with a feeder layer (FL) of BM-derived MSC from a single donor (co-culture system), or without any MSC FL (Fig. II.1).

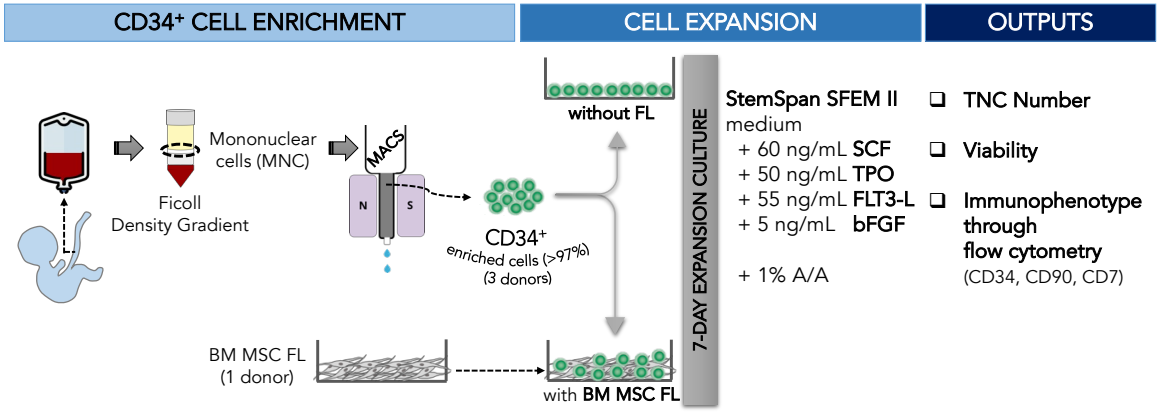

Figure II.1. *Schematic representation of the preliminary study to evaluate the impact of using a feeder layer of mesenchymal stromal cells to expand CD34⁺-enriched cells. Umbilical cord blood-derived CD34⁺-enriched cells were expanded with or without a feeder layer of bone marrow-derived mesenchymal stromal cells for 7 days. A/A: Antibiotic-Antimycotic; BM: bone marrow; FL: feeder layer; MACS: magnetic-activated cell sorting; MSC: mesenchymal stromal cells; TNC: total nucleated cells.*

II.4.1.1. Expansion of UCB HSPC is favored by the presence of a FL of BM-derived MSC

At day 7 of culture, UCB-derived HSPC showed a high viability (>90%) either in co-culture (using a BM MSC FL) or in cultures without a MSC FL (NO FL). The fold increase (FI) in total nucleated cells (TNC) was 53±0.5 for co-cultures and 51±5.1 for NO FL cultures (Fig. II.2A). Specifically, looking at individual cases, two donors presented higher values in the co-culture condition compared to the NO FL condition, while a third

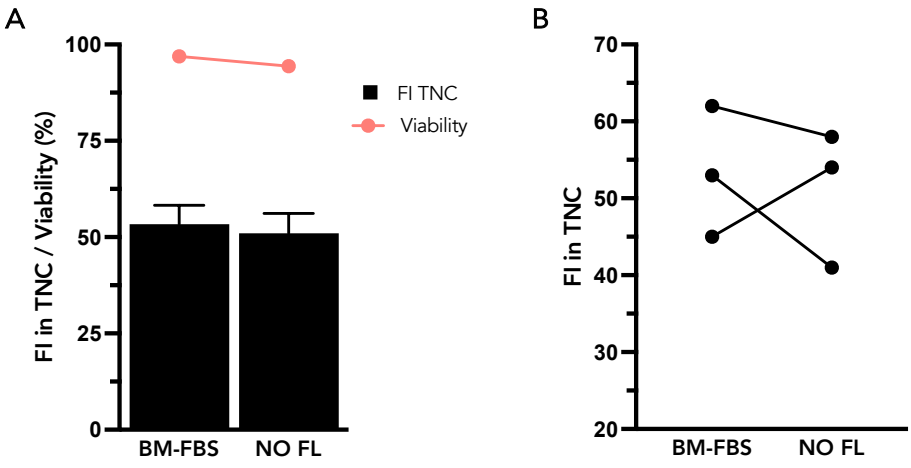

Figure II.2. *Viability and fold increase in total nucleated cells of expanded umbilical cord blood-derived hematopoietic stem/progenitor cells after 7 days of culture with or without a feeder layer of bone marrow-derived mesenchymal stromal cells.* ***(A)*** *Mean values.* ***(B)*** *Individual cases. BM: bone marrow; FBS: fetal bovine serum; FI: fold increase; FL: feeder layer; TNC: total nucleated cells. Values are presented as mean±SEM (n=3).*

donor presented opposing results, i.e., the co-culture condition presented an inferior FI in TNC compared to the NO FL condition (Fig. II.2B). We know, from our extensive experience in HSPC-MSC co-cultures, that expansions with a MSC FL typically present higher values of FI in TNC than the NO FL condition. Thus, in terms of FI in TNC, this donor can be considered an outlier.

Through immunophenotypic characterization of the expanded and non-expanded UCB-derived HSPC, consistent results were attained for both conditions concerning the $CD34^+$ cell population and its subpopulations (Fig. II.3A; Fig. II.4). At day 7, a $CD34^+$

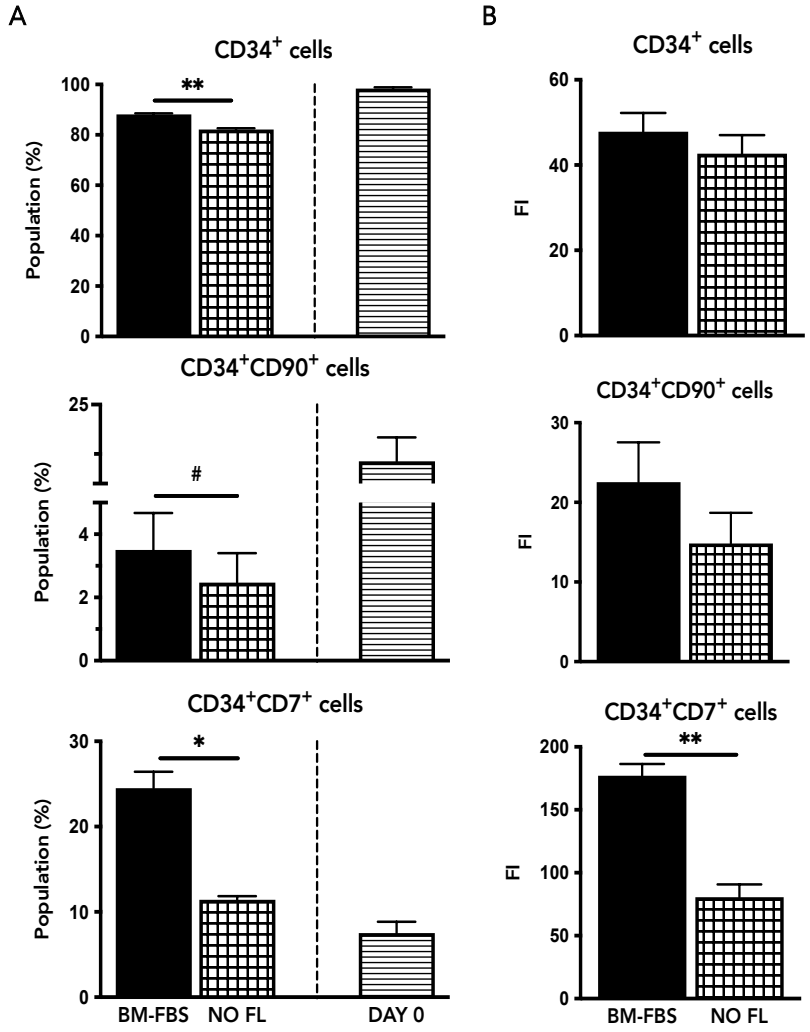

*Figure II.3. Quantitative characterization of the hematopoietic stem/progenitor cell populations after a 7-day expansion in a co-culture system with bone marrow-derived mesenchymal stromal cells or without any feeder layer. (A) Percentage of hematopoietic stem/progenitor ($CD34^+$ cells), more primitive ($CD34^+CD90^+$) and progenitor T cells ($CD34^+CD7^+$) before and after expansion. (B) Fold increase of hematopoietic stem/progenitor ($CD34^+$ cells), more primitive ($CD34^+CD90^+$) and progenitor T cells ($CD34^+CD7^+$) after expansion. BM: bone marrow; FBS: fetal bovine serum; FI: fold increase; FL: feeder layer. Values are presented as mean±SEM (n=3). **: p<0.01; *: p<0.05; #: p=0.05.*

cell population was maintained in culture, which varied between 81.7%, for the NO FL condition, and 88.5% for the co-culture using a BM MSC FL ($p<0.01$). In order to depict the more primitive stem/progenitor content of the UCB cells after culture, the immunophenotypic analysis included the assessment of CD34 and CD90 surface markers, as the subpopulation containing more primitive cells is characterized by its simultaneous expression (i.e., $CD34^+CD90^+$ cells). Even though statistical significance was not reached, there was a tendency ($p=0.05$) for this subpopulation of more primitive UCB HSPC to be higher in the co-culture condition. Another subpopulation of interest that was assessed were the proT cells (i.e., progenitor T cells), defined as cells that co-express the surface markers CD34 and CD7 (i.e., $CD34^+CD7^+$ cells). For the proT cell subpopulation, the immunophenotypic analysis showed that the presence of a BM MSC FL in the culture significantly enhanced this population ($p<0.05$). (Fig. II.3A; Fig. II.4). Expansion levels of the aforementioned subpopulations ($CD34^+$, $CD34^+CD90^+$ and $CD34^+CD7^+$), expressed as FI, followed the tendency observed for cell population content (in percentage) (Fig. II.3B). In particular, the FI of proT cells was significantly higher ($p<0.01$) when UCB $CD34^+$-enriched cells were expanded using a FL of BM MSC (177±16.0) compared to the NO FL condition (80.6±17.7).

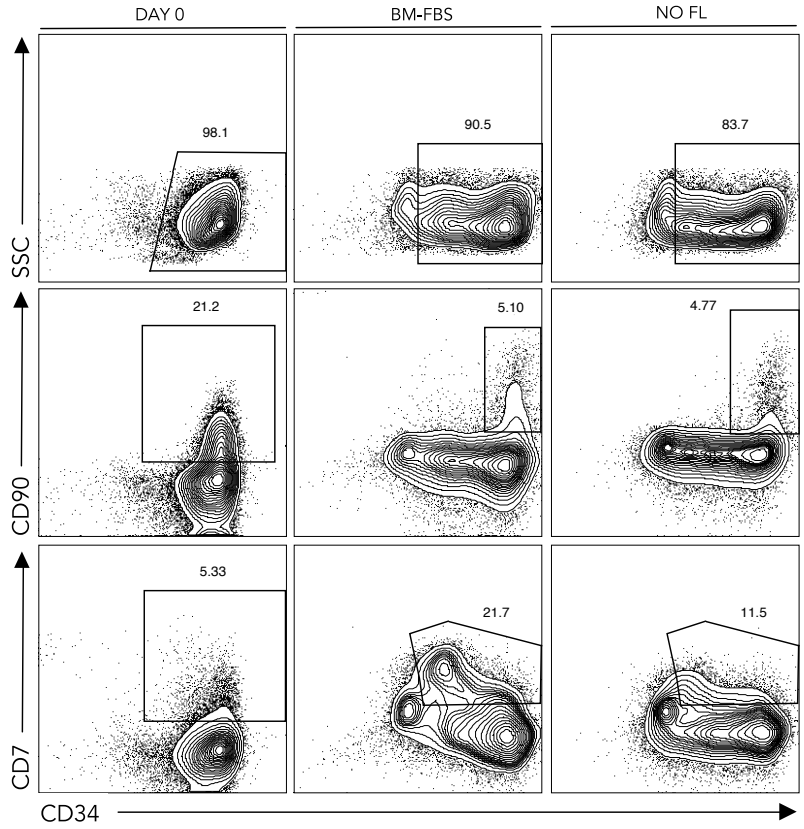

Figure II.4. *Representative immunophenotypic profile of hematopoietic stem/progenitor cells before and after a 7-day expansion in a co-culture system with bone marrow-derived mesenchymal stromal cells or without any feeder layer. Populations are gated on live cells. BM: bone marrow; FBS: fetal bovine serum; FL: feeder layer; SSC: side scatter.*

II.4.2. Influence of the tissue source of MSC on the hematopoietic supportive capacity of UCB-derived CD34⁺-enriched cells

Given the interesting results of the preliminary study in what concerns the better capacity of a co-culture system to support primitive progenitors from UCB *ex-vivo vs* feeder-free conditions, we sought to explore the influence of the MSC tissue source on the hematopoietic supportive capacity of UCB-derived HSPC. In this comprehensive study, CD34⁺-enriched cells from three UCB donors were expanded for 7 days in a co-culture system using different sources of MSC, namely BM, adipose tissue (AT) and umbilical cord matrix (UCM) (Fig. II.5). MSC were previously expanded using medium with either fetal bovine serum (FBS) or human platelet lysate (HPL) and its impact was also studied.

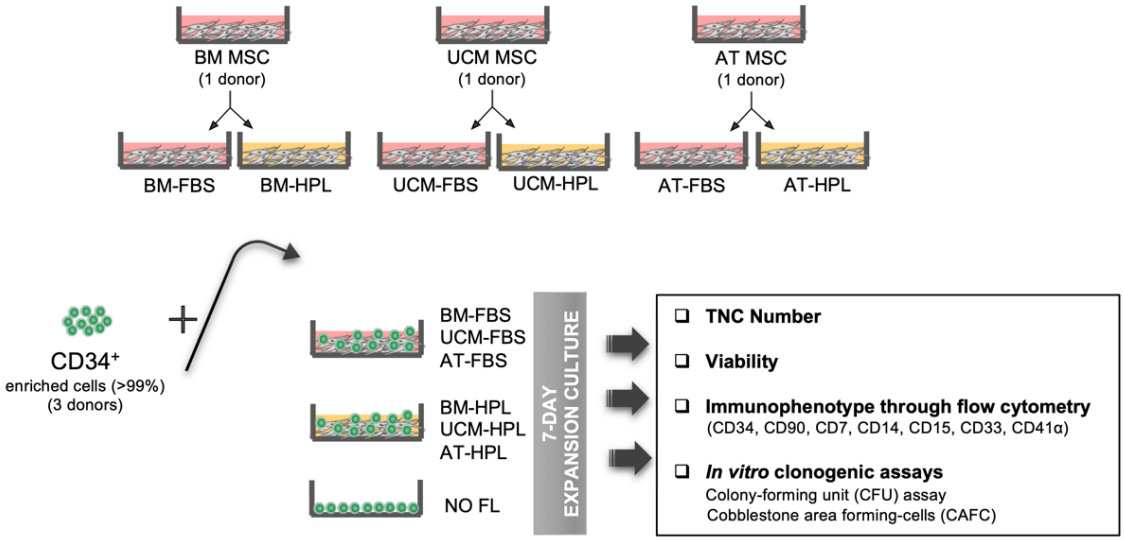

Figure II.5. *Schematic representation of the study using different sources of mesenchymal stromal cells (MSC) to expand umbilical cord blood (UCB) CD34⁺ cells, in a co-culture system, for 7 days. MSC were previously expanded using medium with either fetal bovine serum or human platelet lysate. UCB cells were characterized by immunophenotyping and in vitro clonogenic assays. AT: adipose tissue; BM: bone marrow; FBS: fetal bovine serum; FL: feeder layer; HPL: human platelet lysate; TNC: total nucleated cells; UCM: umbilical cord matrix.*

II.4.2.1. AT MSC outperform UCM MSC in promoting the *ex-vivo* expansion of UCB-derived HSPC

At day 7 of culture, UCB-derived HSPC showed a high viability (>90%) in all co-cultures tested using different MSC feeder layers (BM, AT and UCM), as well as in cultures without a MSC FL (NO FL). FI in TNC ranged from 50 to 83 (Fig. II.6). Co-culture with AT and BM MSC resulted in the highest FI of TNC for UCB cells, with the former allowing slightly higher values (>80 and >70, respectively). In the conditions of our study, UCM-derived MSC resulted in the lowest expansion of UCB cells, with FI TNC values similar to the negative control, i.e., HSPC expanded without a MSC FL. In particular, the

expansion levels in TNC for UCB cells co-cultured with a FL of UCM MSC previously established using either FBS- (UCM-FBS) or fibrinogen-depleted HPL-supplemented medium (UCM-HPL) significantly differed ($p<0.01$ and $p<0.05$, respectively) from the FI values obtained with HSPC co-cultured with a FL of AT MSC previously established with FBS-supplemented medium (AT-FBS). Nevertheless, the culture medium in which MSC were previously expanded (FBS *vs* HPL supplementation) did not seem to have a major impact on the overall expansion of HSPC, as observed by the FI TNC values obtained.

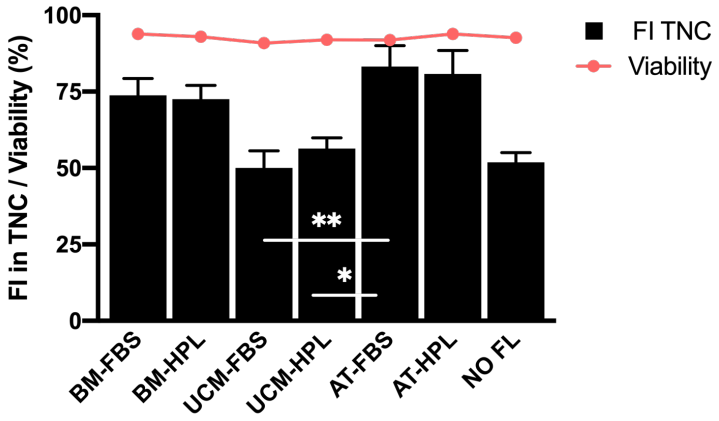

Figure II.6. *Viability and fold increase in total nucleated cells of expanded umbilical cord blood-derived hematopoietic stem/progenitor cells after 7 days of co-culture with mesenchymal stromal cells from different sources. AT: adipose tissue; BM: bone marrow; FBS: fetal bovine serum; FI: fold increase; FL: feeder layer; HPL: human platelet lysate; TNC: total nucleated cells; UCM: umbilical cord matrix. Values are presented as mean±SEM (n=3 for all conditions, with exception of 'NO FL': n=2). **: p<0.01; *: p<0.05.*

II.4.2.2. Impact of the tissue source of MSC and xenogeneic-free culture conditions for the establishment of the FL on the differentiative potential of UCB expanded cells

Through immunophenotypic characterization of the expanded and non-expanded UCB-derived $CD34^+$-enriched cells, different dynamics were observed according to the culture medium in which MSC FL had been previously established (Fig. II.7). At day 7, a $CD34^+$ cell population was maintained in culture, which varied between 30.4 and 69.1% for the co-cultures, with the negative control (NO FL) presenting a population of 43.7±7.0%. Regarding this $CD34^+$ cell population, not only differences between the distinct MSC sources were observed, but also between MSC-FBS and MSC-HPL FL within the same source, with the former presenting a higher $CD34^+$ cell content: 69.1±2.3% (BM-FBS) *vs* 56.2±0.8% (BM-HPL) ($p<0.05$); 45.4±2.9% (UCM-FBS) *vs* 30.4±3.2% (UCM-HPL) ($p<0.01$); 68.6±0.9% (AT-FBS) *vs* 56.1±2.2% (AT-HPL) ($p=0.056$) (Fig. II.8A). In order to highlight the differences observed in what concerns CD34

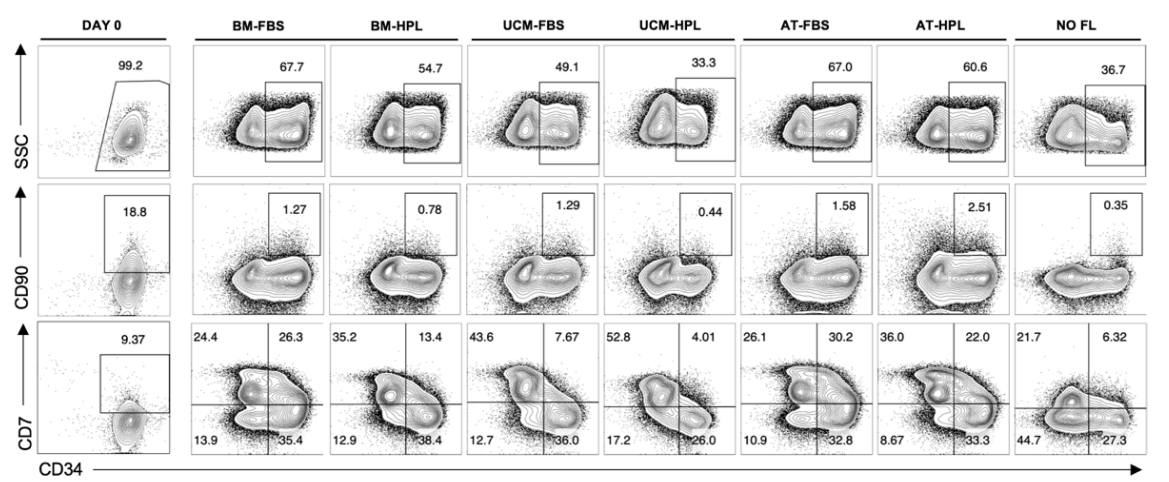

Figure II.7. *Representative immunophenotypic profile of hematopoietic stem/progenitor cells before and after a 7-day expansion in a co-culture system with mesenchymal stromal cells from three different sources (bone marrow, umbilical cord matrix and adipose tissue). Populations are gated on live cells. AT: adipose tissue; BM: bone marrow; FBS: fetal bovine serum; FL: feeder layer; HPL: human platelet lysate; SSC: side scatter; UCM: umbilical cord matrix.*

expression by the expanded UCB in the different culture conditions, we performed a histogram overlay analysis (Fig. II.9A). For all conditions tested, two peaks can be observed: one corresponding to $CD34^+$ cells (positive peak) and the other to $CD34^-$ cells (negative peak). The positive peak (i.e., $CD34^+$ cells) is notably higher and more pronounced for the conditions where BM-FBS and AT-FBS FL were used. For UCB cells expanded in BM-HPL and AT-HPL conditions, the positive peak is not as high or intense as observed for the FBS conditions. Concerning the UCB cells expanded with a FL of UCM MSC, the positive peak is the smallest of all co-cultures, being smaller and less intense for the UCM-HPL condition than the UCM-FBS condition, resembling the behavior observed with HSPC expanded under feeder-free conditions (NO FL). In what concerns the more primitive stem/progenitor content of the UCB HSPC (i.e., $CD34^+CD90^+$ cells), after culture, the immunophenotypic analysis showed that while BM and AT FL were able to maintain a similar percentage of this specific subpopulation of more primitive UCB HSPC, the UCM FL seems to have yielded a smaller percentage. Nonetheless, for all MSC sources studied, the percentage of this subpopulation showed a tendency to be inferior when MSC-HPL were used in the co-culture system: 3.2±1.7% (BM-FBS) *vs* 2.0±1.0% (BM-HPL); 2.9±1.1% (AT-FBS) *vs* 2.3±0.6% (AT-HPL); 1.5±0.3% (UCM-FBS) *vs* 0.9±0.3% (UCM-HPL); 0.6±0.3% (NO FL). For the proT cell subpopulation (i.e., $CD34^+CD7^+$ cells), the immunophenotypic analysis showed the same pattern observed in the subpopulation containing more primitive cells. Of notice, the difference between HPL and FBS conditions is also evident for the proT cell subpopulation, as UCB HSPC that were co-cultured with BM-FBS resulted in an increase of more than 50% on the expression of both CD34 and CD7 markers, when compared to BM-HPL: 32.1±2.9%

vs 19.3±3.2% ($p<0.01$). Co-cultures using the other MSC sources followed the same tendency: 33.4±4.2% (AT-FBS) *vs* 20.2±1.0% (AT-HPL); 8.9±0.7% (UCM-FBS) *vs* 4.1±0.9% (UCM-HPL); 10.1±3.8% (NO FL) (Fig. II.8A; Fig. II.9B). Expansion levels of the aforementioned subpopulations ($CD34^+$, $CD34^+CD90^+$ and $CD34^+CD7^+$), expressed as FI, followed the tendency observed for cell population content (in percentage) (Fig. II.8B).

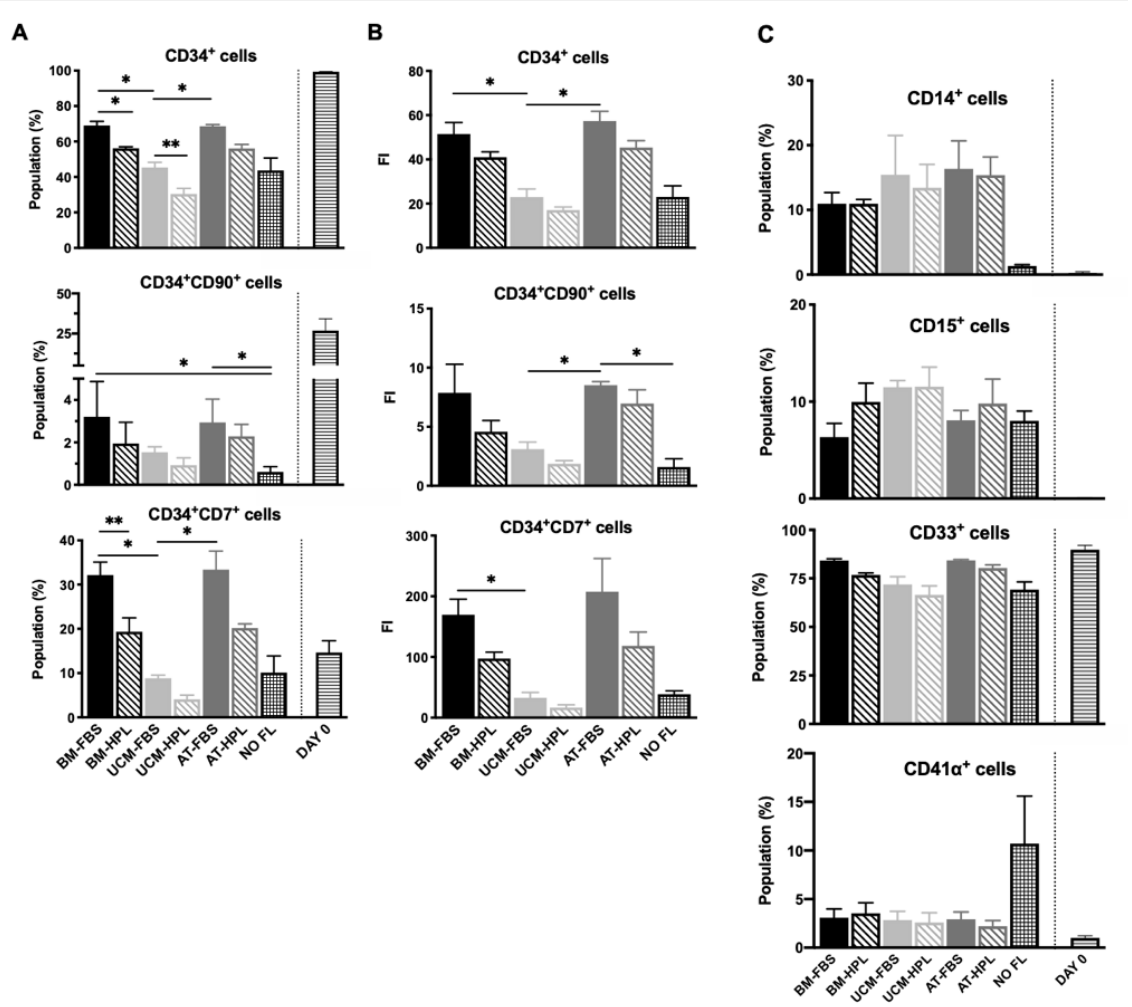

Figure II.8. Quantitative characterization of the hematopoietic stem/progenitor cell populations after a 7-day expansion in a co-culture system with mesenchymal stromal cells from different sources. **(A)** *Percentage of hematopoietic stem/progenitor ($CD34^+$ cells), more primitive ($CD34^+CD90^+$) and progenitor T cells ($CD34^+CD7^+$) before and after expansion.* **(B)** *Fold increase of hematopoietic stem/progenitor ($CD34^+$ cells), more primitive ($CD34^+CD90^+$) and progenitor T cells ($CD34^+CD7^+$) after expansion.* **(C)** *Percentage of cell populations with myeloid potential before and after expansion. AT: adipose tissue; BM: bone marrow; FBS: fetal bovine serum; FI: fold increase; FL: feeder layer; HPL: human platelet lysate; UCM: umbilical cord matrix. Values are presented as mean±SEM (n=3 for all conditions, with exception of 'NO FL': n=2). **: $p<0.01$; *: $p<0.05$ (statistical significance is only showed for FBS conditions).*

In all cultures, the differentiative potential of the expanded UCB cells was mainly shifted towards the myeloid lineage (Fig. II.8C). A high expression of CD33, a myeloid-specific receptor, was observed on non-expanded cells (day 0), but also on expanded cells regardless of the MSC source used in the co-culture system, as well as on the control without FL. Nonetheless, UCB cells expanded over MSC-HPL seem to show a slight decrease of this marker compared to MSC-FBS conditions. $CD14^+$ cells (monocytic potential) were also present on day 7 (11.0-16.4%), without any obvious differences between UCB cells expanded over MSC-FBS or MSC-HPL within each MSC source. On the other hand, UCB cells expanded without FL showed a residual population with monocytic potential (1.3±0.2%). Conversely, hematopoietic cells expanded under feeder-free conditions (NO FL) displayed a considerable population (10.7±4.9%) of $CD41\alpha^+$ cells (megakaryocytic potential) whereas the $CD41\alpha^+$ population varied between 2.2-3.5% in the co-cultures. $CD15^+$ cells (granulocytic potential) were also present among the expanded UCB cells and its percentage varied according to the MSC source used to establish the FL (6.3-11.5%), with no evident influence of culture medium used; UCB cells expanded under feeder-free conditions (control) comprised a population of 8.0±1.0% $CD15^+$ cells.

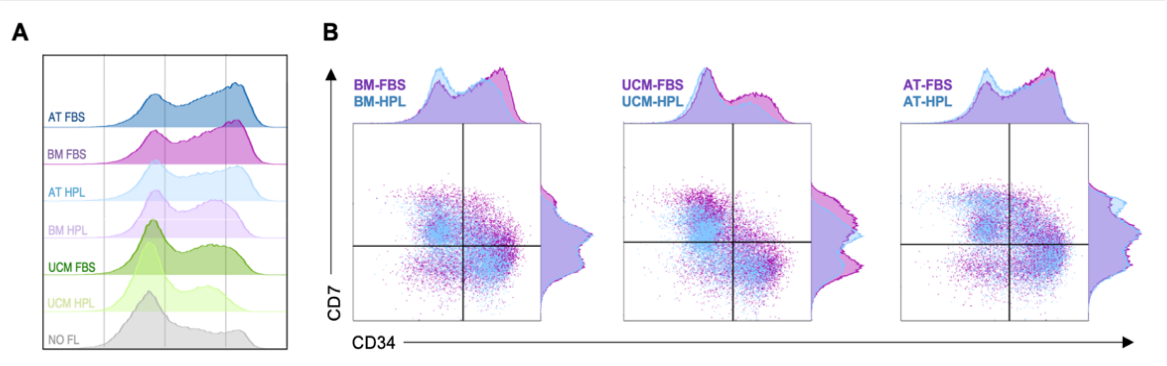

Figure II.9. *Comparison of CD34 and CD34/CD7 expression by expanded umbilical cord blood cells after 7 days of co-culture with mesenchymal stromal cells from different sources previously established using different medium supplementation (fetal bovine serum or human platelet lysate).* ***(A)*** *Histogram overlay of CD34 expression by expanded umbilical cord blood (UCB) cells co-cultured with mesenchymal stromal cells (MSC) feeder layers from different tissue sources that were previously established with fetal bovine serum (FBS)- or human platelet lysate (HPL)-supplemented medium (representative UCB donor).* ***(B)*** *Dot plot overlay of CD34 and CD7 co-expression by expanded UCB cells co-cultured with MSC feeder layers from the same tissue source that were previously established with FBS- or HPL-supplemented medium (representative UCB donor). AT: adipose tissue; BM: bone marrow; FL: feeder layer; UCM: umbilical cord matrix.*

II.4.2.3. UCB expanded cells maintain their clonogenic potential regardless of the MSC tissue source and culture conditions

Besides immunophenotyping, we performed two different assays to identify the presence of primitive cells and the clonogenic potential of the progenitor cells: the cobblestone area-forming cells (CAFC) assay and the colony-forming unit (CFU) assay, respectively. By using our co-culture expansion system, we verified that, regardless of the MSC source used to expand the UCB cells, all of them allowed a FI in the number of CAFC of expanded UCB cells (Fig. II.10A). There seemed to a be a tendency for a FL of BM or AT MSC to allow for a slight increase in the FI, as the mean ranged from 3.4 to 6.3, while the mean FI of CAFC of the expanded cells ranged between 2.4-3.1 when a FL of UCM MSC was used. However, no statistical significance was found among MSC sources. UCB cells expanded without a FL (NO FL) presented the smallest mean FI of CAFC (1.1±1.1).

In what concerns the clonogenic potential, assessed through the CFU assay, as expected, the number of total CFU obtained per 10^5 HSPC was superior for UCB cells before expansion, on day 0 ($2.5x10^4 \pm 1.0x10^3$), than after expansion (Fig. II.10B). After the 7-day expansion in the co-culture system, even though the CFU values obtained with BM-MSC and UCM-MSC slightly differed between them, overall, the number of total CFU was similar for UCB cells expanded in any of the MSC sources, ranging from $1.2x10^4 \pm 1.9x10^3$ (UCM-HPL condition) to $1.5x10^4 \pm 1.2x10^3$ (BM-FBS condition). The culture medium in which MSC were established did not seem to have impact on the CFU total number produced by the UCB cells. Although with no statistical significance, cells expanded without a MSC FL (NO FL) showed an increasing trend in total CFU numbers ($1.6x10^4 \pm 2.5x10^3$) compared to the ones expanded with a MSC FL. We also looked in detail to the type of CFU produced (Fig. II.10C), namely erythroid burst-forming unit (BFU-E), colony forming unit granulocyte-monocyte (CFU-GM) or multilineage colony forming unit (CFU-Mix). For non-expanded cells (UCB cells on day 0), we verified that half of the colonies presented were committed to the myeloid lineage, as 51.5±0.5% of the colonies were CFU-GM, but there was also some erythroid potential, seen not only by the percentage of BFU-E (4.0±0.7%) but also CFU-Mix (44.5±0.5%). For the UCB cells expanded in a co-culture system, regardless of the MSC source used, we observed a shift in the type of colonies produced, as the great majority (>70%) were CFU-GM colonies. The erythroid potential was reduced, as less than 1% of the colonies were BFU-E, with the remaining colonies being CFU-Mix. Interestingly, for the conditions where UCB cells were expanded with MSC-HPL, the percentage of CFU-GM colonies showed a tendency to be slightly greater when compared with MSC-FBS conditions: 83.8±4,1% (BM-HPL) *vs* 75.1±4.1% (BM-FBS) and 84.2±5,5% (AT-HPL) *vs* 79.6±4.1% (AT-FBS). For the UCM MSC source, similar results were found 85.7±4,1% (UCM-HPL) *vs* 84.5±3.0% (UCM-FBS). Of notice, UCB cells that were expanded with NO

FL presented percentages of CFU-GM and CFU-Mix very similar to the non-expanded cells on day 0, with a reduction in the percentage of BFU-E.

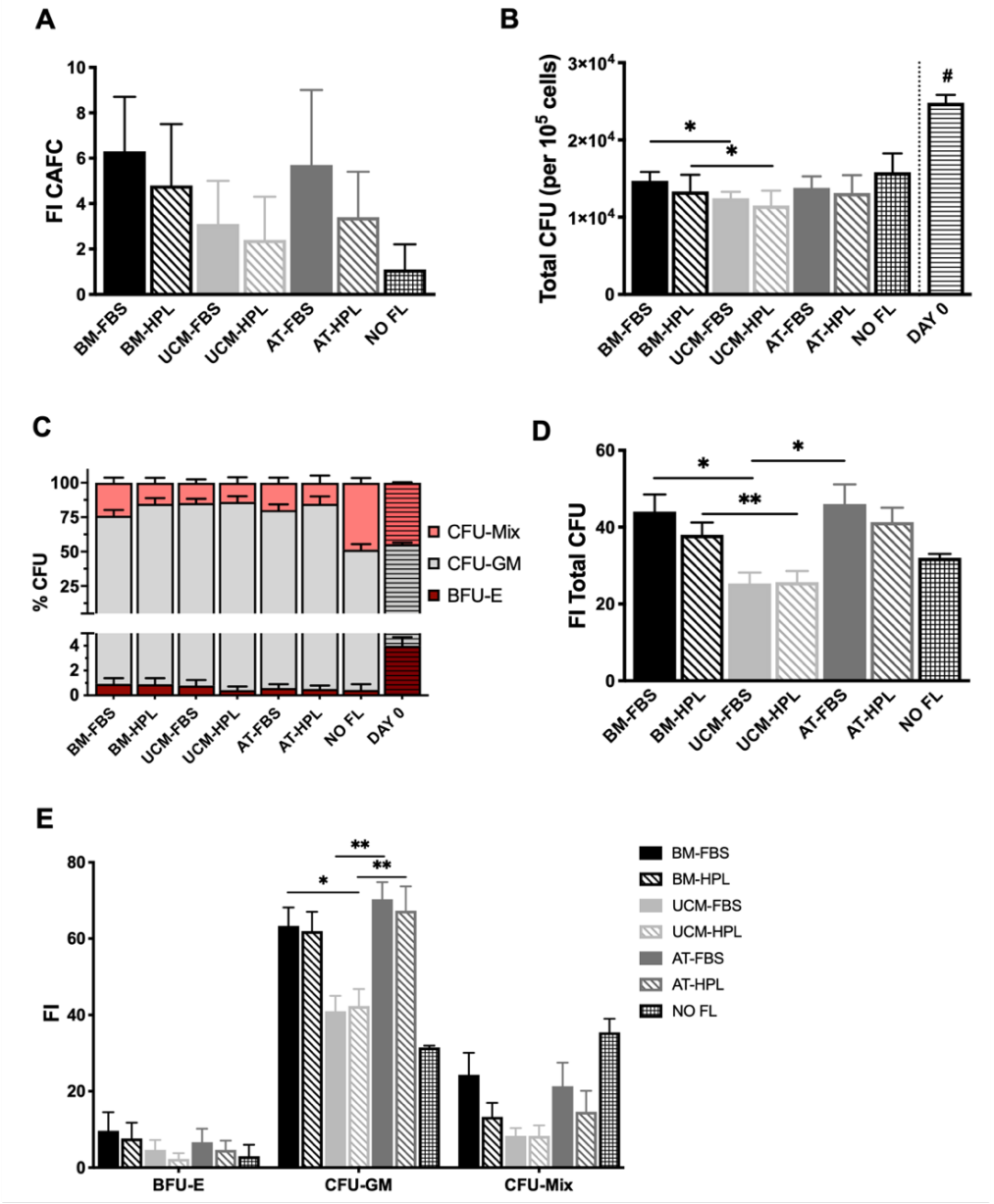

Figure II.10. Cobblestone area-forming cells and colony-forming units produced by hematopoietic stem/progenitor cells before and after a 7-day expansion in a co-culture system with mesenchymal stromal cells from different sources. ***(A)*** *Fold increase (FI) of cobblestone area-forming cells (CAFC).* ***(B)*** *Total colony-forming unit (CFU) obtained per 10^5 cells.* ***(C)*** *Percentage of each CFU type (BFU-E, CFU-GM, CFU-Mix) produced.* ***(D)*** *FI of total CFU.* ***(E)*** *FI of each CFU type (BFU-E, CFU-GM, CFU-Mix). AT: adipose tissue; BFU-E: erythroid burst-forming unit; BM: bone marrow; CFU-GM: colony forming unit granulocyte-monocyte; CFU-Mix: multilineage colony forming unit; FBS: fetal bovine serum; FL: feeder layer; HPL: human platelet lysate; UCM: umbilical cord matrix. Values are presented as mean±SEM (n=3 for all conditions, with exception of 'NO FL': n=2). **: p<0.01; *: p<0.05; #: p<0.01 vs BM-FBS, UCM-FBS, UCM-HPL, AT-FBS and p<0.05 vs BM-HPL, AT-HPL.*

In terms of FI of total CFU, which considers the aforementioned results and the expansion potential of our expansion systems, we verified that it follows the pattern observed for FI in TNC (Fig. II.6). Specifically, UCB cells expanded over a FL of BM or AT MSC presented the highest FI in total CFU (~40x), while the results obtained with a FL of UCM MSC were significantly lower (~25x). No significant differences were observed regarding the establishment of the MSC sources with FBS- or HPL-supplementation (Fig. II.10D). The influence of the MSC source on the expansion potential of UCB cells in what concerns each CFU type (BFU-E, CFU-GM, CFU-Mix) obtained was also explored (Fig. II.10E). In co-cultures with MSC, the highest FI was observed for the CFU-GM, followed by the CFU-Mix and lastly the BFU-E. Although with small differences, BM and AT MSC FL resulted in similar FI of each CFU type for the expanded UCB cells, higher than the ones obtained with UCM MSC. Concerning the culture medium used in the MSC expansion, no influence in the FI of each CFU type seems to exist. On the other hand, expansion of $CD34^+$-enriched cells without a MSC FL allowed for equivalent FI values for CFU-Mix and CFU-GM.

II.5. Discussion

The wide application of umbilical cord blood (UCB) hematopoietic stem/progenitor cells (HSPC) to treat malignant and non-malignant diseases in a hematological context, specifically adult patients, is hampered by the low cell quantity in a single unit. While great efforts are being made to overcome this hurdle, expanding UCB HSPC *ex-vivo* with the support of a bone marrow (BM) mesenchymal stromal cell (MSC) feeder layer (FL) is a clinically-relevant strategy. Indeed, in 2012, the results of a phase I/II clinical trial where 31 patients with hematologic cancers received transplants of two UCB units, one of which containing HSPC expanded *ex-vivo* in a co-culture system with BM MSC, were published[73]. Since transplantation of both UCB units proved to be safe and effective, significantly improving the engraftment compared to unmanipulated UCB only, the study moved to a phase III clinical trial. The study is now completed, but the results were not yet published (ClinicalTrials.gov Identifier: NCT01854567). Despite the encouragement and great advances that these clinical trials present to the field, they also mirror the need for optimization of these co-culture systems. Culture period is one of the parameters that should be optimized. By doing a 2-week expansion of the UCB cells in the co-culture system with MSC, at least one medium change over the first week is demanded, which entails a superior cost of reagents, time and handling. Our expansion protocol was designed to last one week without any medium changes or handling in between, reducing culture manipulation. Additionally, our expansion system, originally established with BM MSC, has its cytokine cocktail optimized for the

maximum expansion without compromising the maintenance of HSPC[107], reducing overall cost of goods. Concerning the two main outputs typically evaluated in the translation of an expansion protocol to a clinical trial, i.e., the fold increase (FI) of total nucleated cells (TNC) and $CD34^+$ cells, the authors were able to reach a FI of 12.2 in TNC, while the $CD34^+$ cell fraction had a FI of 30.1, after 14 days. In this study published by our lab, employing a BM MSC FL in co-culture with the UCB HSPC, we were able to obtain a FI of 73.8 and 51.5, respectively, after 7 days. This increase can easily be explained not only by our optimized co-culture system, but also due to the starting cell product: in this clinical trial[73] mononucleated UCB cells were used, while we started with a highly purified population of UCB $CD34^+$ cells.

In the aforementioned clinical trial, off-the-shelf BM-derived MSC isolated and expanded employing fetal bovine serum (FBS)-supplemented medium were used to prepare the FL for the co-culture system. However, MSC isolated from the BM present some disadvantages related to the source *per se*, since BM collection is a very invasive procedure that entails risks for the donors. In addition, BM collection is not done as frequently as peripheral blood (PB) stem cell mobilization and collection, thus decreasing the availability of this source. While the majority of hematopoietic co-culture studies use BM MSC derived from the iliac crest of the hip bone (from HSPC donors in a hematopoietic cell transplantation (HCT) context), BM samples can also be obtained from routine bone surgeries, namely from knee surgery. However, these medical interventions are normally associated with elderly patients, and it is well known that a decrease in MSC functionality, as well as in the number of subculturing steps (i.e., passages) they are able to withstand, is correlated with an increase in donor age[126]. Thus, although hematopoiesis occurs in the BM and from the physiological point of view the use of BM MSC would be the rational choice, alternative sources are required to ease clinical translation. In this context, there are other sources of MSC readily available, namely adipose tissue (AT) and umbilical cord matrix (UCM), which are commonly discarded as medical waste. Either of these MSC sources can be collected to isolate off-the-shelf MSC, in a similar way to what is done with BM-derived MSC. Direct comparison of MSC from different sources, namely BM, UCM and AT, have already been explored in different areas, such as treatment of graft-*vs*-host disease (GVHD)[127] and immune cell suppression capacity[128]. However, to our best knowledge, no study has performed a comprehensive comparison of the hematopoietic support provided by different sources of MSC to an enriched population of UCB HSPC.

The preliminary study performed herein, in agreement with previous work from our lab[66], suggested that the use of BM-derived MSC favors the expansion/maintenance of $CD34^+$ cell populations in a co-culture setting, in particular an interesting subpopulation with lymphoid potential. Thus, we sought to directly compare how three different tissue sources of MSC – BM, UCM and AT – influence the expansion of UCB-derived $CD34^+$

cells. This highly-enriched population was isolated from cryopreserved mononuclear cells (MNC) of UCB samples. By using cryopreserved samples, our rationale was replicating what is nowadays commonly performed in a clinical setting, since UCB transplants are routinely performed with cryopreserved UCB units. Moreover, since the goal is to create an expansion product that can surpass the cell number issue of a single unit, studies than can achieve so by using cryopreserved samples are closer to reality. Additionally, we went further by exploring a serum-free (SF)/xenogeneic-free (XF) co-culture system, i.e., we compared the expansion capacity and cell profile of expanded UCB cells over a MSC FL previously established using either FBS or fibrinogen-depleted human platelet lysate (HPL).

By using a FL of MSC that were previously expanded in culture medium supplemented with FBS (BM-FBS, UCM-FBS, AT-FBS) in our co-culture systems, we were able to verify that, after seven days of expansion, a FI TNC of more than 70 or 80 for BM and AT, respectively, was achieved. Although one could speculate that the tendency for a higher expansion capacity obtained with AT would be accompanied by a loss of hematopoietic progenitors, the immunophenotypic analysis showed the maintenance of a high population (>65%) of hematopoietic progenitors ($CD34^+$ cells) for both BM and AT sources. Concerning the fraction of expanded hematopoietic cells that suffered a loss of their CD34 expression, a shift towards the myeloid lineage was primarily observed (i.e., expression of CD14, CD15, CD33 and CD41α), as previously described by our group [68]. This behavior was substantiated by a higher percentage of CFU-GM in the co-culture system, regardless of the MSC FL source used. The absence of a FL during *ex-vivo* expansion originated similar percentages of CFU-Mix and CFU-GM. This disparity regarding different CFU populations between expansion systems with and without a MSC FL has been previously observed by our group[107]. Interestingly, a small population that contains more primitive cells ($CD34^+CD90^+$ cells)[129] was also kept in both BM-FBS and AT-FBS conditions, which is aligned with the tendency for higher CAFC-producing capacity observed for these conditions. The CAFC assay is a variant of the long-term culture-initiating cells (LTC-IC) assay that does not require cell replating. In our study, it was used to characterize the more primitive compartment of our expanded HSPC population, as this *in vitro* assay has been proposed as a valid surrogate measurement of hematopoietic reconstitution potential[130]. Our expansion protocol also expanded a particular subpopulation of progenitors that co-express CD34 and CD7, classically defined as proT cells, i.e., progenitor cells with ability to homing the thymus and differentiate into T cells[131]. The expansion of this particular subpopulation is very promising, because not only the myeloid progenitors are being expanded in our co-culture system (as in most *ex-vivo* expansion protocols), but also these precursors of the lymphoid lineage, which are candidates for adoptive T-cell therapies[132]. Also, the significant presence of proT cells in our expanded population pool will contribute

towards improving the recovery of a potential HCT patient, who inevitably is immunocompromised after treatment. An expanded product with such progenitors capable of a faster lymphopoiesis is critical to reduce HCT-related mortality[133,134]. Both BM-FBS and AT-FBS FL allowed a doubling in percentage for this particular UCB cell population after the expansion protocol. Importantly, and as seen in our previous work of 2010[68], the presence of a MSC FL showed to be essential for the expansion of proT cells, as in the feeder-free system the percentage of this population was inferior to non-expanded cells. Of note, a population of $CD34^{-}CD7^{+}$ cells was also present and expanded using any of the MSC FL. While this expanded population can be differentiated into natural killer and dendritic cells[135] that can be used in cellular immunotherapy, a small percentage of this population has been reported to be able to engraft the thymus *in vivo*[131], resulting in a broader redefinition of proT cells and suggesting that this population in our expansion system can also be of interest. On the other hand, the use of UCM-FBS FL resulted in a lower FI TNC (50) that was also accompanied by a decrease in the progenitor populations seen through $CD34^{+}$ expression (<50%). Understandably, this decrease in the progenitor populations is also reflected on specific subpopulations, such as proT cells. Although present, the percentage of this population was smaller than before expansion. Compared to the adult sources, UCM MSC appear to provide less hematopoietic support in the conditions of our study, shown by the reduced expansion capacity and also progenitor population maintenance. Of notice, UCM MSC FL were subjected to a higher Mitomycin-C concentration in their growth-arrest treatment compared to their adult counterparts (5 *vs* 0.5 µg/mL) due to the higher *in vitro* proliferation capacity of these cells[115]. Mitomycin-C has been commonly employed to inhibit MSC proliferation, as an alternative to irradiation, for multiple assays (e.g., immunomodulatory[136–138], FL for embryonic stem cells[139], induced pluripotent stem cells[140], as well as for HSPC[141,142]), and the concentration used varies in a 0.5-50 µg/mL range. Importantly, it has been previously acknowledged that different cells might present an intrinsic sensitivity to this chemoterapeutic and thus a dose-response curve to this agent has to be established for each cell type of interest[143]. In this context, a previous study demonstrated the higher efficiency of using Mitomycin-C concentrations of 4-8 µg/mL compared to a 0-2 µg/mL range to growth-arrest human UCM MSC *in vitro*[124]. Although a possible influence of Mitomycin-C cannot be ruled out, the lower performance of UCM MSC FL in supporting UCB HSPC observed in our study follows the trend present in the field. Other groups have demonstrated an inferior hematopoietic support associated with UCM MSC FL, which was shown using Mitomycin-C-treated[141,142], irradiated[144] and non-inactivated[145] FL.

Despite the fact that MSC have been mostly cultured with FBS-containing media in clinical trials, the risks associated with the usage of this culture medium supplement are

well known, namely the risk of xeno-immunization against bovine antigens and the transmission of pathogens. Ethical issues associated with FBS collection, limited availability and batch-to-batch variability are also concerns to be considered[119]. In the 1980s, HPL successfully started to be used as an alternative to FBS in the culture of several cell lines and is currently used in the manufacturing of MSC for clinical trials[146,147]. This supplement is rich in potent bioactive mediators, including various chemokines and growth factors[148]. Current HPL formulations are fibrinogen-depleted (not requiring supplementation with porcine heparin) and can be gamma irradiated to reduce pathogen content, which highly reduces the risk of transmission of human diseases by known or unknown viruses or prions. In an attempt to make a product more closely available for clinical purposes, we decided to also establish a MSC FL expanded without the use of animal derived components, by using medium supplemented with fibrinogen-depleted HPL. Interestingly, we noticed that the expansion capacity of HSPC was not affected by the change of MSC expansion medium, as the FI TNC was similar for both FBS and HPL conditions within each source. However, a significant decrease in the percentage of $CD34^+$ cells between FBS/HPL conditions within each MSC source was observed for all MSC sources, suggesting a shift from hematopoietic progenitors to more differentiated cells when MSC were expanded with HPL. It is worth mentioning that all differences observed resulted from an adaptation process, as MSC had been isolated with medium supplemented with FBS and first expanded with this medium. Interestingly, previous studies have reported that although HPL-supplemented medium improved the proliferation capacity of MSC in expansion, their immunosuppressive properties were inhibited in comparison to MSC expanded with FBS-supplemented medium. Namely, MSC expanded with fibrinogen-rich HPL showed a reduced capacity to prevent T- and NK-cell proliferation[149,150]. Importantly, another study has shown that fibrinogen depletion from HPL can partially restore MSC immunomodulatory capacities[151]. Here, we could verify that the hematopoietic support provided by MSC can be modulated by the environment in which MSC grow and the source itself is not the only important factor. Considering our results and the absence of comparative studies concerning the hematopoietic supportive capacity of MSC cultured with HPL, further experiments are needed.

Few studies exploring the hematopoietic support given by a FL of AT MSC exist. Without using exogenous cytokines, comparable levels of UCB HSPC expansion were attained when using a BM MSC FL or an AT MSC FL. Curiously, $CD7^+$ cell percentage was significantly higher using the AT FL, while the $CD34^+$ cell percentage was significantly enhanced using a BM FL[112]. Compared to BM MSC FL, a FL of AT MSC, either from mice or human, favored granulocyte differentiation from PB stem cells ($CD34^+$ cells) and the growth of progenitor cells *in vitro* to a higher extent. It was suggested that this better support could be attributed to chemokine CXCL12, a critical

regulator of hematopoiesis, found to be expressed three-fold higher in AT MSC than BM MSC[152,153], even though less than 1% of genes were found to be differentially expressed between AT and BM MSC[154]. By seeding UCB MNC upon an AT MSC FL and making successive removals of non-adherent cells, Andreeva and colleagues[155] were able to verify that AT MSC enabled the selection of functionally active $CD34^+$ HSPC at normoxia (20% O_2) and hypoxia levels (5% O_2) after seven days of expansion. Even though they used an interesting strategy to enrich $CD34^+$ cells during culture, their expansion levels were quite low (6-10x) compared to our FI of $CD34^+$ cells (60x), which can easily be explained by their lack of exogenous cytokines besides using an expansion system that still relies on FBS usage.

UCM MSC, namely Wharton's jelly MSC, have also been studied concerning hematopoietic support to UCB $CD34^+$ cells. In order to simulate the growth of HSPC *in vivo*, Zhao and collaborators[116] studied the influence of oxygen percentage in the co-culture system without adding any cytokines, finding out that normoxia values enhanced FI of TNC (3x), $CD34^+$ cells and CFU. Although hypoxia levels of 1% O_2 did not allow the expansion of TNC, they were able to maintain a higher percentage of $CD34^+$ cells. By changing the expansion medium from H5100 medium to StemSpan medium supplemented with SCF, FLT3-L, and TPO cytokines, this group attained a higher FI in TNC (>300x), as well as in $CD34^+$ cells (90x)[156]. Although similar to our co-culture system, we were able to maintain a higher percentage of $CD34^+$ cell population, despite the lower FI in this population. Nevertheless, these differences could be explained by their higher period of expansion (10 days). When Klein and colleagues[145] directly compared MSC from amnion, chorion and Wharton's jelly to BM MSC, they verified that a FL of the latter source was significantly superior in expanding UCB $CD34^+$ cells. Although their approach was different, as they started the expansion with unfractioned MNC cultured in medium supplemented with FBS over 14 days, BM MSC were shown to be a better source over UCM MSC, which is coherent with our results.

Overall, HSPC *ex-vivo* expansion through co-culture with MSC can be influenced by multiple experimental variables. Whether by using different expansion media, oxygen levels or starting HSPC population, as well as usage of exogenous cytokines, the resulting expansion outcome will inevitably vary. While MSC donor variability could also be considered an important experimental parameter, its impact on the robustness of co-culture HSPC expansions can be controlled. Similar to the manufacturing model for Alofisel, an approved expanded AT MSC-based cell therapy, we expect that a cell bank produced from a single donor will be able to provide innumerous cell doses for MSC FL production. Additionally, by introducing AT as an alternative MSC source, donor availability for co-culture expansions will be significantly improved. Both these points will facilitate the definition of MSC donor acceptance criteria, contributing towards process standardization and current good manufacturing practices (cGMP) compliance.

Ultimately, by aiming at the production of clinical-grade expanded UCB HSPC, we envision exploring the scalability of the co-culture system using AT MSC to evaluate the feasibility of attaining numbers with clinical significance. Our co-culture system is currently limited to a two-dimensional (2D) surface and performed in static conditions. Translating the co-culture setting into a three-dimensional (3D) environment (e.g., using a scaffold for MSC anchorage) and developing a bioreactor to introduce a flow environment could help improve its scalability and overall viability in producing a potential approved cell-based product. At the same time, it would be important to investigate and clarify the differences and/or similarities behind the supportive hematopoietic capacity of each MSC source at a cellular level. If they could be tracked to individual cell features (e.g., MSC-derived soluble cytokines, extracellular vesicles, adhesion molecules, extracellular matrix molecules, or other[157]), we could potentiate their effect by bioengineering it in a novel expansion system.

III. Exploiting the artificial thymic organoid system to support T cell differentiation from (expanded) umbilical cord blood hematopoietic stem/progenitor cells

III.1. Summary

T cells are essential players in the adaptive immune response. Shortage of mature T cells in umbilical cord blood (UCB) units delays their activity after transplantation, leaving patients vulnerable to opportunistic infections. Since donor lymphocyte infusions are unavailable for unmanipulated UCB, patients receiving these grafts have no adoptive therapy options based on T cells. Given their importance, *in vitro* T cell differentiation has been pursued, though challenging to attain. This is mainly due to their dependence on a three-dimensional organization combined with Notch signaling. By mixing hematopoietic/stem progenitor cells (HSPC) and MS5 cells ectopically expressing a Delta ligand, artificial thymic organoids (ATOs) emerged as an interesting serum-free approach that allowed differentiation of mature $CD8^+$ T cells after a few weeks in culture. In this chapter, we established and verified the robustness of the ATOs system for differentiating UCB-derived HSPC into $CD8^+$ T cells. Moreover, its potential to differentiate T cells was further explored by establishing ATOs with HSPC that had been previously expanded using our co-culture system, as these cells showed to possess enhanced lymphoid potential. Remarkably, after 5 weeks, ATOs established with HSPC previously expanded over mesenchymal stromal cells allowed a 5-fold increase in the percentage of $CD3^+TCR\alpha\beta^+$ T cell population as well as in terms of absolute numbers of mature $CD8^+$ T cells, in comparison with ATOs established with fresh isolated umbilical cord blood-derived HSPC.

III.2. Background

In humans, as in all vertebrates, adaptive immunity provides protection against infection, invading pathogens and tumor cells. T cells play a major role due to a particular feature, the T cell receptor (TCR), which is different for each T cell and specific for a given antigen. T cells are also responsible for maintaining immunological memory and self-tolerance[75]. Being a neonatal source, umbilical cord blood (UCB) is predominantly composed of naïve T cells[158]. Consequently, UCB transplant (UCBT) recipients are faced with increased immunological vulnerability. The absence of donor lymphocyte infusions (DLI) for UCBT patients makes it harder to cover those needs. However, by taking advantage of another important cell population enriched in UCB (i.e., hematopoietic stem/progenitor cells (HSPC)), T cells may be produced *in vitro*. During normal adult hematopoiesis, T cells derive from HSPC that reside in the bone marrow (BM). However, T cells require the specific microenvironment of the thymus to develop, in contrast with other hematopoietic lineages that fully differentiate within the BM[159]. Thus, after leaving the BM and through circulation, BM-derived progenitors with

lymphoid potential seed the thymus where they complete their maturation and differentiation process. This thymic dependence is related to the thymus three-dimensional (3D) organization, comprised by an ordered architecture of thymic stromal cells (TSC) of mesenchymal and epithelial origin. As developing thymocytes migrate through supporting TSC, the 3D microarchitecture maximizes connections between them, which is essential for both cell type survival. The maturation process is mediated by thymic epithelial cells (TEC), through Notch signaling, until thymocytes reach a double positive (DP) stage ($CD4^+CD8^+$). DP cells are then subjected to a selection process, originating CD4 or CD8 single positive (SP) T cells. At last, $CD4^+$ and $CD8^+$ T cells exit the thymus to circulation, exhibiting a naïve phenotype.

Given the essential role of 3D thymic organization for thymopoiesis, the first *in vitro* models that generated T cells recreated this architecture by doing organ cultures of embryonic thymic lobes, i.e., the fetal thymic organ culture (FTOC) technique[160]. By adding deoxyguanosine (dGuo) to the culture, all thymocytes were virtually depleted while the stroma was spared[161]. Cellular interactions needed for T-cell development were further investigated through the reaggregate thymic organ culture (RTOC) technique, which combined the dGuo treatment with an enzymatic dissociation to isolate surviving TSC. A mixture of thymocytes and TSC were then centrifuged, with the resulting cell aggregate resembling a thymic lobe. Importantly, by mixing cellular components from different genetic backgrounds, the RTOC technique allowed interactions between major histocompatibility complex (MHC) molecules and TCR to be explored during thymocyte selection[162]. On the other hand, two-dimensional (2D) monolayer cultures of TSC failed to support T lymphopoiesis. TSC inability to support T cell development was due to the incapacity of maintaining Notch ligands expression, Delta-like (DLL) 1 and DLL4, in 2D systems[159]. The OP9-DLL1 system establishment was therefore a breakthrough regarding *in vitro* models for T cell generation, as it made possible to generate T cells on a monolayer, outside thymic tissue[163]. In this system, OP9 cells (a mouse BM-derived stromal cell line) were transduced to ectopically express a Notch ligand, being OP9-DLL1 the cell line most used. They were used as a feeder layer to HSPC, in a co-culture system, where HSPC progressively developed into the different stages of T lymphopoiesis, culminating in the differentiation of mature $CD8^+$ T cells. Even though this system does not depend on thymic tissue availability, T cell differentiation is highly dependent on the fetal bovine serum (FBS) lot used. It is also time consuming and inefficient, as it takes 60-70 days to attain 2-4% of mature $CD8^+$ T cells[164].

In 2017, artificial thymic organoids (ATOs) emerged as an alternative system[165] that recovered the 3D dynamic, in a similar way to the RTOC technique. This system relies on mixing and compacting two cell types through centrifugation, resulting in a 3D-like structure. HSPC from any source (umbilical cord blood (UCB), BM or peripheral blood)

are combined with MS5-hDLL1 cells, a mouse BM-derived stromal cell line transduced to express the human DLL1 (hDLL1). T cells differentiated in this system showed mature naïve phenotypes, a diverse TCR repertoire and TCR-dependent function, in a similar way to T cells found in the thymus. The production of T cells with antigen-specific cytotoxicity when TCR-engineered HSPC were used in the ATOs system is also described[165]. Later, this system was also used to differentiate mature conventional T cells from human induced pluripotent stem cells (iPSC)-derived embryonic mesodermal progenitors, using MS5-hDLL4[166].

In the present study, we established the ATOs system as a platform for differentiating UCB-derived HSPC into $CD8^+$ T cells. Specifically, UCB-derived HSPC were cultured as recommended and differentiation through the different stages of T lymphopoiesis was evaluated. We also took advantage of our UCB HSPC expansion knowledge, where enhanced lymphoid potential was observed when UCB cells were expanded in a co-culture setting with BM MSC, yielding a greater population of progenitor T cells ($CD34^+CD7^+$) (Chapter II). By establishing ATOs with cells that are more committed to the T cell lineage, we hypothesized that this approach could not only accelerate differentiation into mature T cells, but also enhance the cell yield. Hence, in the present study, we further explored the potential of ATOs to attain $CD8^+$ T cells by comparing expanded UCB HSPC *vs* freshly isolated $CD34^+$ cells as starting cell product.

III.3. Material and Methods

III.3.1. Maintenance and expansion of MS5-hDLL4 cells

A vial of MS5-hDLL4 cells was gently provided by Prof. Gay Crook's group (UCLA, United States of America (USA)). Upon arrival at our lab, cells were immediately thawed and washed using Dulbecco's Modified Eagle's Medium (DMEM) (Cat. #52100-039, Gibco, USA) supplemented with 20% (v/v) fetal bovine serum (FBS) (Cat. #10270106, Thermo Fisher Scientific, USA). Afterwards, cells were resuspended in DMEM supplemented with 10% (v/v) FBS (DMEM-10% FBS), counted and plated at a cell density of 3000 cells/cm^2 in T-flasks. They were maintained in a humidified atmosphere at 37°C and 5% CO_2. When 70-80% confluence was reached, cells were treated with 0.05% (v/v) trypsin (Cat. #15090-046, Gibco) and 1 mM ethylenediamine tetraacetic acid (EDTA) (Cat. #03690-100mL, Sigma-Aldrich, USA) in phosphate buffered saline (PBS) (Cat. #21600-044, Gibco), for 5 min at 37°C and 5% CO_2. After washing with DMEM-10% FBS, cells were passaged at the same cell density. All media used was supplemented with 1% (v/v) Antibiotic-Antimycotic (A/A) (Cat. #15240-062, Gibco).

III.3.2. Fluorescence-activated cell sorting (FACS) of MS5-hDLL4 brightest cells

Cells were resuspended in a PBS solution containing 2% (v/v) FBS (PBS-2% FBS), at a concentration of $3x10^6$ cells/mL. Both LIVE/DEAD (1:1000) (Cat. #L34974, Invitrogen, USA) and mouse anti-human DLL4 primary antibody (1:250) (Cat. #346502, BioLegend, USA) were added to the cell suspension. Cells were incubated for 30 min at 4°C, in the dark, and washed with 10 mL of PBS-2% FBS, at 350 *g* for 5 min. After resuspension with PBS-2% FBS, at a concentration of $3x10^6$ cells/mL, the goat anti-mouse IgG1 Alexa Fluor 488 secondary antibody (1:1000) (Cat. #A-2112, Invitrogen) was added to the cell suspension and incubated for 30 min at 4°C, in the dark. Cells were washed with 10 mL of PBS-2% FBS, at 350 *g* for 5 min, and resuspended with PBS-2% FBS supplemented with 1% A/A, at a concentration of $2x10^7$ cells/mL. Cells were kept in ice, in the dark, until cell sorting. Cell sorting of MS5-hDLL4 brightest cells was performed using a FACSAria IIu (Instituto Gulbenkian de Ciência (IGC), Lisboa). Cells were collected in DMEM supplemented with 50% FBS and 1% A/A and kept in ice. Afterwards, cells were counted and seeded as described in "III.3.1. Maintenance and expansion of MS5-hDLL4 cells". After one passage post-sorting, cells were cryopreserved using Recovery Cell Culture Freezing Medium (Cat. #12648-010, Gibco) and stored in a liquid/vapor phase nitrogen tank.

III.3.3. Generation of umbilical cord blood (UCB)-derived hematopoietic stem/progenitor cells (HSPC)

$CD34^+$ HSPC from UCB were isolated as previously described in "II.3.4. Enrichment for $CD34^+$ cells". When applicable, expanded UCB-derived $CD34^+$-enriched cells were attained as previously described in "II.3.5. *Ex-vivo* expansion of $CD34^+$-enriched cells". Cells were resuspended in R-B27 medium (preparation of this medium is described below in III.3.5. Preparation of ATOs complete medium), at $1\text{-}2x10^5$ cells/mL and kept on ice until generation of artificial thymic organoids (ATOs).

III.3.4. Isolation of thymocytes from human thymic fragments

Using a syringe plunger (10 mL syringe), a small thymic fragment (<1 cm) was mashed over a 70 µm cell strainer (Cat. #352350, Falcon, USA). After washing the strainer with RPMI 1640 supplemented with 10% (v/v) FBS, the cell suspension was collected to a tube. Following dilution with PBS, 10 mL of the cell suspension was carefully placed over a 5 mL Ficoll (Cat. #17544203, GE Healthcare, USA) layer, in a 15 mL tube. After density gradient centrifugation at 500 *g* for 30 min, thymocytes were collected to a new tube and washed with PBS at 500 *g* for 7 min. Following cell count, thymocytes were cryopreserved using Recovery Cell Culture Freezing Medium and stored in a liquid/vapor phase nitrogen tank.

III.3.5. Preparation of ATOs complete medium

ATOs complete medium was composed by RPMI 1640 medium (Cat. #21875034, Gibco) supplemented with 1% (v/v) Glutamax (Cat. #35050038, Gibco), 1% (v/v) A/A, 4% (v/v) B-27 supplement (Cat. #17504-044, Gibco), 30 µM ascorbic acid (L-Ascorbic acid 2-phosphate sesquimagnesium salt hydrate; Cat. #A8960-5G, Sigma-Aldrich), 5 ng/mL of recombinant human IL-7 (Cat. #200-07, PeproTech, USA) and 5 ng/mL of recombinant human Flt3-L (Cat. # AF-300-19, PeproTech).

The preparation of ATOs complete medium started with the preparation of R-B27 medium, i.e., RPMI 1640 supplemented with 1% (v/v) Glutamax, 1% (v/v) A/A, 4% (v/v) B-27 supplement (freshly thawed) and 30 µM ascorbic acid (freshly prepared). R-B27 medium was stable to be used within approximately 2 weeks, if stored at 4°C. ATOs complete medium was done when freshly thawed IL-7 and Flt3-L were added to a working volume of R-B27 medium.

III.3.6. Generation of ATOs

1.1 mL of ATOs complete medium was added to each well of a 6-well plate. Using tweezers, a 0.4 µm cell culture insert (Cat. #PICM0RG50, Merck, Germany) was placed inside each well, taking care that only the bottom of the insert membrane contacts the medium. The plate was left aside in the laminar flow hood until further use. MS5-hDLL4 cells were treated with 0.05% (v/v) trypsin and 1 mM EDTA in PBS solution, for 5 min at 37°C and 5% CO_2. Cells were washed with DMEM-10% FBS, passed through a 70 µm cell strainer (if cell agglomerates were visible), and centrifuged at 500 *g* for 7 min. Afterwards, cells were resuspended in R-B27 medium, counted and kept on ice until ATOs generation.

According to the number of ATOs to be generated (e.g., 1 ATO: 7 500 $CD34^+$ HSPC + 150 000 MS5-hDLL4$^+$ cells; 10 ATOs: 75 000 $CD34^+$ HSPC + 1 500 000 MS5-hDLL4$^+$ cells), the appropriate number of UCB $CD34^+$ HSPC (or expanded HSPC, when applicable) and MS5-hDLL4$^+$ cells were added to an 1.5 mL microcentrifuge tube, not exceeding a maximum of 12 ATOs per tube. The cell suspension was centrifuged at 300 *g*, for 5 min, using a swinging-bucket centrifuge. Following careful aspiration of the supernatant, the cell pellet was resuspended by briefly vortexing, using small pulses at low/medium velocity. The volume of the cell suspension was adjusted to be approximately 5 µL/ATO, by adding R-B27 medium.

Immediately before plating an ATO, the insert was removed from the medium (using tweezers) and placed in the borders between two adjacent wells, to remove medium excess. Using a 10 µL pipette tip, 5 µL of the cell suspension (i.e., 1 ATO) was gently released as a drop in the middle of the insert membrane, producing an ATO (resembling a small spherical dome). A maximum of 2 ATOs were plated in the same insert. In those cases, they were plated as close as possible to the insert center, separated by

approximately 1 cm. Using tweezers, the insert was placed back to the medium-containing well. Of note, medium should never directly contact the upper surface of the ATO. Once all ATOs for one plate were generated, the lid was placed back. ATOs were incubated for 5 weeks, in a humidified atmosphere at 37°C and 5% CO_2, with media change every 3-4 days.

III.3.7. Medium change of ATOs

To allow aspiration of the exhausted media, the plate was slightly tilted. Care was taken to not overspill media over the surface of the cell insert. Of note, during aspiration, approximately 100 µL was left underneath the cell insert to prevent it from drying. 1 mL of ATOs complete medium was added to the well, between the cell insert and the side of the well.

III.3.8. Harvesting cells from ATOs

1 mL of cold PBS supplemented with 0.5% (v/v) bovine serum albumin (Cat. #A8327-50ML, Sigma-Aldrich) and 2 mM EDTA (MACS buffer) was added to the surface of the cell culture insert, immersing ATOs. By pipetting up and down, ATOs were detached from the insert membrane and the hematopoietic cells were released to the medium. Of note, solid tissue "debris" that did not mechanically disrupt contained mostly stromal cells. The cell suspension was transferred to a tube, as well as the subsequent washes of the cell insert and well with cold MACS buffer. After passing through a 70 µm cell strainer to remove debris, cells were centrifuged at 350 *g* for 5 min and resuspended in the desired medium. After counting, cells were characterized by immunophenotyping.

III.3.9. Immunophenotypic characterization

After washing with PBS, the cell pellet was resuspended in 50 µL of PBS. Zombie Violet (1:1000) (Cat. #423113, BioLegend) was added and incubated for 10-15 min, in the dark. Without washing the cells, surface antibodies (Table III.1) were added and incubated for 15-20 min, in the dark. After washing the cells with 2 mL of FACS Buffer (PBS solution containing 2% (v/v) FBS and 0.1% (v/v) NaN_3 (Cat. #S2002-100G, Sigma-Aldrich)) at 350 *g* for 5 min, cells were resuspended in 150 µL of FACS Buffer. Until acquisition, cells were kept in ice, in the dark. Cells were acquired using a BD LSRFortessa X-20 flow cytometer (BD Biosciences, USA), at IGC, and data was analyzed using FlowJo v10 software (FlowJo LLC, USA).

Table 0.1. Panel of surface antibodies used.

Antigen	Fluorochrome	Clone	Brand	Cat #	1st Exp	2nd Exp
CD1α	PE	HI149	BioLegend	300106	X	X
CD5	PE-Cy7	UCHT2	BioLegend	300622	X	X
CD7	FITC	CD7-6B7	BioLegend	343104	X	X
CD34	PerCP-Cy5.5	8G12	BD Biosciences	347222	X	X
CD4	BV605	OKT4	BioLegend	317438	X	X
CD8	BV711	RPA-T8	BioLegend	301044	X	X
CD3	BV510	OKT3	BioLegend	317332	X	
CD3	BV510	UCHT1	BioLegend	300448		X
TCRβ^{ic}	APC	8A3 (βF1)	BD Pharmingen (USA)	566052	X	
TCRαβ	APC	IP26	BioLegend	306718		X

III.4. Results

III.4.1. Artificial thymic organoids (ATOs) were successfully established and maintained but with limited T cell differentiation

In order to successfully establish the ATOs system, a first study using a single donor of umbilical cord blood (UCB) was done. ATOs were established by mixing freshly isolated UCB-derived CD34$^+$-enriched cells and MS5-hDLL4 cells. Differentiation through the T cell lineage was followed for 5 weeks (Fig. III.1).

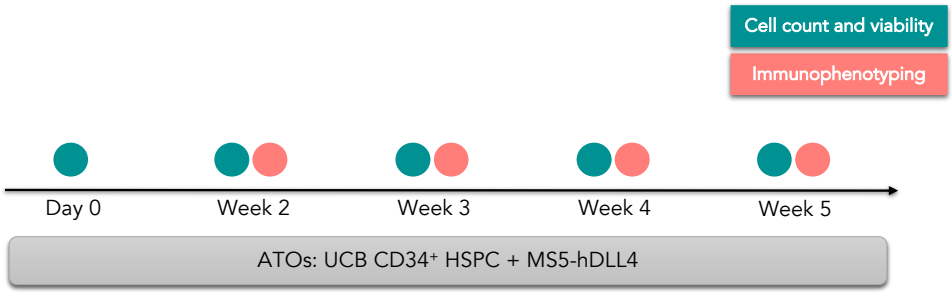

Figure 0.1. Schematic representation of the first study for the establishment of the artificial thymic organoids (ATOs) system. ATOs were established by mixing umbilical cord blood-derived hematopoietic stem/progenitor cells and MS5-hDLL4 cells and were cultured for five weeks. T cell lineage differentiation was evaluated through immunophenotyping. Cell count and viability were also determined. HSPC: hematopoietic/stem progenitor cells; UCB: umbilical cord blood.

A macroscopic evaluation of the ATOs integrity was done throughout the study (Fig. III.2). On day 0 they looked translucid (Fig. III.2A), but after some weeks they became more opaque and slightly bigger (Fig. III.2B), suggesting cell proliferation was occurring. This was confirmed through cell counting (Fig. III.3A), that revealed an increase in cell number between weeks 2 and 4. On week 4, a peak of 446 000 cells per ATO was reached, representing a fold increase (FI) in total cell number of 59. On week 5, a decrease of cell number was observed (350 000 cells/ATO) which was accompanied by a loss of viability (Fig. III.3B).

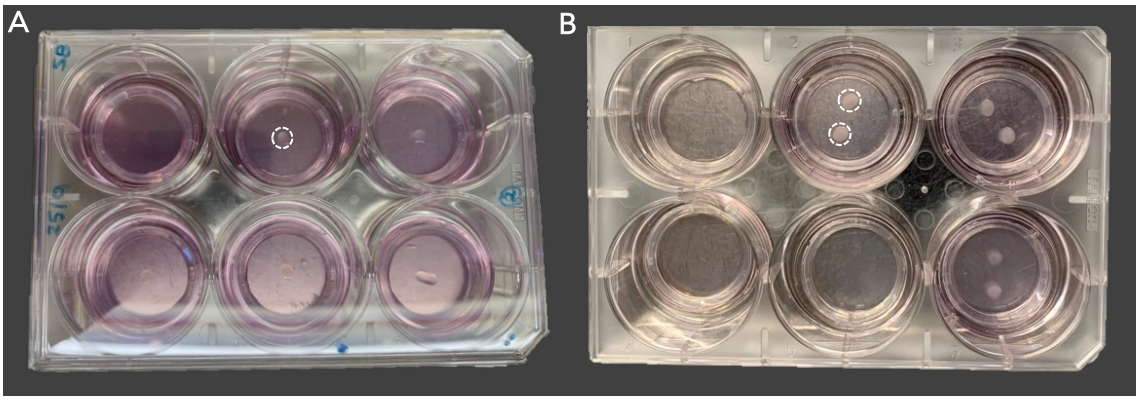

Figure 0.2. *Artificial thymic organoids (ATOs) on day 0* ***(A)*** *and on week 4* ***(B)****. Representative ATOs are depicted by white dashed circles.*

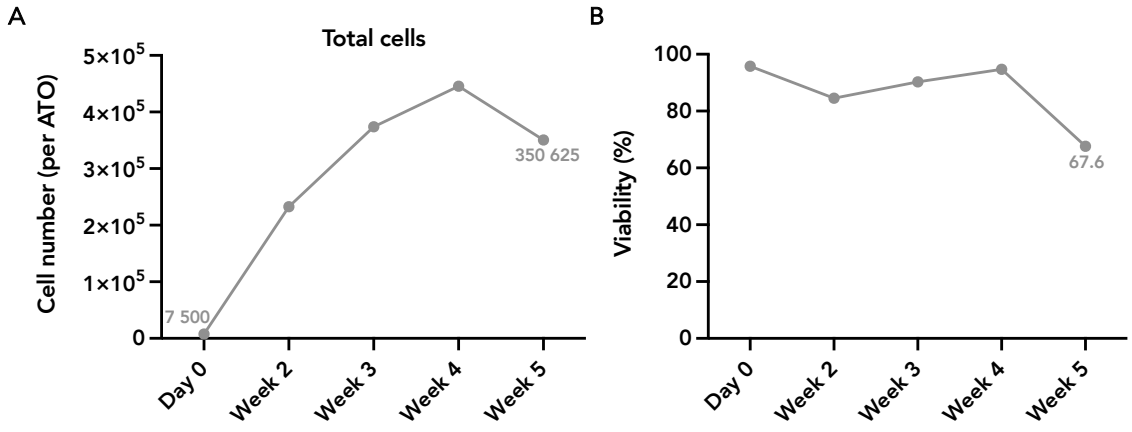

Figure 0.3. *Cell number and viability of umbilical cord blood-derived hematopoietic stem/progenitor cells used to establish artificial thymic organoids.* ***(A)*** *Total cell number.* ***(B)*** *Viability. ATO: artificial thymic organoid.*

At week 2, more than 60% of the cells were committed to the T cell lineage, as shown by the presence of $CD5^+CD7^+$ T lineage cells (Fig. III.4). Additionally, $CD4^+CD3^-$ immature single positive (ISP) and $CD4^+CD8^+$ double positive (DP) T cell precursors were seen in week 2. More mature $CD3^+$ cells emerged by week 4 (1.2%). By week 5, the number of $CD3^+$ cells was relatively the same (1.6%), indicating a lack of cell growth for this population. As the original ATOs article stated a significant and progressive increment in this cell population, starting on week 4, the present study was terminated on week 5. However, despite the lack of growth, some $CD3^+$ cells in our study were indeed $CD8^+$ single positive (SP) and $CD4^+$ SP T cells. Both cell types were observed in weeks 4 and 5, revealing that positive selection occurred within ATOs. As expected, within the $CD3^+$ cell population, the amount of $CD4^+CD8^+$ DP T cells were greater than $CD8^+$ SP and $CD4^+$ SP T cells. Nonetheless, by week 5, 22% of the $CD3^+$ cells were $CD8^+$ SP T cells (Fig. III.4).

During the period of the study, long-term maintenance of $CD34^+$ cell progenitors was observed in ATOs, even though with expected decrease over time (e.g., 8.3% by week 2 and 4.3% by week 3) (Fig. III.4). Specifically, ATOs allowed recapitulation of the three phenotypic stages of thymic T cell progenitors, i.e., multipotent $CD34^+CD7^-CD1\alpha^-$ early thymic progenitors (ETP) and developmentally downstream $CD34^+CD7^+CD1\alpha^-$ ($CD1\alpha^-$ Pro-T) and $CD34^+CD7^+CD1\alpha^+$ ($CD1\alpha^+$ Pro-T) cells. From week 2 to week 3, it was possible to identify a decrease of ETP with a concomitant increase of $CD1\alpha^-$ and $CD1\alpha^+$ Pro-T cells. Using an alternative classification scheme, based on CD5 and CD7 markers, Pro-T1 ($CD34^+CD7^+CD5^-$) and Pro-T2 ($CD34^+CD7^+CD5^+$) cells were also identified within the $CD34^+$ cell population. Namely, from week 2 to week 3, a decrease was seen in ETP ($CD34^+CD7^-CD5^-$) while the great majority of $CD34^+$ cell progenitors were Pro-T2 cells.

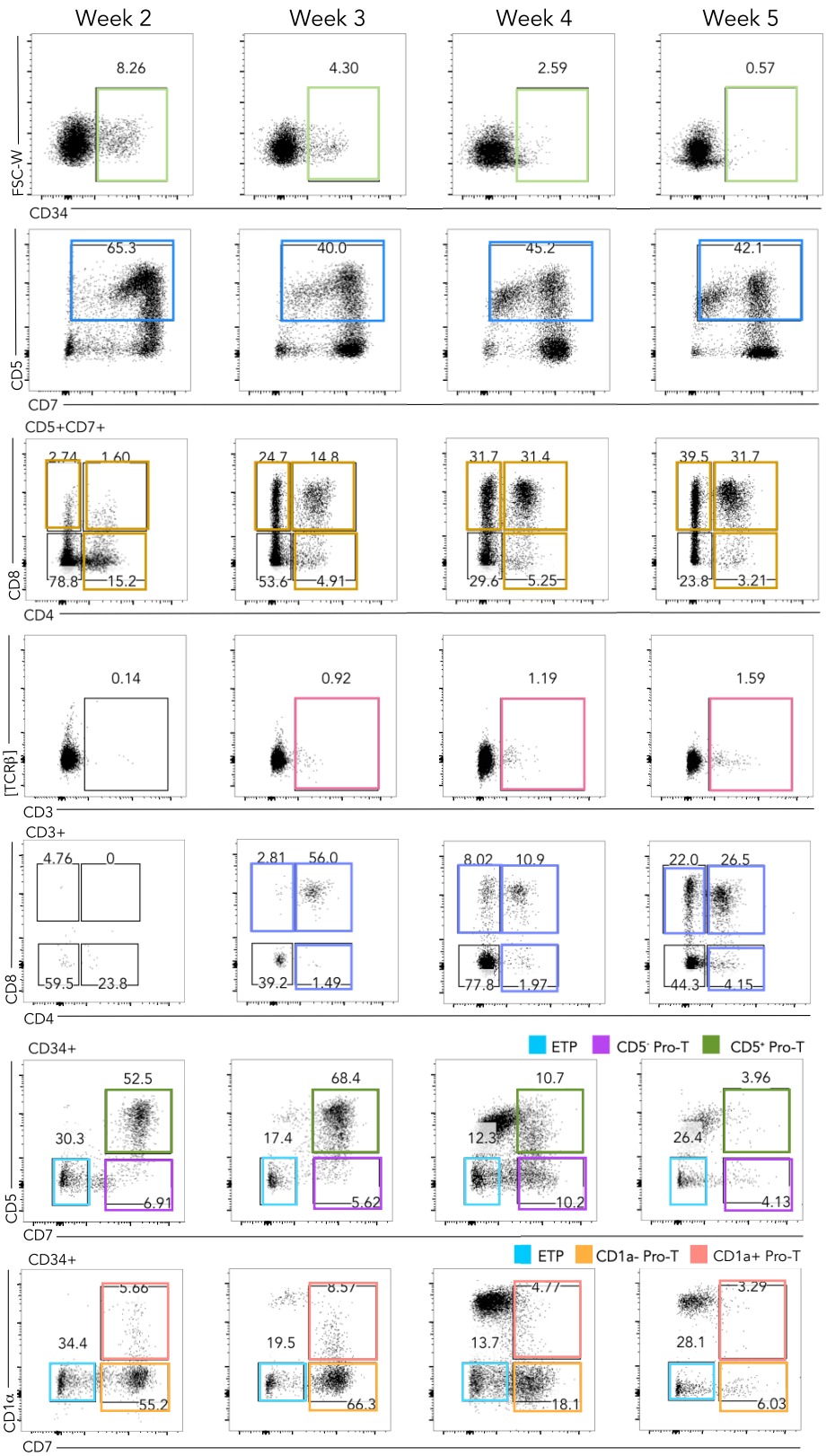

Figure 0.4. *Kinetic analysis of T cell differentiation from umbilical cord blood-derived hematopoietic stem/progenitor cells, using the artificial thymic organoids system, at the indicated time points. Populations are gated on live cells. Subsequent parent gates are shown above each panel. ETP: early thymic progenitors; FSC-W: forward scatter-width.*

III.4.2. Previous expansion of UCB-derived CD34⁺-enriched cells over bone marrow (BM)-derived mesenchymal stromal cells (MSC) accelerates differentiation towards CD8⁺ T cells using the ATOs system

Our first study using ATOs provided satisfatory results since we successfully established ATOs for five weeks and were able to differentiatie T cells after four weeks using this system. However, as T cell differentiation rates were not as expected, considering what is published in the literature, a second study was conducted to validate the first results. Also, in this second study, not only "standard ATOs" (i.e, freshly isolated UCB-derived CD34⁺-enriched cells mixed with MS5-hDLL4 cells) were established, but also two additional sets of ATOs. In these additional sets, instead of freshly isolated cells, previously expanded UCB-derived hematopoietic stem/progenitor cells (HSPC) were mixed with MS5-hDLL4 cells. One of the sets used HSPC that were previously expanded with a feeder layer of BM-derived MSC ("expMSC ATOs") while the other used HSPC that were expanded with cytokines only ("exp ATOs") (Fig. III.5).

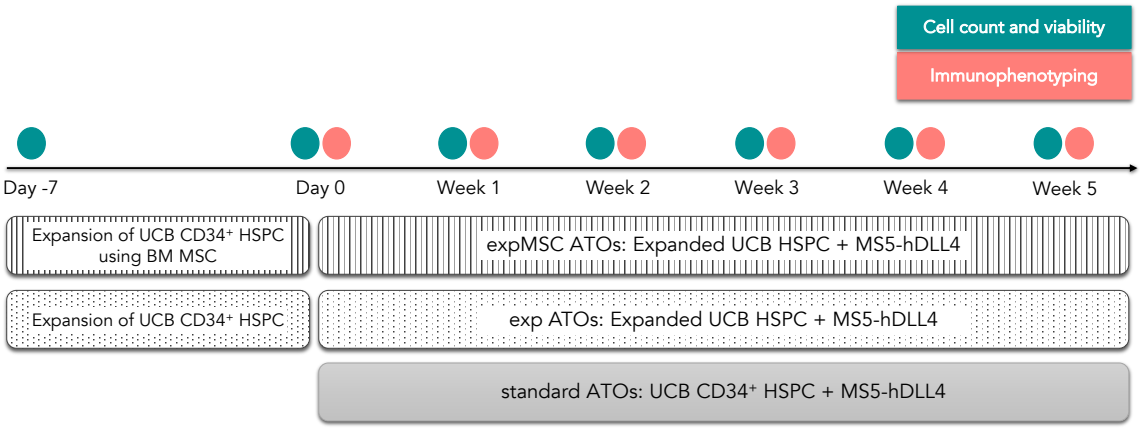

Figure 0.5. *Schematic representation of the second study using the artificial thymic organoids (ATOs) system. Three different sets of ATOs were established and cultured for five weeks. One set was established using freshly isolated umbilical cord blood (UCB)-derived CD34⁺ hematopoietic stem/progenitor cells (HSPC) and MS5-hDLL4 cells ("standard ATOs"). The other two sets were established using previously expanded UCB-derived HSPC, with ("expMSC ATOs") or without ("exp ATOs") a feeder layer of bone marrow-derived mesenchymal stromal cells, and MS5-hDLL4 cells. The same unit of UCB was used in this study. T cell lineage differentiation was evaluated through immunophenotyping. Cell count and viability were also determined. BM: bone marrow; MSC: mesenchymal stromal cells.*

Cell counting showed an exponential cell increase starting on day 0 for the three sets of ATOs (Fig. III.6.A). This exponential increase stopped for "expMSC ATOs" and "exp ATOs" on week 3, with similar values (493 000 and 478 000 cells/ATO, respectively). In the case of "standard ATOs", the exponential increase stopped by week 2, even though cells continued to grow till week 3, where a peak of 260 000 cells/ATOs was reached. Then, after the decline observed on week 4, cell number kept stable on week 5 (130 000

cells/ATO). In what concerns "expMSC ATOs" and "exp ATOs", cell number decreased in both weeks 4 and 5, first abruptly and then more moderately. By week 5, each "expMSC ATO" generated 85 000 cells, while each "exp ATO" produced 125 000 cells. Concerning cell viability (Fig. III.6.B), all sets of ATOs showed a substantial decrease immediately on week 1. This decline was especially evident for "expMSC ATOs" (39%). However, on week 2, viability increased and was higher than 87% for the three sets. After that, viability decreased smoothly over time, with a final accentuated decline for "expMSC ATOs" on week 5 (55%), while the "exp ATOs" and "standard ATOs" had similar higher values (69% and 71%, respectively).

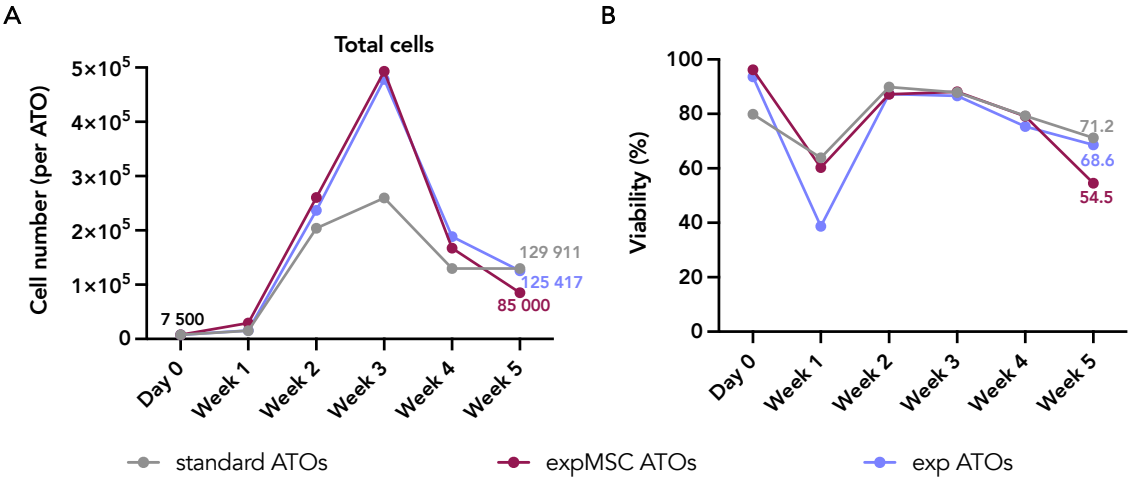

Figure 0.6. Cell number and viability of umbilical cord blood-derived hematopoietic stem/progenitor cells used to establish artificial thymic organoids. ***(A)*** *Total cell number.* ***(B)*** *Viability. ATOs: artificial thymic organoids; MSC: mesenchymal stromal cells.*

On day 0, 32% of the cells in "expMSC ATOs" (Fig. III.7) were already committed to the T cell lineage, as shown by the presence of $CD5^+CD7^+$ T lineage cells, while only 13% of the "exp ATOs" (Fig. III.8) were DP for these markers. After one week, this cell population was still substantially and considerably higher in "expMSC ATOs" (80%) than in "exp ATOs" (64%). However, from week 2 on, the pattern was similar and almost all cells were $CD5^+CD7^+$ for both sets. In the case of "standard ATOs" (Fig. III.9), $CD5^+CD7^+$ T lineage cells showed up after 1 week (44%), on week 2 the percentage doubled (87%) and throughout the rest of the study was above 90%. As in the first study, by week 2, $CD4^+CD3^-$ ISP and $CD4^+CD8^+$ DP T cell precursors were seen in "standard ATOs" but this time with higher percentages: 33% and 17%, respectively. More mature $CD3^+TCR\alpha\beta^+$ T cells showed up a week earlier, on week 3, totalizing 10.5% of all cells. By week 4, this percentage decreased to half and on week 5 ended up with 6.6%. Importantly, within the $CD3^+TCR\alpha\beta^+$ T cell population, by week 3, 85% of the cells were $CD4^+CD8^+$ DP and 2% were already $CD8^+$ SP. On week 4, 71% of the cells were $CD4^+CD8^+$ DP and 19% were $CD8^+$ SP. By the end of the study, 45% of the cells were

$CD4^+CD8^+$ DP while 30% were $CD8^+$ SP and 2% were $CD4^+$ SP. In what concerns ATOs established with HSPC that were previously expanded, by week 1, the presence of $CD4^+CD3^-$ ISP was already noticeable (especially for "expMSC ATOs" (4.5%)), being superior to "standard ATOs" on week 2. $CD4^+CD8^+$ DP T cell precursors only emerged on week 2, for both ATOs sets, and with similar values as "standard ATOs". Mature $CD3^+TCR\alpha\beta^+$ T cells residually (<1%) showed up during week 2, but notably, accounted for one quarter of the cells in both sets by week 3. As observed with "standard ATOs", at week 4, the percentage of this cell population underwent a high decrease to 8.5% and 5.3% in "expMSC ATOs" and "exp ATOs", respectively. Then, on week 5, this population recovered considerably in both sets, achieving its highest value in the case of "expMSC ATOs" (38%) and being 15% in the case of "exp ATOs". Within the $CD3^+TCR\alpha\beta^+$ T cell population, in both weeks 3 and 4, "expMSC ATOs" and "exp ATOs" followed the pattern observed in "standard ATOs", namely, an initial dominance of $CD4^+CD8^+$ DP that progressively turned into $CD8^+$ SP. In the last week (week 5), "exp ATOs" still had more $CD4^+CD8^+$ DP cells (60%) than $CD8^+$ SP (32%), similar to "standard ATOS". However, "expMSC ATOs" underwent an impressive change with $CD8^+$ SP T cells becoming the dominant cell population (47%), while $CD4^+CD8^+$ DP cells represented 42% of the cells.

The percentage of $CD34^+$ cell progenitors was very high (97%) in "standard ATOs" (Fig. III.9), on day 0. As expected, it was much lower in "expMSC ATOs" (Fig. III.7) and "exp ATOs" (Fig. III.8), as these sets were established with HSPC already expanded for 7 days. Nevertheless, "expMSC ATOs" presented almost double of these cells (67%) compared to "exp ATOs" (37%), on day 0. On the following weeks, "expMSC ATOs" always presented slightly higher values than "exp ATOs". However, in both sets, this cell population became almost inexistent from week 4 on. On the other hand, "standard ATOs" still presented a considerable population (57%) on week 1 and, by the end of the study, 2% of the cells were still $CD34^+$. Within the $CD34^+$ cell population, in all three sets, it was possible to observe recapitulation of the three phenotypic stages of thymic T cell progenitors, i.e., multipotent $CD34^+CD7^-CD1\alpha^-$ ETP and developmentally downstream $CD1\alpha^-$ Pro-T and $CD1\alpha^+$ Pro-T cells. Interestingly, for both "expMSC ATOs" and "exp ATOs", it was evident that although the majority of cells were ETP in the beginning of the study, the progression to $CD1\alpha^-$ Pro-T and $CD1\alpha^+$ Pro-T cells was faster than for "standard ATOs". The same trend was observed using the alternative classification scheme, based on CD5 and CD7 markers. Namely, both "expMSC ATOs" and "exp ATOs" were faster in differentiating Pro-T2 ($CD34^+CD7^+CD5^+$) cells than "standard ATOs". Human thymocytes were also phenotypically characterized as a control. As expected, $CD34^+$ cell progenitors were almost null and the majority of cells were $CD3^+TCR\alpha\beta^+$ T cells (65%). From these, and also as expected, the vast majority were $CD4^+$ SP (69%), 17% were $CD8^+$ SP and, at last, 7.5% were $CD4^+CD8^+$ DP cells.

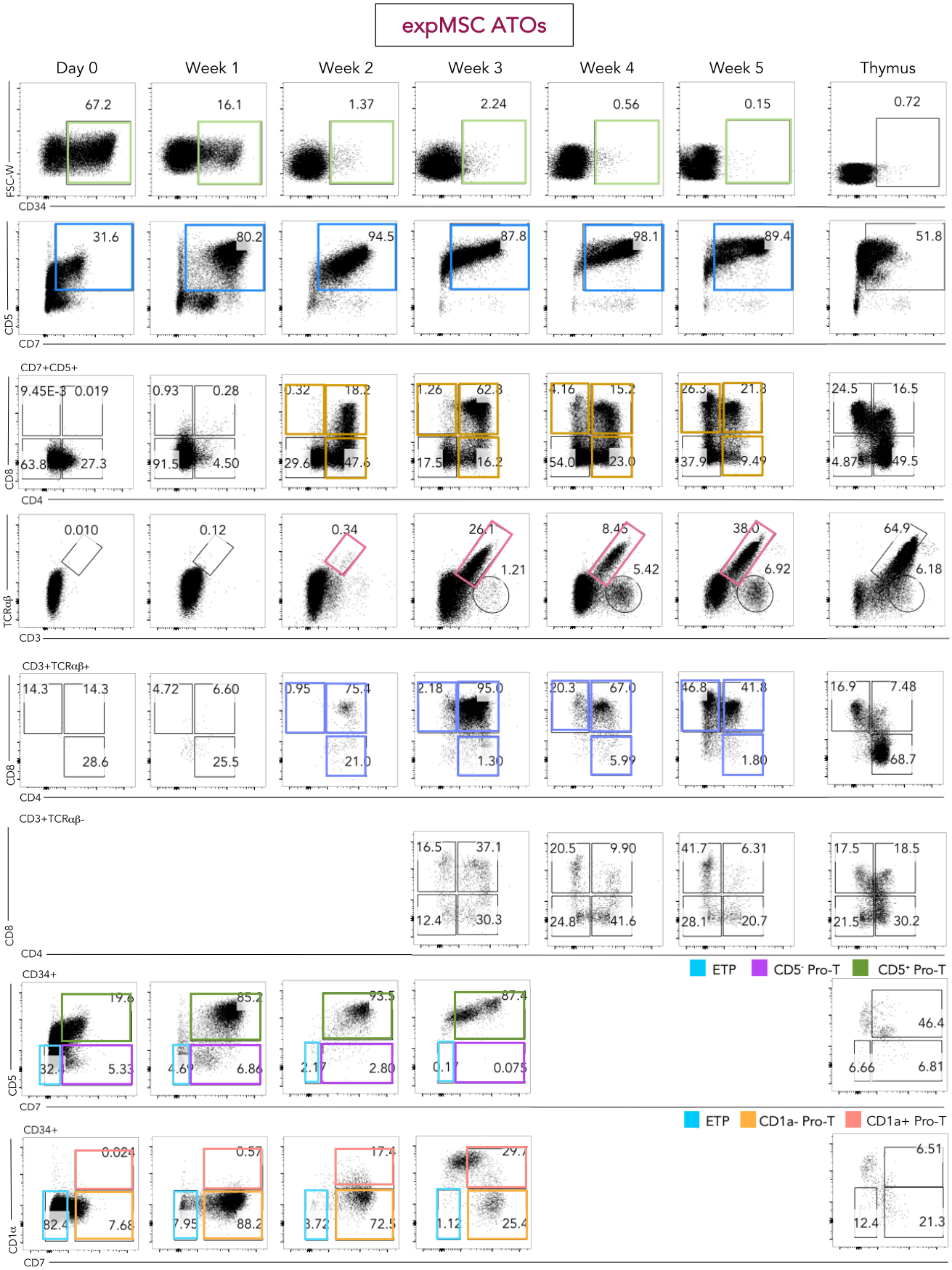

Figure 0.7. Kinetic analysis of T cell differentiation from umbilical cord blood-derived hematopoietic stem/progenitor cells, using the artificial thymic organoids system, for "expMSC ATOs". Populations are gated on live cells. Subsequent parent gates are shown above each panel. ETP: early thymic progenitors; FSC-W: forward scatter-width.

Figure 0.8. *Kinetic analysis of T cell differentiation from umbilical cord blood-derived hematopoietic stem/progenitor cells, using the artificial thymic organoids system, for "exp ATOs". Populations are gated on live cells. Subsequent parent gates are shown above each panel. ETP: early thymic progenitors; FSC-W: forward scatter-width.*

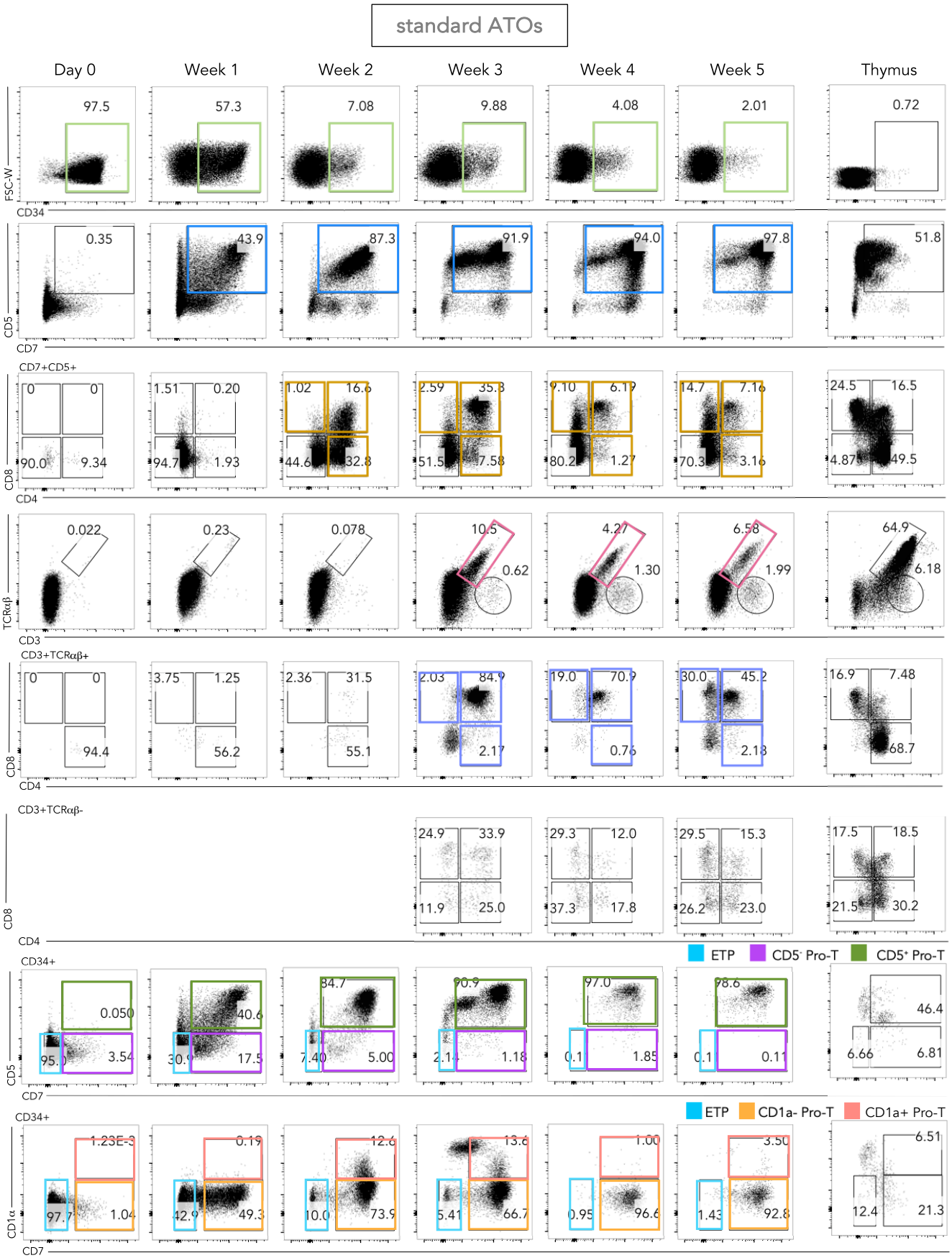

Figure 0.9. *Kinetic analysis of T cell differentiation from umbilical cord blood-derived hematopoietic stem/progenitor cells, using the artificial thymic organoids system, for "standard ATOs". Populations are gated on live cells. Subsequent parent gates are shown above each panel. ETP: early thymic progenitors; FSC-W: forward scatter-width.*

We also calculated the absolute number of specific cell populations of interest, such as CD3⁺TCRαβ⁺ T cells (Fig III.10.A) and CD3⁺TCRαβ⁺CD8⁺ T cells (Fig III.10.B). These values were obtained by combining cell population percentages (Figs. III.7-III.9) with viable cell number per ATO (Fig. III.6.A). Each ATO was initially seeded with 7 500 HSPC. For all sets of ATOs, the peak for CD3⁺TCRαβ⁺ T cell population was observed at week 3. At this week, each "standard ATO" provided approximately 27 000 CD3⁺TCRαβ⁺ T cells, while a "expMSC ATO" and a "exp ATO" provided 129 000 and 121 000 cells, respectively. At the end of the study, by week 5, a reduction of 69, 75 and 85%, respectively, was observed in each set for this cell population. On the other hand, the maximum production of CD3⁺TCRαβ⁺CD8⁺ T cells was observed on week 5 in all ATOs sets. Remarkably, at the end of the study, each "standard ATO" generated approximately 2 500 CD8⁺ SP, while a "expMSC ATO" and a "exp ATO" produced 15 000 and 6 000 CD8⁺ SP, respectively.

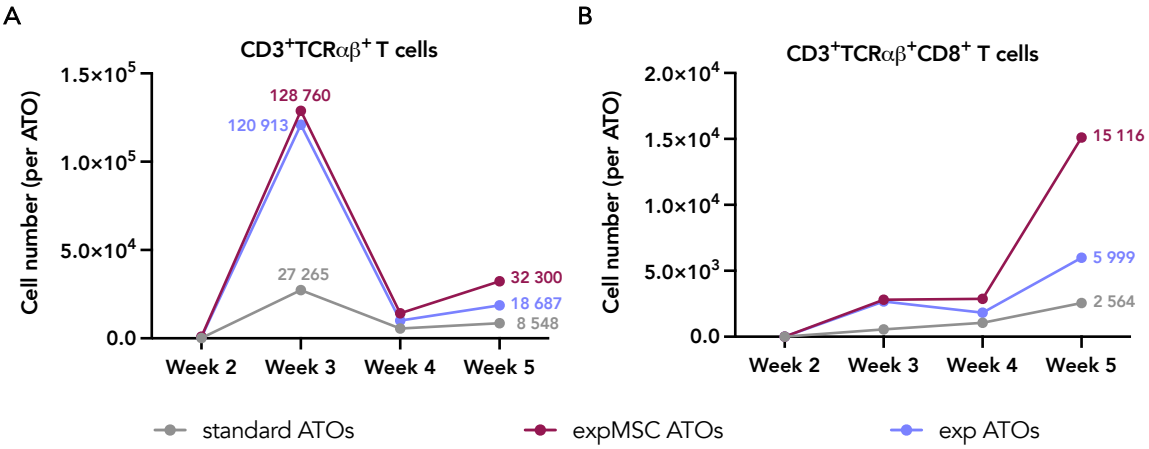

Figure 0.10. *Cell number evolution of specific populations throughout the second study using artificial thymic organoids.* ***(A)*** *CD3⁺TCRαβ⁺ T cells.* ***(B)*** *CD3⁺TCRαβ⁺CD8⁺ T cells. ATO: artificial thymic organoid; MSC: mesenchymal stromal cells.*

III.5. Discussion

The use of hematopoietic stem/progenitor cells (HSPC) derived from umbilical cord blood (UCB) is considered a suitable option in the context of allogeneic hematopoietic cell transplantation (HCT). This is especially relevant for patients lacking a suitable human leukocyte antigen (HLA)-matched donor, because UCB-derived HSPC present lower immunogenicity, allowing a greater degree of HLA mismatch between recipient and donor, and are also less prone to cause graft-*vs*-host disease (GVHD)[39,40]. To overcome low cell numbers, the use of two UCB units combined with improved conditioning regimens has become an effective therapeutic option for adult patients

and high weight children. Still, the delay in engraftment and immune reconstitution, partly caused by the low cell number but also by the immaturity of immune cells, results in a prolonged period of immune incompetence. As recipients rely on immunity of the transplanted cells to fight opportunistic infections (OI), which are uniformly naïve, there is a high incidence of OI in the first 100 days after UCB transplantation (UCBT), particularly viral infections. Indeed, OI are the major cause of death during the first six months after UCBT[37,38]. In this context, another disadvantage is the lack of donor cells for post-transplant adoptive therapies, such as donor lymphocyte infusions (DLI), due to ethical reasons. DLI are commonly employed to enhance donor-derived immunity to treat infections, but also mixed chimerism or disease relapse. Despite these limitations, the number of UCBT performed is increasing, becoming crucial to find adoptive cell therapy strategies to improve recipient survival[37–39].

One option to circumvent the lack of DLI availability is to attain sufficient T cells *in vitro* that could be used in UCBT patients after transplant. In Sweden, a group paved the way in 2010 by expanding the T cells present in 5% (1.5-28 x 10^6 $CD3^+$ cells) of the grafts used in UCBT context[167]. After an 8-10 day-protocol, sufficient T cells (median: 639 x 10^6 T cells; range: 2.2-2240) were attained to cover the needs of a DLI protocol for children and adult patients (DLI doses varied between 5 x 10^3 and 1 x 10^6 T cells/kg of patient weight). These expanded T cells, with an activated profile, where used as DLI in four patients after UCBT. Fortunately, no adverse effects were reported that could be associated with UCB DLI. Possible therapeutic benefits were seen, but without certainty of being associated with DLI treatment[168]. Attaining T cells through this expansion approach faces some constraints, namely the variability of expansion efficiency associated with different T cell units[167]. There is also the possibility of *in vitro* expansion causing exhaustion of cell proliferative capacity. Additionally, as expanded T cells are in an activated state, there is an increased risk of GVHD induction.

Another approach that can be pursued to attain T cells *in vitro* is to differentiate them from HSPC. However, in opposition to other cell types that are easily differentiated using two-dimensional (2D) systems, mature T cells are extremely difficult to attain using this approach. The most recognized 2D system, the OP9-DLL1 system, was developed by Zúñiga-Pflücker[163] and combines a mouse stromal cell line that ectopically expresses the Notch ligand DLL1 – OP9-DLL1 cells – with UCB-derived HSPC, in a co-culture system[169]. This system is not only labor intensive, as it requires fresh OP9-DLL1 feeder layers every four days but is also dependent on fetal bovine serum (FBS) usage. Furthermore, differentiation efficiency is highly variable between different lots of FBS used[170,171]. Lastly, using this system, only 2-4% of the cells differentiated were mature CD8 single positive (SP) T cells after a culture period of 8-10 weeks[164]. Thus, the OP9-DLL1 system is time-consuming with a very low efficiency rate. Attaining T cells *in vitro* using this approach turned out to be difficult due to the lack of a three-dimensional (3D)

structure. The 3D configuration, in combination with Notch signaling, maximizes connections between hematopoietic cells but also with stromal cells. These enhanced connections facilitate positive selection of maturating cells, a process essential for differentiation of mature T cells.

These limitations were completely overcome when the group of Gay Crooks (UCLA) developed the artificial thymic organoids (ATOs) system in 2017[165]. Through a simple process of compacting two cell types, MS5-hDLL1 and UCB-derived HSPC, $CD3^+TCR\alpha\beta^+$ T cells emerged by week 4, comprising about 6% of total cells. At week 6, this population increased to 31%. Within this population, the great majority (~72%) were CD4 and CD8 double positive (DP) T cells and about 23% were CD8 SP T cells (i.e., approximately 7% of total cells). By week 6, they reported a mean of 2×10^6 cells/ATO and a mean of 1.4×10^5 CD8 SP T cells/ATO (data from 11 independent experiments; in 2 experiments the values were 0.5×10^5 CD8 SP T cells/ATO). In our first study, although we had been able to successfully establish the ATOs system in our lab and differentiate T cells, we were far away from obtaining the values reported by Crook's group. In accordance with their study, T cells emerged by week 4, but by week 5, our values were still inferior to 2%. The total cell number we had per ATO on week 5, 3.5×10^5 cells, was also inferior to their reported 2×10^6 cells/ATO. These differences in the final T cell yield and the total cell number per ATO, challenge the reproducibility of the ATOs system when trying to be adapted by other groups.

Using the same approach, two years later, this group improved their work by generating T cells from human pluripotent stem cells (PSC-ATOs)[166]. They also directly compared the efficiency of T cell development using MS5-hDLL1 and MS5-hDLL4 and although both lines supported T cell differentiation, better results were attained using the second one. In that particular study, $CD3^+TCR\alpha\beta^+$ T cells emerged by week 3 (14.1%), accounting for approximately 90% of the cells on week 5 and 95% on week 7. Impressively, on week 3 the majority of the cells were CD4 and CD8 DP (86.2%), and on week 5 there was a shift to CD8 SP T cells (79.6%) which increased to 89.9% on week 7. They reported that a small-scale experiment, of 100 embryonic mesoderm organoids (EMOs)/ATOs, generated 1.5×10^6 CD8 SP T cells by week 7 (from 1×10^6 human embryonic mesodermal progenitors (hEMPs) initially seeded), which means that 1 EMO/ATO was able to provide approximately 15 000 CD8 SP T cells. Impressively, we were able to obtain the same number of CD8 SP T cells two weeks earlier (by week 5) with our "expMSC ATOs", in our second study. In this study of PSC-ATOs, they observed that $CD3^+TCR\alpha\beta^+$ T cells emerged one week earlier (by week 3) compared to their original study (week 4). Remarkably, in our second study, we also observed that $CD3^+TCR\alpha\beta^+$ T cells emerged at week 3, representing 10.5% of all cells in "standard ATOs" and one quarter in "expMSC ATOs" and "exp ATOs". Expectably, almost all $CD3^+TCR\alpha\beta^+$ T cells at this point were CD4 and CD8 DP. Thus, the considerable cell

loss observed in the following week (week 4), can easily be attributed to cell death by apoptosis of DP T cells that did not undergo positive selection to finally become CD4 or CD8 SP T cells. Indeed, the DP state is a very important check point, where the great majority of T cell precursors die. Thus, while a generalized cell decrease was observed from week 4 to week 5 (considering total cell count), a slight increase was noticed when looking specifically to the $CD3^{+}TCR\alpha\beta^{+}$ T cell population. Interestingly, in the final weeks, for both standard and expanded ATOs, a progressive substitution of DP cells for, essentially, CD8 SP T cells, but also CD4 SP, was observed.

In our second study we were able to corroborate that positive selection occurs in the ATOs system, as we were able to differentiate mature CD8 and CD4 SP T cells. As discussed elsewhere[165,166], given the absence of thymic epithelial cells (TEC), it is hypothesized that positive selection of mature CD8 SP T cells occurs through neighboring hematopoietic cells within the ATOs, that ubiquitously present selective major histocompatibility complex (MHC) I ligands. This has also been previously suggested in the OP9-DLL1 system[172]. On the other hand, positive selection of mature CD4 SP T cells is presumed to occur via MHC class II presented by rare dendritic cells developed within ATOs. The higher frequency of CD8 T cells, rather than CD4 SP, can thus be partially explained by the ubiquitous expression of MHC class I on hematopoietic cells and the rarity of MHC class II-expressing cells. Very importantly, these studies showed that optimal positive selection and T cell maturation observed in the ATOs system is dependent on all three ATOs components, namely: 3D structure, MS5-hDLL1 cells and ATOs complete medium. Specifically, neither monolayer cultures using ATOs components, nor OP9-DLL1 cells in 3D organoids were able to support T cell development[165]. Of note, impact of non-TEC mediated positive selection should be clarified to rule out any impact on *in vivo* T cell functionality. Importantly, if selection mechanisms in ATOs are as described, the amount of CD8 or CD4 SP cells generated per ATO could, in the future, be changed to favor one or the other.

Notably, T cell maturation in ATOs was shown not to be species-specific nor MS5-specific factor dependent. Development of mature T cells in ATOs was also attained using immortalized human bone marrow-derived mesenchymal stromal cells (MSC) transduced to express DLL1 (MSC-DLL1), even though with lower efficiency[165]. Considering our exciting results using ATOs with previously expanded HSPC from our MSC co-culture system, a synergistic approach is foreseeable. Co-culture expansion of UCB HSPC and T cell differentiation could be sequentially performed *in situ*, by using MSC-DLL1 or MSC-DLL4 as stromal cells. Firstly, HSPC would be expanded in 3D MSC co-culture aggregates using described cytokine-based culture conditions[173]. Then, after increasing the number of HSPC and favoring lymphoid priming, the ATOs system protocol would be started using the same 3D aggregates already formed. This approach would help to solve two drawbacks present in the ATOs system, namely the presence

of murine cells and their final T cell yield being dependent on the number of initially isolated HSPC. By removing the MS5 cell line (becoming a completely xeno-free protocol) and having a pre-expansion and lymphoid priming of the starting HSPC population (through our co-culture expansion), the ATOs system could take a big step towards its clinical application.

By taking advantage of UCB-derived HSPC expansion before T cell differentiation, there is a rational use of UCB resources and creation of added value for units with limited cell numbers, by the inclusion of an expansion stage prior to T cell generation. It is estimated that only about 20% of the cryopreserved units in banks contain sufficient cell doses for transplanting 75 kg patients (considering a recommended threshold dose of >2-2.5 x 10^7 total nucleated cells (TNC)/kg, with at least a 4/6 HLA matching)[174,175], meaning that there is definitively an unmet clinical need with a great market impact. Ultimately, generated differentiated T cells can become a readily available source of cells for adoptive transfer immunotherapies, namely DLI upon OI after UCBT, contributing to boost and widen the clinical use of UCB cells.

Even with the above mentioned improvements, the ATOs system is very laborious and time-consuming, requiring extensive manual manipulation. Ideally, to facilitate production of T cells *in vitro*, they should be differentiated using a feeder cell-free system[176]. As mentioned before, Notch signaling is needed for T cell commitment and maturation. However, Notch ligands, DLL1 or DLL4, must be immobilized to activate Notch signaling, as soluble Notch ligands fail to do so[177]. Some groups have followed the stromal cell-free system approach by immobilizing delta ligands either on the surface of tissue-culture plates[178,179] or microbeads[180,181]. Approaches that use immobilized ligands in plate-bound systems have a higher limitation of space, as plates are restricted to 2D. On the contrary, beads can take advantage of 3D to increase the amount of interactions between cells and Notch signaling ligands. This makes them compatible with scalable systems for hematopoietic cells, such as the G-Rex system and the WAVE bioreactor[181]. However, these feeder-free systems lack the 3D structure necessary to promote full T lineage differentiation. Consequently, proT cell production has gained more interest, which is compatible with feeder-free and other systems that cannot replicate thymus-mediated T cell receptor (TCR) rearrangement and positive selection.

In general, our improvement of the ATOs system would be very compatible with antigen-specific T cell therapy, potentiating its translation.

IV. Decellularization of human thymic tissue: a platform for T cell differentiation *in vitro*

IV.1. Summary

Three-dimensional organization, a distinctive characteristic of the thymus, is key for T cell differentiation to occur *in vivo* and *in vitro*. While thymic epithelial cells are essential to induce T cell differentiation, the non-cellular component of the thymus – the extracellular matrix (ECM) – provides a physical scaffold for cells to anchor, as well as growth factors and bioactive molecules that promote cell differentiation and homeostasis. Human thymic fragments were subjected to a 3-day decellularization protocol that included the use of a hypotonic buffer, a sodium dodecyl sulfate solution and DNase treatment, to produce a natural thymic bioscaffold. Decellularization efficiency was confirmed through macroscopic visualization, as a white-to-translucid appearance was observed. Immunohistochemistry of decellularized thymic sections revealed absence of nuclear content and maintenance of the main ECM components: type I collagen, type IV collagen, fibronectin and laminin. Thymic structure, typically organized in lobules, was maintained after decellularization. DNA quantity was determined for both native and decellularized fragments and an extensive reduction of at least 95% was observed. Following lyophilization of the natural thymic samples, powdering of thymic ECM was pursued, to enhance the applicability of this product.

IV.2. Background

The use of natural scaffolds, such as decellularized tissues, that can be repopulated by cells of autologous or allogeneic origin is a promising approach in the field of tissue engineering and regenerative medicine. When applied to organs, this approach arose as a way to solve the problem of organ donor shortage, since there is a great gap between the number of patients candidate to organ transplantation and the number of organs available[182]. Natural scaffolds have been obtained through decellularization methods that allow the preservation of three-dimensional (3D) architecture and extracellular matrix (ECM) of several tissues and organs[183]. The choice of the best decellularization agent is dependent on many factors related with the tissue or organ nature, including thickness, cell density, tissue cellularity and lipid content. Regardless of the decellularization agent used, damage of some degree will inevitably occur in ECM ultrastructure and components[90]. On the other hand, several groups have also developed alternative strategies to deliver the acellular ECM directly or to combine them with cells[184,185]. For instance, ECM slurries require sample post-processing but are versatile to use, while cell-derived ECM sheets are not dependent on organ donation and can be produced *in vitro*. In this way, scaffold complexity can be reduced, diversifying the use of decellularized ECM and creating more applications.

The human thymus is divided into two main lobes. Each lobe is composed of several lobules and each lobule presents two regions morphologically and functionally distinct, the cortex and the medulla. Each region possesses its own distinct population of thymic epithelial cells (TEC), the cortical TEC (cTEC) and the medullary TEC (mTEC). These cells, together with other thymic stromal cells (TSC), produce homing signals for the immigration of bone marrow (BM)-derived lymphocyte progenitors, but also trophic factors necessary for T cell differentiation and maturation[186,187]. While there is a mutual dependency between TEC and developing thymocytes, as the cross talk between them is essential for their mutual survival and proliferation[188], TEC maturation, survival and function is also dependent on the unique architecture of the thymic stroma. TEC form a 3D sponge-like network that is essential for their function. Consequently, TEC have been shown to have lower capacity to support T cell differentiation *in vitro* in a two-dimensional (2D) system[189]. Key genes for TEC specification and proliferation were also shown to be dependent on the 3D organization of the thymic stroma[159,190].

Mice acellular thymic scaffolds were able to support TEC survival in culture during their repopulation. When transplanted to athymic nude mice, these bioengineered thymic organoids were able to promote homing of lymphocyte progenitors and support T cell differentiation. Interestingly, tolerance to skin allografts was achieved when the thymic organoids were made with TEC co-expressing both syngeneic and allogenic major histocompatibility complexes (MHC), or a mixture of donor and recipient TEC[97]. Also using murine thymi, the efficiency of several detergent-based decellularization solutions to preserve the main ECM components of the primary lymphoid organ have been tested[98]. CHAPSO-treated decellularized thymic lobes seeded with TEC were able to engraft in nude mice, attract hematopoietic precursors and produce mature T cells.

Here, we were able to establish a decellularization protocol to produce acellular thymic scaffolds from human thymic fragments. Decellularization efficiency of this protocol was confirmed through macroscopic evaluation, characterization of ECM components and structure, as well as DNA quantification. These natural thymic scaffolds are intended to be used as a platform to produce T cells *in vitro*. Additionally, instead of using the entire scaffold, acellular thymic fragments were also processed into a lyophilized powder to be potentially incorporated in different biomaterials to boost their thymic biomimetic properties (e.g., fibers).

IV.3. Material and Methods

IV.3.1. Human thymic samples

Thymic samples were attained from children who underwent pediatric cardiac surgery at Hospital de Santa Marta, Centro Hospitalar de Lisboa Central, under informed and

written consent of tutors. Samples were stored in RPMI medium (Cat. #61870-036, Gibco, USA) supplemented with 10% (v/v) fetal bovine serum (FBS) (Cat. #10270106, Thermo Fisher Scientific, USA) and 1% (v/v) Antibiotic-Antimycotic (A/A) (Cat. #15240-062, Gibco) at 4°C. Until 48 hours after collection, samples were transported in ice and processed at Stem Cell Engineering Research Group (SCERG) lab, at Institute for Bioengineering and Biosciences, Instituto Superior Técnico (iBB-IST). After washing the thymic samples with cold phosphate buffered saline (PBS) (Cat. #21600-044, Sigma-Aldrich, USA) in a petri dish, small thymic fragments (<1cm^3) were cut using a scalpel and serrated tweezers. Thymic fragments were immersed in optimal cutting temperature (OCT) compound (Cat. #361603E, VWR, USA), frozen in dry ice-cooled isopentane (Cat. #24872.298, VWR) and stored at -80°C until further use (maximum of 6 months).

IV.3.2. Decellularization process

A 3-day decellularization protocol was adapted (Fig. IV.1) from A.C. Silva and colleagues, originally established for fetal and adult murine heart specimens[191]. The protocol required previous preparation of the following decellularization solutions: PBS; hypotonic buffer (10 mM Tris, 3.42 mM ethylenediamine tetraacetic acid (EDTA), pH 7.8); 0.2% (w/v) sodium dodecyl sulfate (SDS) (0.2% SDS, 10 mM Tris, pH 7.8); hypotonic wash buffer (10 mM Tris, pH 7.8) and DNase treatment solution (20 mM Tris, 2 mM $MgCl_2$, 50 U/mL DNase I, pH 7.8). All solutions were filtered through a 0.22 µm membrane filter after preparation. They were stored at room temperature (RT) for no

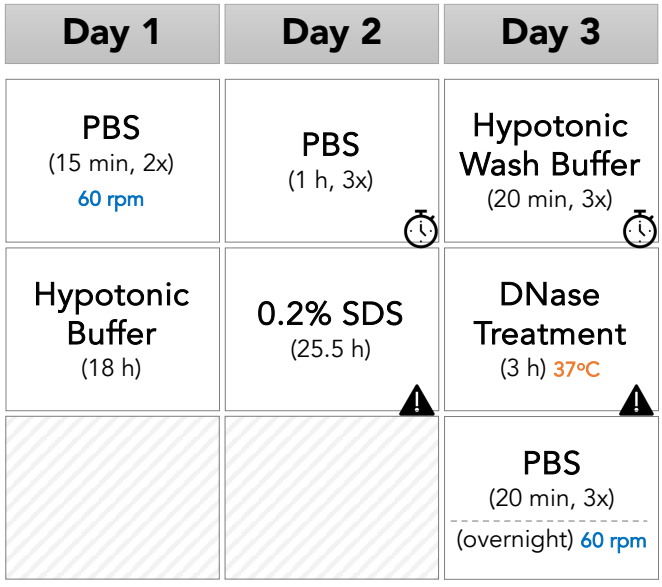

Figure IV.1. Schematic representation of the 3-day decellularization protocol for human thymic fragments. Every step was performed at 170 rpm and 25°C, except in cases where a different agitation or temperature are mentioned. Caution symbol: check point; PBS: phosphate buffered saline; Stopwatch symbol: optional pause point; SDS: sodium dodecyl sulfate.

longer than three months, with the exception of 0.2% SDS solution that was freshly prepared and used. Detailed description of decellularization solution preparation can be found in the Appendix section (VIII.1.1. Preparation of the decellularization solutions).

Every step of the decellularization protocol was performed at 170 rpm and 25°C, except in cases where a different agitation or temperature are mentioned. On day 1, thymic fragments were thawed at RT and immersed in PBS to complete OCT dissolution. Using an ES-20 orbital shaker-incubator (Biosan, Latvia), at 60 rpm, samples were washed twice with PBS for 15 min. Each fragment was placed into a well of a 24-well plate and 1.5 mL of hypotonic buffer supplemented with 1% A/A was added to each well. Samples were incubated for 18 h. On day 2, the hypotonic buffer was carefully aspirated, and samples were washed three times with PBS, for 1 h. When needed, samples were kept for 24 h in PBS supplemented with 1% A/A, at 4°C, in static conditions (optional pause). PBS was carefully aspirated and 1.5 mL of freshly prepared 0.2% SDS solution supplemented with 1% A/A was added to each well and incubated for 25.5 h. After SDS treatment, samples presented a white to translucid appearance (check point). On day 3, as samples were very gelatinous, SDS solution was carefully aspirated using a Pasteur pipette. Samples were then washed three times with hypotonic wash buffer, for 20 min. When needed, samples were kept for 18 h in hypotonic wash buffer supplemented with 1% A/A, at 4°C, in static conditions (optional pause). Hypotonic wash buffer was carefully aspirated, and 1.5 mL of DNase treatment solution was added to each well. Samples were incubated at 37°C for 3 h. After DNase treatment, samples presented a complete white to translucid appearance and were reduced in size (check point). As samples lost their gelatinous appearance and were fragile, DNase treatment solution was carefully aspirated. Samples were then washed three times with PBS, for 20 min. A final wash with PBS supplemented with 1% A/A was performed overnight, at 60 rpm.

Macroscopic images of thymic samples and fragments (before and during the decellularization process) were taken using a camera of an iPhone X (Apple, USA). Close-up images were taken using the abovementioned camera over a SZX10 stereoscopic microscope (Olympus, Japan), through a 4x objective.

IV.3.3. Immunohistochemistry of thymic fragments

Maintenance of extracellular matrix (ECM) structure and components was evaluated through immunohistochemistry of frozen sections from thymic fragments. Native (n=2) and decellularized (n=2 for 0.2% SDS; n=1 for 0.1% SDS) samples were fixed for 3 h (or overnight) in 2% (w/v) buffered formaldehyde (Cat. #P6148, Sigma-Aldrich) with 4% (w/v) sucrose (Cat. #S7903, Sigma-Aldrich), at 4°C on a roller. Afterwards, samples were prepared for cryosectioning. Specifically, they were incubated with PBS with 4% sucrose, followed by a second incubation with PBS with 15% sucrose, both over a full

day (or overnight) at 4°C, on a roller. A third incubation was done with PBS supplemented with 15% sucrose and 7.5% gelatin (Cat. #G2500, Sigma-Aldrich) for 1 h, at 37°C, on a roller. Samples were then placed in aluminum "boats", embedded in new liquified gelatin solution (previously warmed at 37°C) and solidified at RT. At last, the aluminum boats were frozen through contact with liquid nitrogen-chilled isopentane and stored at -80°C until cryosectioning. Using a CM1860 UV cryostat (Leica, Germany), 12-µm sections were cut, placed into slides (Cat. #631-9483, VWR) and dried at RT for 30 min. Sections were then washed three times with PBS, in a Coplin Jar, for 10 min with agitation (50 rpm). Afterwards, they were blocked with a drop of PBS supplemented with 5% (v/v) bovine serum albumin (BSA) (Cat. #A8327-50ML, Sigma-Aldrich), for 30 min at RT, in a humidified chamber. Incubation of the sections with primary antibodies anti-collagen I (1:200, Cat. #ab34710, Abcam, United Kingdom), -collagen IV (1:500, Cat. #ab6311, Abcam), -fibronectin (1:1000, Cat. #ab6328, Abcam) and -laminin (1:200, Cat. #ab11575, Abcam) was performed overnight, at 4°C, in a humidified chamber. Sections were then washed three times with PBS, for 10 min with agitation. Secondary antibodies Alexa 488-conjugated goat anti-mouse (1:500, Cat. #A21121, Invitrogen, USA) and Alexa 546-conjugated goat anti-rabbit (1:500, Cat. #A11010, Invitrogen) were then added and incubated for 2 h, at RT, in a humidified chamber. Both primary and secondary antibodies were diluted in PBS with 1% BSA. Following three washes with PBS 4x, for 10 min with agitation, slides were immersed for 30 sec in a Coplin Jar containing 0.1% (v/v) Triton X-100 supplemented with 5 µg/mL DAPI (Cat. #62248, Thermo Fisher Scientific) in PBS. After two final washes of 15 min with PBS 4x and PBS 1x, respectively, slides were mounted with 50 mg/mL Propyl gallate (Cat. #P3130, Sigma-Aldrich) in PBS:glycerol (1:9) (Cat. #56-81-5, Thermo Fisher Scientific). Controls were done as described above, but without adding primary antibodies, only secondary. All images were acquired on a BX60 microscope (Olympus), with an ORCA-R2 C10600 camera (Hamamatsu, Japan), and processed using ImageJ v.2.0.0-rc-69/1.52p software.

IV.3.4. DNA quantification

DNA content removal was assessed by quantifying the amount of DNA in both native and decellularized thymic fragments, and calculating the percentage of DNA removal between both samples. Firstly, snap-frozen native and decellularized samples were subjected to lyophilization using a CoolSafe freeze dryer (LaboGene, Denmark) for 24-48 h. Afterwards, samples were roughly minced and total DNA was isolated using the DNeasy Blood & Tissue Kit (Cat. #69504, Qiagen, Netherlands), according to the manufacturer's instructions for purification of total DNA from animal tissues (spin-column protocol). Briefly, samples were weighed and the suitable amount (≤10 mg) of tissue was mixed with a digestion buffer containing proteinase K, in an 1.5 mL microcentrifuge tube. Samples were incubated at 56°C, overnight, in a thermomixer

with agitation. After lysis, buffering conditions for the lysate were adjusted in order to provide optimal DNA-binding onto the spin-column. Contaminants and enzyme inhibitors were removed in two wash steps, and DNA was then eluted in deionized water (200 µL and 50 µL, for native and decellularized samples, respectively). Eluted DNA was stored at -20°C until use or immediately measured using a NanoVue Plus spectrophotometer (Biochrom, United Kingdom).

IV.3.5. Production of thymic ECM powder

After being lyophilized as previously described in "IV.3.4. Quantification of DNA content removal", decellularized samples were subjected to a milling process using the mixer mill MM 40 (Retsch, Germany). Specifically, a 12.5 mL stainless steel milling chamber was filled with several fragments in addition to two 10 mm stainless steel milling balls. Fragments were milled for 1 min, at 28 Hz, until a powder was formed. The powder was removed with a spatula into a plastic container, sealed tightly and stored at RT.

IV.4. Results

The efficiency of the decellularization protocol here described was confirmed through three main evaluations: macroscopic visualization, maintenance of extracellular matrix (ECM) structure and composition using immunohistochemistry, and lack of nuclear content through DNA quantification (but also immunohistochemistry).

IV.4.1. Human thymic fragments showed a white-to-translucid appearance after decellularization

Following washing of thymic samples, small fragments were cut. They were selected from cleaner areas, free of the main blood vessels, coagulated parts and fat tissue (Fig.

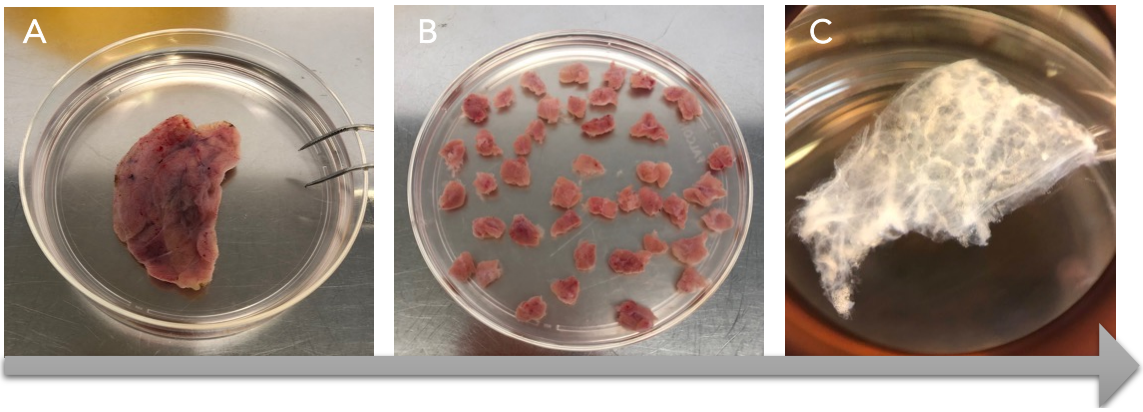

Figure IV.2. *From a pediatric thymic sample to a decellularized thymic fragment.* ***(A)*** *Thymic sample after collection and wash.* ***(B)*** *Small thymic fragments cut with a scalpel (<1 cm^3).* ***(C)*** *One thymic fragment after complete decellularization.*

IV.2). To optimize the decellularization protocol, two different SDS concentrations were tested: 0.1% and 0.2%. Macroscopic visualization is the most straightforward validation of a successful decellularization. After SDS treatment, fragments presented a white-to-translucid appearance, using both SDS concentrations. No macroscopic differences were seen between them during the decellularization procedure. Thus, at least at a macroscopic level, thymic fragments showed to be efficiently decellularized (Fig. IV.3).

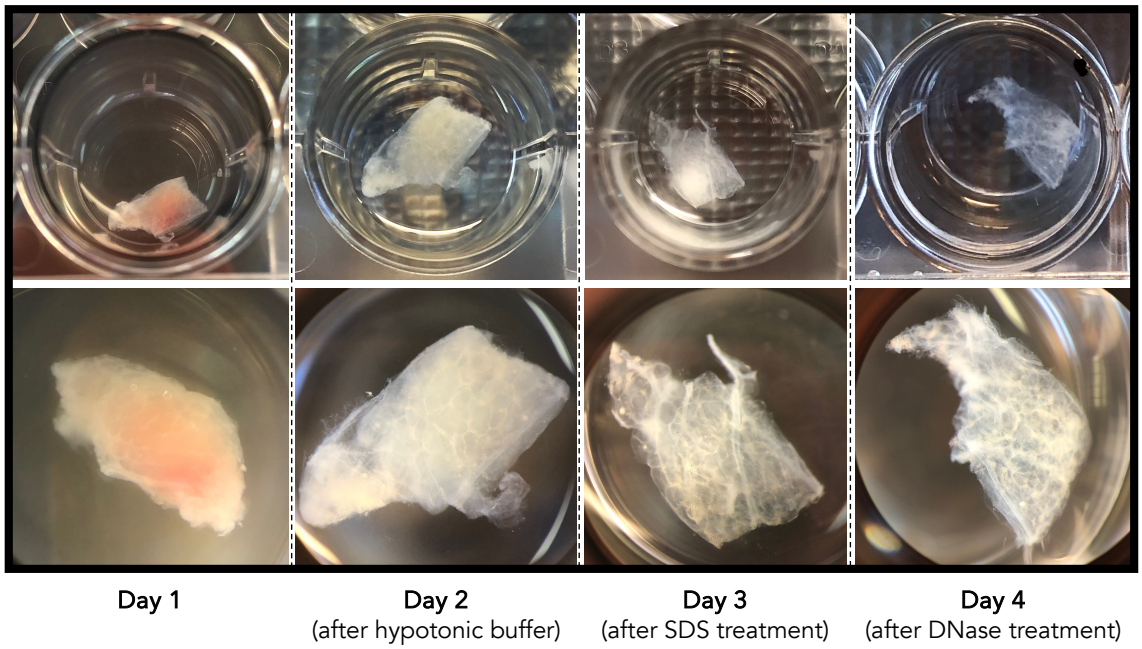

Figure IV.3. *Evolution of the decellularization process of a human thymic fragment. After complete decellularization, the fragment showed a white-to-translucid appearance. SDS: sodium dodecyl sulfate.*

IV.4.2. Thymic ECM components and structure were maintained after decellularization

Immunofluorescence analysis showed the presence of specific ECM proteins in native and decellularized samples of thymic fragments (Fig. IV.4). It also allowed observation of a lobule organization, characteristic of the thymus, present in the native samples and also maintained after decellularization (Fig. IV.4.B). No significant differences were seen between decellularized samples that were processed with 0.2% SDS or 0.1% SDS. Specifically, there seemed to be no loss of ECM components or structure when a higher detergent concentration was used. As 0.2% SDS samples seemed to have less debris (data not shown), this concentration was chosen to be further used in the decellularization protocol. Immunofluorescence analysis showed, very clearly, the presence of a considerable number of cells in native samples, through DAPI staining for the nucleic acids. After decellularization there was no DAPI staining visible, confirming the absence of cells, which is in accordance with the macroscopic visualization. Native

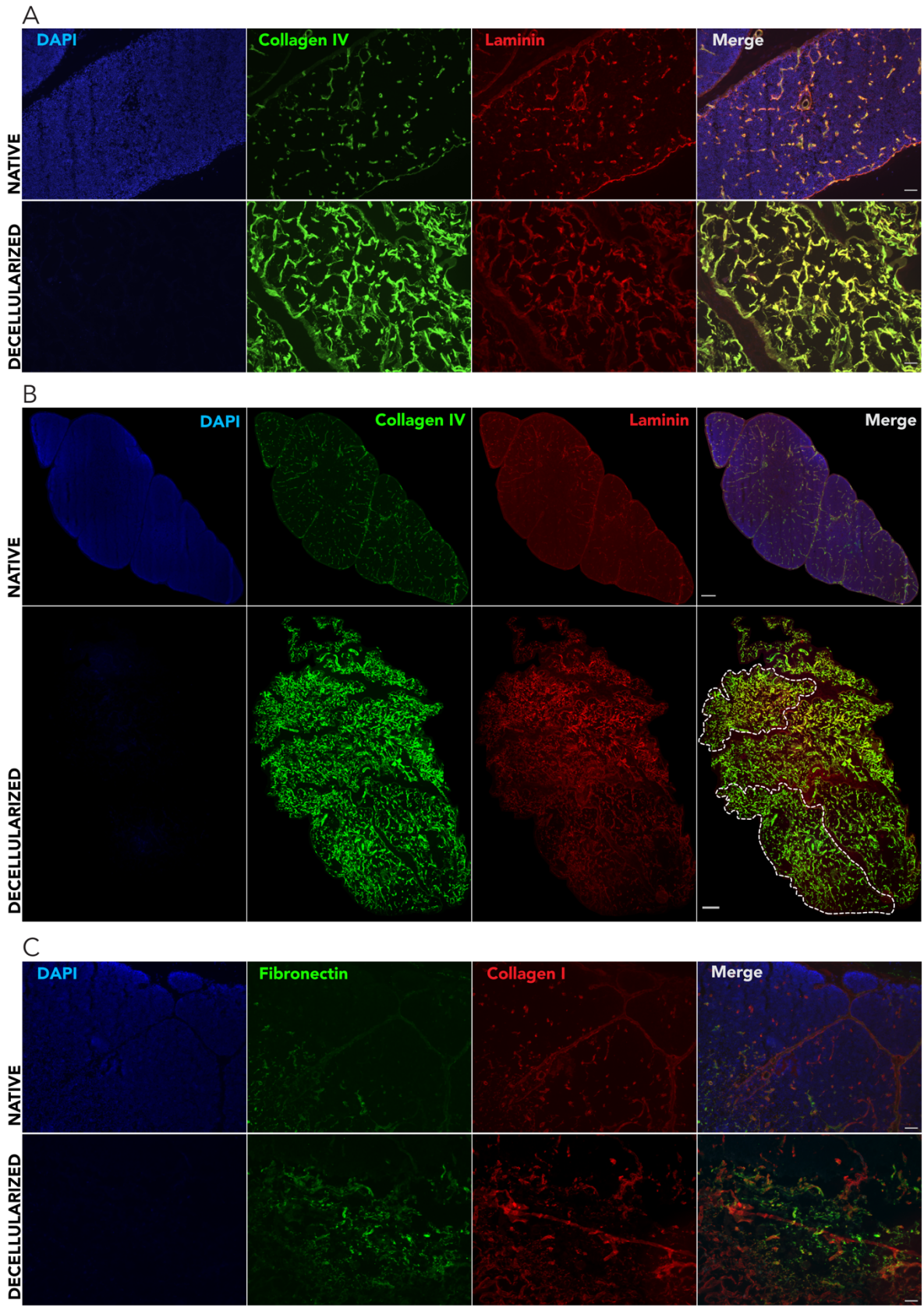

Figure IV.4. *Native and decellularized thymic fragments stained for the main extracellular matrix components.* ***(A)*** *Type IV collagen and laminin. Scale bar: 50 µm.* ***(B)*** *Panel collage presenting the full image of a section. Dashed lines highlight the maintenance of thymic structure, organized in lobules, after decellularization. Scale bar: 200 µm.* ***(C)*** *Type I collagen and fibronectin. Scale bar: 50 µm.*

samples presented the main ECM components analyzed, i.e., laminin, type IV collagen, type I collagen and, to a less extent, fibronectin. Type I collagen clearly stained thymic septa, in both native and decellularized samples (Fig. IV.4.C). Besides that, type I collagen organization in fibrils was very perceptible within the lobules. In native samples was possible to observe co-localization of both type I collagen and fibronectin, but, generally, expression of type I collagen was higher. Type I collagen also stained blood vessels very clearly as evidenced in Fig.IV.5. Fibronectin was not much abundant in native specimens. Therefore, its presence on decellularized samples was also reduced. Type IV collagen and laminin had a strong presence in native samples, that was maintained after decellularization. There was a clear spatial overlay of both ECM components, revealing their co-localization, mainly within thymic lobules. Laminin was also clearly present in thymic septa. As decellularized samples underwent a reduction in size (due to sample compaction), fluorescence intensity evidencing expression of both these ECM proteins was higher than in native samples (Fig. IV.4.A).

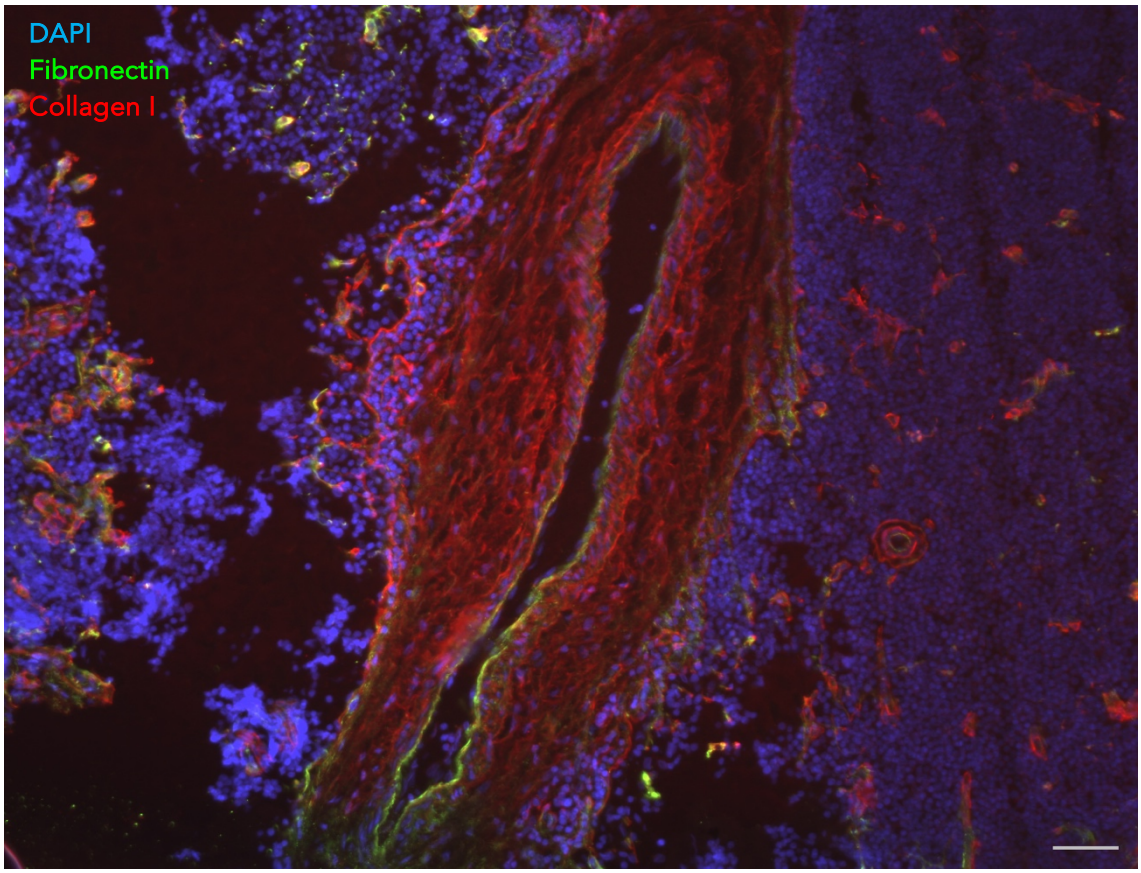

Figure IV.5. *Native thymic fragment stained for type I collagen and fibronectin, showing a blood vessel in detail. Scale bar: 50 µm.*

IV.4.3. Decellularized thymic samples showed residual DNA

Many difficulties were faced using the DNeasy Blood & Tissue Kit (Qiagen). For general tissues, up to 25 mg of tissue was recommended. For tissues with a very high number

of cells, no more than 10 mg starting material was suggested to be used (giving spleen as an example). The first attempts to isolate DNA from both native and decellularized tissues were done with wet tissue, i.e., without being lyophilized. While with decellularized samples (that, expectedly, had very low DNA content) the lysis process with proteinase K was successful, lysis of native samples was always incomplete. All Qiagen suggested recommendations were followed, which included: i) increase in lysis time from 1-3 h to overnight; ii) use of a thermomixer with agitation; iii) increase of the amount of proteinase K (from 20 µL to 40 µL). Although different kit lots were used and very low amounts of native tissue (1-2 mg) (much lower than the 10 mg given as reference for tissues with high cell numbers), proper lysis never occurred. Qiagen state, that after lysis, samples "may appear viscous, but should not be gelatinous, as it may clog the DNeasy Mini spin column". They also state that "a white precipitate may form on addition of Buffer AL and ethanol. This precipitate does not interfere with the DNeasy procedure. Some tissue types (e.g., spleen, lung) may form a gelatinous lysate after addition of Buffer AL and ethanol. In this case, vigorously shaking or vortexing the preparation is recommended." Even though the vortexing suggestion was followed, a white gelatinous lysate always formed upon addition of Buffer AL and ethanol. The presence of this gelatinous lysate (DNA not degraded) not only clogged the DNeasy Mini spin column, compromising DNA purification, but also did not allow proper DNA quantification, as only a part of the existing DNA content was purified. Bearing in mind that these results (Table IV.1) are not accurate for native samples, they clearly show absence of DNA in decellularized samples, by comparison to the native ones.

Table IV.1. *DNA quantification of wet thymic tissue samples, before and after decellularization. DNA (ng/µL) values are the mean of three measures. Nat: native; Dec: decellularized.*

Sample ID	Sample state	Sample weight (mg)	DNA (ng/µL)	Vol (µL)	DNA (ng)	ng DNA/mg wet tissue
#19	Nat	10	84.5	200	16 900	1 690
#19	Nat	7	42.5	200	8 500	1 210
#21	Nat	2.3	85.8	200	17 200	7 500
#21	Nat	1.6	58.0	200	11 600	7 250
#21	Nat	4	66.8	200	13 400	3 340
#19	Dec	48	4.7	50	235	4.9
#19	Dec	57	5.5	50	273	4.8
#20	Dec	81	6.7	50	337	4.2
#20	Dec	74	11.3	50	567	7.7

After lyophilizing the samples, the problem persisted. Even weighting insignificant quantities of native tissue (inferior to 1 mg), using an analytical scale (Pioneer PA224C) with a readability of 0.1 mg, lysis with proteinase K was never complete (Table IV.2). Results of DNA quantification from both wet and lyophilized samples are summarized in Fig. IV.6. For wet tissues, at least 99% of DNA removal was verified. For lyophilized samples, results showed, at least, a DNA removal of 95%.

Table IV.2. *DNA quantification of lyophilized thymic tissue samples, before and after decellularization. DNA (ng/µL) values are the mean of three measures. Nat: native; Dec: decellularized.*

Sample ID	Sample state	Sample weight (mg)	DNA (ng/µL)	Vol (µL)	DNA (ng)	ng DNA/mg dry tissue	µg DNA/mg dry tissue
#22	Nat	0.3	93.2	200	18 600	62 100	62.1
#22	Nat	0.5	124	200	24 700	49 500	49.5
#22	Nat	1.2	135	200	27 000	22 500	22.5
#22	Nat	1.1	189	200	37 900	34 400	34.4
#22	Dec	2	66	50	3 300	1 650	1.7
#22	Dec	1.8	82.2	50	4 100	2 280	2.3

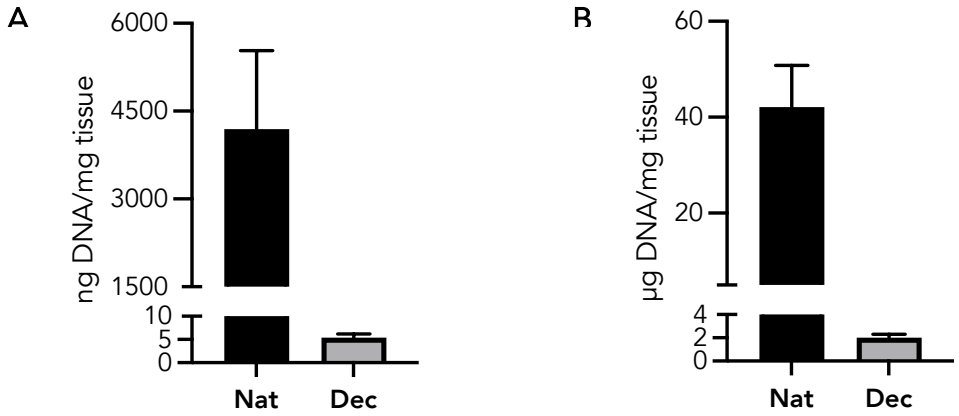

Figure IV.6. *DNA quantification of thymic tissue samples, before and after decellularization.* ***(A)*** *Wet tissue.* ***(B)*** *Dry (lyophilized) tissue. Nat: native; Dec: decellularized. Values are presented as mean±SEM.*

IV.5. Discussion

In order to provide umbilical cord blood (UCB)-derived donor lymphocyte infusions (DLI) for UCB transplant patients, a novel approach for *in vitro* T cell differentiation was hypothesized. Knowing the importance of the thymus for T cell generation and functional maturation, we attempted to take advantage of the native thymic niche clues

to improve T cell differentiation protocols *in vitro*. To this end, we developed a protocol for decellularization of human thymic tissue using individualized thymic fragments, dissected from the donated portion of the whole organ. Choosing between the use of thymic fragments or the whole thymus can have implications for future applications. In our case, the use of fragments was imposed by our collection method, namely taking advantage of samples obtained through pediatric cardiac surgeries. To access the heart, physicians need to partially remove the thymus, as this organ is localized in front of and above the heart. Nevertheless, the goal of these surgeries is to remove only the necessary amount of thymic tissue, guaranteeing there is enough thymus left to assure future thymic function[192]. Therefore, our samples, that were until now considered medical waste, were never of a whole thymus. Attaining human whole thymic samples would be difficult, as these surgeries (i.e., thymectomy) are rare and are normally due to the existence of a thymoma (which would disqualify the sample for donation)[193]. Also, the thymus is highly cellularized and does not possess central vasculature[98]. Perfusion of decellularization agents through the central vasculature is usually the decellularization method used for whole organs[90,194]. Given the absence of central vasculature of the thymus, perfusion is not an option. While diffusion (the method we used to decellularize the thymic fragments) could be an alternative, this would definitely be harder to do given the abovementioned characteristics of the thymus. Small thymic fragments benefit from a relatively easy and fast decellularization protocol, through diffusion. Still, if thymus recellularization is to be performed, using the whole organ would have the benefit of ensuring that the extracellular matrix (ECM) microarchitecture would be completely intact, i.e., that both cortical and medullary regions would be present. Both regions are essential for complete T cell differentiation. Thus, by having the whole organ, these regions would surely be represented. When having small fragments, there is the possibility that inadvertently some region could be missed. Although thymic samples collected in the hospital are not whole, they are big enough to produce hundreds of fragments. Therefore, one single donated thymic sample would be sufficient to generate numerous mini-platforms of natural scaffolds to produce T cells *in vitro*.

In this study, isolation of total DNA and its quantification turned out to be difficult to establish. While macroscopic and microscopic visualization suggested the absence of DNA, a more quantifiable assay that could confirm it was needed. The selected kit for DNA quantification did not specify requiring wet or dry (i.e., lyophilized) tissues, therefore initial attempts were performed with wet tissues. The kit manufacturer provided a table with typical DNA yields from different animal tissues. For tissue with a high number of cells, which was based on data from spleen, 5-30 µg of DNA from 10 mg of tissue were expected. Indeed, thymi are commonly defined as being densely populated with cells. However, every kit recommendation to attain a complete tissue

lysis failed, being unable to quantify existing DNA in native samples. Additionally, use of wet tissues also introduces an undesirable factor, i.e., water content. Water content has an obvious impact on sample weight. Consequently, DNA quantifications would be directly influenced by variable water content, preventing sample comparison. Therefore, further attempts were performed using lyophilized samples, to overcome these concerns. However, new (and old) issues arose. Even when using insignificant amount of native tissue (0.3-1.1 mg), complete lysis was not achieved. This was further corroborated by our DNA quantifications, where a negative correlation was observed between sample weight and DNA quantity per mg of tissue, when a positive correlation should be expected. Specifically, for the same thymic sample, 0.3 mg of native tissue presented almost 3x more DNA per mg (62.1 µg) than 1.2 mg of native tissue (22.5 µg). These results were in agreement with what was visualized during lysis, i.e., smaller fragments led to better lysis, but still incomplete. Importantly, care should be taken when comparing values of DNA quantity per weight of dry tissue to assess decellularization processes. Weight of lyophilized native tissue is not the same as weight of lyophilized decellularized tissue. After decellularization and lyophilization, decellularized thymic fragments get much lighter. Thus, several decellularized fragments are necessary to reach the weight of a single native fragment. So, ideally, for a proper comparison to be done, two separate native thymic fragments should be cut in an equal size (with the same weight). After decellularizing one of them, both should be lyophilized and undergo DNA quantification. Then, the DNA mass obtained for the native fragment should be directly compared with the DNA mass from the decellularized fragment, in order to determine the percentage of DNA removal. Although this was the initial plan, due to aforementioned technical issues, it was not feasible. Thus, in future work, the use of another kit or method to isolate DNA from these samples should be explored. Of note, criteria to confirm a successful decellularization have been previously proposed, based on immunophenotypic confirmation (lack of DAPI staining), amount of residual DNA (<50 ng/mg dry tissue) and length of existing DNA fragments (<200 bp)[90]. The importance of using dry tissue might be underestimated, since lyophilization is not always mentioned during DNA quantification descriptions[100].

Upon lyophilization of decellularized thymic samples, we also started to explore other avenues for these samples. We recognized the potential of transforming our samples into powder. Initially, we tried a simple milling process, using a pestle and mortar. However, besides being a manual technique, samples were full of static electricity, hindering their handling. Additionally, decellularized thymic samples presented very elastic properties, leading to inefficient milling and flattened samples. Therefore, we were unable to macerate them. To circumvent this hurdle, we tried an approach that had been previously used to produce ECM-derived foams and microcarriers[195]. In that particular study, cryomilling was performed, i.e., they filled a 25 mL stainless steel

milling chamber with lyophilized ECM and two 10 mm stainless steel milling balls. After submerging the milling chamber in liquid nitrogen, frozen samples were milled in a programmable laboratory ball mill system (3 min at 30 Hz). These steps were repeated until a fine powder was produced. We attempted to reproduce this system, using a similar ball mill system. Of note, an initial test was done without cryo-temperatures. Performing only a 1 min cycle, we were able to mill the ECM samples to a rough powder. New attempts should be tried, with more ECM quantity (i.e., more decellularized thymic fragments), in order to not compromise the milling chambers that are fragile and can break. Using more ECM quantity would also allow more cycles to be done and, subsequently, the production of a fine powder. On the other hand, the produced powder got contaminated with stainless steel filings from the mill chamber. Contamination coming from the balls or the chamber during milling has been previously reported, being a known characteristic of this technique[196]. Thus, in order to be used in further applications, either the process must be optimized to reduce contamination, or the stainless steel filings must be removed from the powder afterwards.

By introducing the contribution of human thymic tissue, our approach brings significant novelty to the current state of *in vitro* T cell differentiation. Our two explored strategies (whole and powdered fragments) allow for a range of possible applications for improved *in vitro* generation of T cells. Each one has their own benefits, which should be correctly taken advantage of to maximize their potential effect. Using the entire decellularized fragment opens up recellularization options, maintaining the native and unique three-dimensional (3D) structure. Possible repopulation cell types include the original thymic populations (i.e., cortical and medullary thymic epithelial cells (cTEC and mTEC, respectively)) or established cell lines that were manipulated to express Notch signaling molecules required for T cell differentiation (e.g., OP9-DLL1). While TEC repopulation would provide the ideal environment, mimicking the thymus *ex vivo*, TEC isolation is not trivial and progenitors with expansion capacity would be required to be able to reach relevant numbers for recellularization[197]. Enzymatic digestion of 5 murine thymi followed by sorting of TEC ($CD45^{-}MHC\ II^{+}EpCAM^{+}$) led to the isolation of approximately one million cells[197]. On the other hand, the use of cell lines facilitates reaching necessary numbers for recellularization, since they normally possess extensive expansion capacity and are adapted to *in vitro* conditions. Also, since the recellularized thymus would only serve as a platform for T cell differentiation *in vitro*, stromal cell lines would not be transplanted into the patient. While Notch signaling and 3D interaction with stromal cell lines have been shown to be enough for T cell differentiation[165], existing cell lines (e.g., OP9 or MS5) are currently unable to completely mimic TEC phenotype. Human mesenchymal stromal cells (MSC) are an interesting cell candidate for recellularization, since they possess extensive expansion potential *in vitro*, have been previously evaluated as a stromal compartment of the artificial thymic organoid (ATOs) system and

are common targets of genetic engineering[165,198]. Interestingly, our acellular thymic scaffolds could even be used to improve the ATOs system, developed in the previous chapter (Chapter III). Namely, we would use the scaffolds as a 3D platform for T cell differentiation to occur, injecting both MS5-hDLL4 and previously expanded UCB-derived hematopoietic stem/progenitor cells (HSPC). By providing the natural ECM of the thymus, including its growth factors and bioactive molecules, we foresee an improvement in T cell production, not only in the amount of T cells produced but also a reduction in the time needed. Additionally, immobilization of delta ligands in the scaffolds can also be explored, instead of using MS5 cells. These approaches would undoubtedly enrich the ATOs system, as the system would benefit from a native 3D structure and become xenogeneic-free.

Preserving the native structure of a decellularized tissue can also be viewed as a limitation, since its shape cannot be adapted for a specific purpose[199]. To improve their versatility, decellularized thymic fragments were also explored as ECM powder. Although there is loss of the native 3D organization, produced ECM powder becomes much more compatible with other bioengineering strategies for T cell differentiation. As a powder, it can be incorporated into an endless range of biocompatible biomaterials that can then be shaped into a specific geometry[200]. Electrospun fibers, polymeric hydrogels and 3D bioinks for bioprinting are some possibilities for thymic ECM incorporation. Electrospinning-based synthetic structures, previously improved with decellularized thymic ECM, could be employed to create an artificial environment for T cell differentiation. These nanofibers allow controlled porosity, which could be useful to replicate the medullary and cortical regions of the thymus. Fibronectin and laminin-2 were successfully immobilized in 3D meshes made of electrospun fibers as scaffolds for mTEC and cTEC, respectively[201,202]. Although being typically homogenous, hydrogels can provide a stiffness similar to biological structures, such as organs[203]. Additionally, porous hydrogels can have a controlled diffusion of bioactive molecules originated from the added decellularized thymic ECM. Nanostructured bifunctional hydrogels have been evaluated as platforms to support *in vitro* T cell differentiation, with limited success[204]. Incorporating thymic ECM in these hydrogels might be key to reaching relevant numbers of differentiated T cells *in vitro*. Finally, use of bioinks for 3D bioprinting has recently gained considerable interest, due to its versatility in creating customized scaffolds in an automated way[205]. Use of this technology for artificial thymic platforms is also expected. Supplementation of mentioned bioinks with thymic ECM would definitely increase their biological impact in applications of T cell differentiation. Decellularized thymic tissue can have a significant impact in creating *in vitro* conditions for T cell differentiation. Either as whole fragments or as soluble powder, taking advantage of the native thymus may provide the remaining stimuli required to finally reach a robust platform for reproducible mature T cell production.

V. Final Remarks and Future Directions

Recovery of functional adaptive immunity remains one of the biggest hurdles for hematopoietic cell transplantation (HCT), in what concerns survival and quality of life of transplanted patients. We have identified the obvious need to improve and accelerate T cell production for patients, specifically those receiving umbilical cord blood (UCB) transplants (UCBT), as these rely mainly on uniformly naïve T cells in UCB grafts. We tackled this issue by trying to develop a novel way to differentiate T cells *in vitro*. Inspired by the *in vivo* multi-step T cell differentiation, each chapter of this thesis contributed towards different steps of our proposed *in vitro* bioengineering approach for T cell differentiation.

Thinking of the whole therapeutic process that begins with HCT, we began our approach by taking advantage of UCB as a valuable source of hematopoietic stem/progenitor cells (HSPC) for HCT. As medical waste, their considerable availability allows reaching a great variety of human leukocyte antigen (HLA) combinations for donor-patient matching. In Chapter II, the objective was to have a clinically relevant number of starting UCB-derived HSPC, so as not to limit our T cell platform on the restricted number of isolated HSPC. Taking advantage of our established co-culture HSPC expansion system using mesenchymal stromal cells (MSC), we explored other relevant sources of supportive MSC (i.e., adipose tissue (AT) and umbilical cord matrix (UCM)) in order to maximize our HSPC expansion. Additionally, we studied our *ex vivo* HSPC expansion system in a distinctive perspective, focused on possible priming of HSPC towards the lymphoid lineage. This would allow possible development of a system joining both HSPC expansion and initial differentiation into the lymphoid line. This systematic comparison showed that UCB-derived $CD34^+$-enriched cells were more efficiently expanded, while preserving the stem/progenitor content, over a feeder layer (FL) of MSC derived from AT. Notably, a substantial population of progenitor T (proT) cells ($CD34^+CD7^+$ cells) was also expanded, demonstrating a priming effect from the supportive MSC FL. We went further by exploring if MSC FL established using serum-free (SF)/xenogeneic-free (XF) conditions, i.e., using fibrinogen-depleted human platelet lysate (HPL) instead of fetal bovine serum (FBS), would impact the already established SF co-culture system. While the expansion capacity was not affected by this alteration, we noticed a shift from hematopoietic progenitors to more differentiated cells. Still, further studies are needed to fully understand the impact of using HPL (instead of the commonly used FBS) in MSC FL establishment in what concerns its ability to support human HSPC *in vitro*. Overall, our study provides important insights concerning the possibility of expanding UCB HSPC in a co-culture system with MSC, derived from other more accessible sources than BM and in a SF/XF context, paving the way towards clinical translation. Also, the developed protocols used herein show a high compatibility with current good manufacturing practices (cGMP), since few adjustments would be needed, including the use of the CliniMACS platform (for $CD34^+$ cell

purification) and the incorporation of a clinical-grade XF hematopoietic expansion medium until a suitable fully chemically defined version can be adopted. Therefore, we were able to reach our chapter objectives of improving our HSPC expansion system by incorporating an AT-derived MSC FL, which had a double effect of supporting further HSPC and promoting lymphoid priming with the generation of a substantial proT cell population.

Having increased the availability of HSPC and lymphoid-primed progenitors from UCB in the previous section, in Chapter III, we focused our efforts in establishing an *in vitro* protocol for T cell differentiation, with the aim of reaching single positive (SP) CD8 T cells. While our approach is based on introducing the native thymic microenvironment, we started by taking advantage of existing advanced methods for T cell generation. Recognizing the importance of a three-dimensional (3D) structure present in the thymus during *in vivo* T cell generation, we chose to base our differentiation on the artificial thymic organoid (ATOs) system. This would allow a direct comparison to our bioengineered approach, since this system is able to induce T cell maturation, producing a high yield of SP CD8 T cells. We were successful in establishing the ATOs system, being able to generate SP CD8 T cells. Due to our promising results in Chapter II, we explored the improvement of the ATOs system by combining it with our HSPC expansion co-culture system, expecting our lymphoid priming to accelerate *in vitro* T cell differentiation. Impressively, HSPC expanded with our co-culture system significantly increased the yield (i.e., 5-fold) of $CD3^{+}TCR\alpha\beta^{+}CD8^{+}$ T cells, increasing productivity of SP CD8 T cells, which considerably impacts the field. By demonstrating highly competitive differentiation yields and expanding cell scalability through the use of expanded HSPC, our improvement facilitates production of expected numerous doses of T cells required for patient infusion. In terms of process translation, the ATOs system is compatible with SF and XF reagents, keeping our aim of reaching great compatibility with cGMP. However, organoids present in this system still use a murine cell line for Notch ligand presentation (e.g., MS5-hDLL4) and 3D support. We consider that substituting MS5-hDLL4 with a human equivalent would finally allow T cell differentiation to become completely XF, while possibly showing benefits to the differentiation itself. Knowing the contribution of MSC to the hematopoietic niche and taking advantage of their use in our HSPC expansion co-culture system, development of a MSC cell line expressing DLL4 would be an excellent candidate to test. Also, as expected, we verified the lack of process scalability of the ATOs system, which is based on cell aggregates that have a very limited size restriction due to nutrient diffusion. We foresaw great potential in our proposed bioengineered approach, since the native thymic structure is much more organized as a scaffold and presents important differentiation signals that ATOs cannot replicate. Still, we confirmed that by using our

lymphoid-primed expanded HSPC, *in vitro* T cell differentiation can be accelerated, experimentally validating our HSPC expansion co-culture step.

After establishing an advanced T cell differentiation protocol with successful production of SP CD8 T cells and showing that our HSPC co-culture expansion system is able to accelerate differentiation, in the following chapter we tackled the incorporation of human thymic microenvironment cues. Although several studies explore murine thymi, we ambitioned working with human thymi to reach a breakthrough in the field. Our proposed novel bioengineered approach aimed at using decellularized thymic fragments as scaffolds to promote T cell differentiation. We were able to secure thymic fragments from pediatric patients undergoing cardiac surgery. To manipulate and use these fragments as scaffolds, we worked to establish a decellularization protocol, with optimization of detergent concentrations. Effective decellularization was achieved, maintaining the native macroscopic thymic structures (e.g., lobules), relevant extracellular matrix (ECM) molecules and removing most genomic contaminants. To our knowledge, this is the first successful attempt at decellularizing human thymic tissue. To further increase the versatility of decellularized human thymic fragments, other tissue processing techniques were explored. Ball milling was chosen to macerate decellularized thymic fragments into a powder. Overall, we were able to develop a workflow for decellularization of human thymic fragments, originating entire fragments as whole scaffolds or powdered thymic decellularized ECM. In this way, we completed our objective of producing the desired scaffold to incorporate in our proposed bioengineered approach. Efforts should be made in determining if important regions of the thymus (i.e., medullary and cortical) are present in our fragmented samples. The impact of using human thymic tissue is very significant, contributing towards making our approach completely XF.

Throughout each chapter, individual sections of our newly proposed bioengineering approach were developed. Considering our ambitious goal, we consider to have made substantial contributions to the field. To complete this approach, all developed sections have to be combined in a single workflow. Altogether, UCB-derived HSPC would first be expanded in our co-culture system, increasing their number and promoting their early lymphoid differentiation potential. Then, primed expanded HSPC would be infused into a previously repopulated thymic scaffold with a cell type expressing Notch signaling. Infused cells would be maintained in the scaffold to promote their differentiation and maturation into T cells. Finally, batches of produced T cells could potentially be isolated from the scaffold, being ready to be infused into a HCT patient during their recovery. However, before joining all pieces, recellularization of thymic scaffolds must be assured. Besides MS5-hDLL4 or its human equivalent (i.e., MSC-DLL4), other cell types of interest include isolated thymic epithelial cells (TEC) or induced pluripotent stem cell-derived TEC. When completing this task, our approach

can finally be tested as a whole and compared with other existing T cell differentiation platforms in what concerns cell yields.

VI. Publications and Communications

Publications in Peer-Reviewed International Scientific Journals

Bucar S, Branco ADM, Mata MF, Milhano JC, Caramalho Í, Cabral JMS, Fernandes-Platzgummer A, Lobato da Silva C. Influence of the mesenchymal stromal cell source on the hematopoietic supportive capacity of umbilical cord blood-derived $CD34^+$-enriched cells. *Stem Cell Research & Therapy.* 12:399 (2021). https://doi.org/10.1186/s13287-021-02474-8

Branco A, Bucar S, Moura-Sampaio J, Lilaia C, Cabral JMS, Fernandes-Platzgummer A, Lobato da Silva C. Tailored Cytokine Optimization for ex vivo Culture Platforms Targeting the Expansion of Human Hematopoietic Stem/Progenitor Cells. *Frontiers in Bioengineering and Biotechnology*. 8:573282 (2020). doi: 10.3389/fbioe.2020.573282

Pinto CIG, Bucar S, Alves V, Fonseca A, Abrunhosa AJ, Silva CL, Guerreiro JF, Mendes F. Copper-64 Chloride Exhibits Therapeutic Potential in Three-Dimensional Cellular Models of Prostate Cancer. *Frontiers in Molecular Biosciences.* 7:609172 (2020). doi: 10.3389/fmolb.2020.609172

Poster Communications in Conferences

Bucar S, Branco A, Mata M, Lilaia C, Caramalho Í, Cabral JMS, Fernandes-Platzgummer A, Lobato da Silva C. Ex-vivo Hematopoietic Supportive Capacity Of Mesenchymal Stromal Cells From Different Tissues. *IST PhD Open Days 2020*. Lisbon, Portugal, October 2020

Bucar S, Branco A, Lilaia C, Cabral JMS, Fernandes-Platzgummer A, Lobato da Silva C. Promoting the lymphoid potential of human hematopoietic stem/progenitor cells through a co-culture system with mesenchymal stem/stromal cells. *11th International Meeting of the Portuguese Society for Stem Cells and Cell Therapies*. Lisbon, Portugal, October 2019

VII. References

1. Doulatov, S., Notta, F., Laurenti, E. & Dick, J. E. Hematopoiesis: A human perspective. *Cell Stem Cell* **10**, 120–136 (2012).

2. Liggett, L. A. & Sankaran, V. G. Unraveling Hematopoiesis through the Lens of Genomics. *Cell* **182**, 1384–1400 (2020).

3. Till, J. E. & McCulloch, E. A. A direct measurement of the radiation sensitivity of normal mouse bone marrow cells. *Radiat. Res.* **14**, 213–222 (1961).

4. Dzierzak, E. & Speck, N. A. Of lineage and legacy: The development of mammalian hematopoietic stem cells. *Nat. Immunol.* **9**, 129–136 (2008).

5. Ivanovs, A. *et al.* Human haematopoietic stem cell development: From the embryo to the dish. *Dev.* **144**, 2323–2337 (2017).

6. Morrison, S. J. & Weissman, I. L. The long-term repopulating subset of hematopoietic stem cells is deterministic and isolatable by phenotype. *Immunity* **1**, 661–673 (1994).

7. Morrison S. J, Wandycz A. M, Hemmati H.D, Wright D.E & Weissman I.L. Identification of a lineage of multipotent hematopoietic progenitors. *Development* **124**, 1929–1939 (1997).

8. Velten, L. *et al.* Human haematopoietic stem cell lineage commitment is a continuous process. *Nat. Cell Biol.* **19**, 271–281 (2017).

9. Laurenti, E. & Göttgens, B. From haematopoietic stem cells to complex differentiation landscapes. *Nature* **553**, 418–426 (2018).

10. Notta, F. *et al.* Isolation of single human hematopoietic stem cells capable of long-term multilineage engraftment. *Science (80-.).* **333**, 218–221 (2011).

11. Dorrell, C., Gan, O. I., Pereira, D. S., Hawley, R. G. & Dick, J. E. Expansion of human cord blood CD34+CD38- cells in ex vivo culture during retroviral transduction without a corresponding increase in SCID repopulating cell (SRC) frequency: Dissociation of SRC phenotype and function. *Blood* **95**, 102–110 (2000).

12. Fares, I. *et al.* EPCR expression marks UM171-expanded CD34+ cord blood stem cells. *Blood* **129**, 3344–3351 (2017).

13. Tomellini, E. *et al.* Integrin-α3 Is a Functional Marker of Ex Vivo Expanded Human Long-Term Hematopoietic Stem Cells. *Cell Rep.* **28**, 1063-1073.e5 (2019).

14. Hughes, M. R. *et al.* A sticky wicket: Defining molecular functions for CD34 in hematopoietic cells. *Exp. Hematol.* **86**, 1–14 (2020).

15. Panch, S. R., Szymanski, J., Savani, B. N. & Stroncek, D. F. Sources of Hematopoietic Stem and Progenitor Cells and Methods to Optimize Yields for Clinical Cell Therapy. *Biol. Blood Marrow Transplant.* **23**, 1241–1249 (2017).

16. Goodman, J. W. & Hodgson, G. S. Evidence for stem cells in the peripheral blood of mice. *Blood* **19**, 702–714 (1962).

17. Metcalf, D. The colony stimulating factors discovery, development, and clinical applications. *Cancer* **65**, 2185–2195 (1990).

18. Korbling, M., Przepiorka, D., Gajewski, J., Champlin, R. E. & Chan, K. W. With first successful allogeneic transplantations of apheresis-derived hematopoietic progenitor cells reported, can the recruitment of volunteer matched, unrelated stem cell donors be expanded substantially? [1]. *Blood* **86**, 1235 (1995).

19. Broxmeyer, H. E. *et al.* Human umbilical cord blood as a potential source of transplantable hematopoietic stem/progenitor cells. *Proc. Natl. Acad. Sci. U. S. A.* **86**, 3828–3832 (1989).

20. Gluckman, E. & Rocha, V. History of the clinical use of umbilical cord blood hematopoietic cells. *Cytotherapy* **7**, 219–227 (2005).

21. Bazinet, A. & Popradi, G. A general practitioner's guide to hematopoietic stem-cell transplantation. *Curr. Oncol.* **26**, 187–191 (2019).

22. Dickinson, A. M. *et al.* Graft-versus-leukemia effect following hematopoietic stem cell transplantation for leukemia. *Front. Immunol.* **8**, (2017).

23. Passweg, J. R. *et al.* Hematopoietic cell transplantation and cellular therapies in Europe 2021. The second year of the SARS-CoV-2 pandemic. A Report from the EBMT Activity Survey. *Bone Marrow Transplant.* **58**, 647–658 (2023).

24. Shah, N. *et al.* Hematopoietic Stem Cell Transplantation for Multiple Myeloma: Guidelines from the American Society for Blood and Marrow Transplantation. *Biol. Blood Marrow Transplant.* **21**, 1155–1166 (2015).

25. Majhail, N. S. *et al.* Indications for Autologous and Allogeneic Hematopoietic Cell Transplantation: Guidelines from the American Society for Blood and Marrow Transplantation. *Biol. Blood Marrow Transplant.* **21**, 1863–1869 (2015).

26. Pasqualini, C. *et al.* Tandem high-dose chemotherapy with thiotepa and busulfan-melphalan and autologous stem cell transplantation in very high-risk neuroblastoma patients. *Bone Marrow Transplant.* **51**, 227–231 (2016).

27. Gajjar, A. *et al.* Risk-adapted craniospinal radiotherapy followed by high-dose chemotherapy and stem-cell rescue in children with newly diagnosed medulloblastoma (St Jude Medulloblastoma-96): long-term results from a prospective, multicentre trial. *Lancet Oncol.* **7**, 813–820 (2006).

28. Peinemann, F. *et al.* First-line matched related donor hematopoietic stem cell transplantation compared to immunosuppressive therapy in acquired severe aplastic anemia. *PLoS One* **6**, (2011).

29. Dalle, J. H. & de Latour, R. P. Allogeneic hematopoietic stem cell transplantation for inherited bone marrow failure syndromes. *Int. J. Hematol.* **103**, 373–379 (2016).

30. Gluckman, E. *et al.* Sickle cell disease: an international survey of results of HLA-identical sibling hematopoietic stem cell transplantation. *Blood* **129**, 1548–1556 (2017).

31. Baronciani, D. *et al.* Hemopoietic stem cell transplantation in thalassemia: A report from the European Society for Blood and Bone Marrow Transplantation Hemoglobinopathy Registry, 2000-2010. *Bone Marrow Transplant.* **51**, 536–541 (2016).

32. Wahlstrom, J. T., Dvorak, C. C. & Cowan, M. J. Hematopoietic Stem Cell Transplantation for Severe Combined Immunodeficiency. *Curr. Pediatr. Rep.* **3**, 1–10 (2015).

33. Krivit, W., Sung, J. H., Shapiro, E. G. & Lockman, L. A. Microglia: The Effector Cell for Reconstitution of the Central Nervous System following Bone Marrow Transplantation for Lysosomal and Peroxisomal Storage Diseases. *Cell Transplant.* **4**, 385–392 (1995).

34. Hügle, T. & Daikeler, T. Stem cell transplantation for autoimmune diseases. *Haematologica* **95**, 185–188 (2010).

35. Mancardi, G., Sormani, M. P., Muraro, P. A., Boffa, G. & Saccardi, R. Intense immunosuppression followed by autologous haematopoietic stem cell transplantation as a therapeutic strategy in aggressive forms of multiple sclerosis. *Mult. Scler. J.* **24**, 245–255 (2018).

36. Wolff, S. N. Second hematopoietic stem cell transplantation for the treatment of graft failure, graft rejection or relapse after allogeneic transplantation. *Bone Marrow Transplant.* **29**, 545–552 (2002).

37. Berglund, S., Magalhaes, I., Gaballa, A., Vanherberghen, B. & Uhlin, M. Advances in umbilical cord blood cell therapy: the present and the future. *Expert Opin. Biol. Ther.* **17**, 691–699 (2017).

38. Szabolcs, P. & Niedzwiecki, D. Immune reconstitution after unrelated cord blood transplantation. *Cytotherapy* **9**, 111–122 (2007).

39. Ballen, K. K., Gluckman, E. & Broxmeyer, H. E. Umbilical cord blood transplantation: the first 25 years and beyond. *Blood* **122**, 491–498 (2013).

40. Munoz, J. *et al.* Concise Review: Umbilical Cord Blood Transplantation: Past, Present, and Future. *Stem Cells Transl. Med.* **3**, 1435–1443 (2014).

41. Stiff, P. J. *et al.* Cohort-Controlled Comparison of Umbilical Cord Blood Transplantation Using Carlecortemcel-L, a Single Progenitor–Enriched Cord Blood, to Double Cord Blood Unit Transplantation. *Biol. Blood Marrow Transplant.* **24**, 1463–1470 (2018).

42. Kindwall-Keller, T. L. & Ballen, K. K. Alternative Donor Graft Sources for Adults with Hematologic Malignancies: A Donor for All Patients in 2017! *Oncologist* **22**, 1125–1134 (2017).

43. Zimran, E., Papa, L. & Hoffman, R. Ex vivo expansion of hematopoietic stem cells: Finally transitioning from the lab to the clinic. *Blood Rev.* **50**, 100853 (2021).

44. Bozhilov, Y. K., Hsu, I., Brown, E. J. & Wilkinson, A. C. In Vitro Human Haematopoietic Stem Cell Expansion and Differentiation. *Cells* **12**, 896 (2023).

45. Costa, M. H. G., de Soure, A. M., Cabral, J. M. S., Ferreira, F. C. & da Silva, C. L.

Hematopoietic Niche – Exploring Biomimetic Cues to Improve the Functionality of Hematopoietic Stem/Progenitor Cells. *Biotechnol. J.* **13**, (2018).

46. Wilkinson, A. C., Igarashi, K. J. & Nakauchi, H. Haematopoietic stem cell self-renewal in vivo and ex vivo. *Nat. Rev. Genet.* **21**, 541–554 (2020).

47. Li, J. *et al.* Development and clinical advancement of small molecules for ex vivo expansion of hematopoietic stem cell. *Acta Pharm. Sin. B* **12**, 2808–2831 (2022).

48. Peled, T. *et al.* Nicotinamide, a SIRT1 inhibitor, inhibits differentiation and facilitates expansion of hematopoietic progenitor cells with enhanced bone marrow homing and engraftment. *Exp. Hematol.* **40**, 342-355.e1 (2012).

49. Horwitz, M. E. *et al.* Umbilical cord blood expansion with nicotinamide provides long-term multilineage engraftment. *J. Clin. Invest.* **124**, 3121–3128 (2014).

50. Horwitz, M. E. *et al.* Phase I/II Study of Stem-Cell Transplantation Using a Single Cord Blood Unit Expanded Ex Vivo With Nicotinamide. *J. Clin. Oncol.* **37**, 367–374 (2018).

51. Horwitz, M. E. *et al.* Omidubicel vs standard myeloablative umbilical cord blood transplantation: results of a phase 3 randomized study. *Blood* **138**, 1429–1440 (2021).

52. FDA approves cord-blood therapy. *Nat. Biotechnol.* **41**, 589–589 (2023).

53. Khan, D. M. I. O., Karmaus, P. W. F., Bach, A., Crawford, R. B. & Kaminski, N. E. An in vitro model of human hematopoiesis identifies a regulatory role for the aryl hydrocarbon receptor. *Blood Adv.* **7**, 6253–6265 (2023).

54. Boitano, A. E. *et al.* Aryl hydrocarbon receptor antagonists promote the expansion of human hematopoietic stem cells. *Science (80-.).* **329**, 1345–1348 (2010).

55. Wagner, J. E. *et al.* Phase I/II Trial of StemRegenin-1 Expanded Umbilical Cord Blood Hematopoietic Stem Cells Supports Testing as a Stand-Alone Graft. *Cell Stem Cell* **18**, 144–155 (2016).

56. Wagner, J. E. *et al.* Phase 2 Trials with Mgta-456, Single Cord Blood Units (CBU) Expanded with an Aryl Hydrocarbon Receptor (AHR) Antagonist, Demonstrate Uniform Engraftment and Rapid Hematopoietic Recovery in Patients Following Myeloablative or Non-Myeloablative Conditioning. *Blood* **130**, 662–662 (2017).

57. Stefanski, H. *et al.* Mgta-456, an Aryl Hydrocarbon Receptor (AHR) Antagonist Based Expansion of CD34+ Hematopoietic Stem Cells (HSC), Permits Selection of Better HLA Matched Cord Blood Units (CBUs) and Promotes Faster Neutrophil Recovery and Uniform Engraftment with Potential. *Blood* **134**, 804–804 (2019).

58. Orchard, P. J. *et al.* Mgta-456 Cell Therapy in Inherited Metabolic Disease (IMD) Yields Rapid and Durable Long-Term Improvement of Disease-Specific Outcomes in a Phase 2 Trial. *Biol. Blood Marrow Transplant.* **26**, S19 (2020).

59. Fares, I. *et al.* Pyrimidoindole derivatives are agonists of human hematopoietic stem cell self-renewal. *Science (80-.).* **345**, 1509–1512 (2014).

60. Cohen, S. *et al.* Hematopoietic stem cell transplantation using single UM171-expanded cord blood: a single-arm, phase 1–2 safety and feasibility study. *Lancet Haematol.* **7**, e134–e145 (2020).

61. Harrell, C. R. *et al.* Molecular mechanisms responsible for therapeutic potential of mesenchymal stem cell-derived secretome. *Cells* **8**, (2019).

62. Pinho, S. & Frenette, P. S. Haematopoietic stem cell activity and interactions with the niche. *Nat. Rev. Mol. Cell Biol.* **20**, 303–320 (2019).

63. García-Fernández, C., López-Fernández, A., Borrós, S., Lecina, M. & Vives, J. Strategies for large-scale expansion of clinical-grade human multipotent mesenchymal stromal cells. *Biochem. Eng. J.* **159**, 107601 (2020).

64. Kusadasi, N., Koevoet, J., van Soest, P. & Ploemacher, R. Stromal support augments extended long-term ex vivo expansion of hemopoietic progenitor cells. *Leukemia* **15**, 1347–1358 (2001).

65. Wang, J. F. *et al.* Mesenchymal stem/progenitor cells in human umbilical cord blood as support for ex vivo expansion of CD34+ hematopoietic stem cells and for chondrogenic differentiation. *Haematologica* **89**, 837–844 (2004).

66. Da Silva, C. L. *et al.* A human stromal-based serum-free culture system supports the ex vivo expansion/maintenance of bone marrow and cord blood hematopoietic stem/progenitor cells. *Exp. Hematol.* **33**, 828–835 (2005).

67. Gonçalves, R., Lobato da Silva, C., Cabral, J. M. S., Zanjani, E. D. & Almeida-Porada, G. A Stro-1+ human universal stromal feeder layer to expand/maintain human bone marrow hematopoietic stem/progenitor cells in a serum-free culture system. *Exp. Hematol.* **34**, 1353–1359 (2006).

68. da Silva, C. L. *et al.* Dynamic cell-cell interactions between cord blood haematopoietic progenitors and the cellular niche are essential for the expansion of CD34 + , CD34 + CD38 − and early lymphoid CD7 + cells. *J. Tissue Eng. Regen. Med.* **4**, 149–158 (2010).

69. Jing, D. *et al.* Hematopoietic stem cells in co-culture with mesenchymal stromal cells - modeling the niche compartments in vitro. *Haematologica* **95**, 542–550 (2010).

70. Freund, D. *et al.* Polarization of human hematopoietic progenitors during contact with multipotent mesenchymal stromal cells: Effects on proliferation and clonogenicity. *Stem Cells Dev.* **15**, 815–829 (2006).

71. Corselli, M. *et al.* Perivascular support of human hematopoietic stem/progenitor cells. *Blood* **121**, 2891–2901 (2013).

72. McNiece, I. K., Harrington, J., Turney, J., Kellner, J. & Shpall, E. J. Ex vivo expansion of cord blood mononuclear cells on mesenchymal stem cells. *Cytotherapy* **6**, 311–317 (2004).

73. De Lima, M. *et al.* Cord-blood engraftment with ex vivo mesenchymal-cell coculture. *N. Engl. J. Med.* **367**, 2305–2315 (2012).

74. Chaudhry, M. S., Velardi, E., Malard, F. & van den Brink, M. R. M. Immune Reconstitution after Allogeneic Hematopoietic Stem Cell Transplantation: Time To T Up the Thymus. *J. Immunol.* **198**, 40–46 (2017).

75. Kumar, B. V., Connors, T. J. & Farber, D. L. Human T Cell Development, Localization, and Function throughout Life. *Immunity* **48**, 202–213 (2018).

76. Gameiro, J., Nagib, P. & Verinaud, L. The thymus microenvironment in regulating thymocyte differentiation. *Cell Adh. Migr.* **4**, 382–390 (2010).

77. Radtke, F., Fasnacht, N. & MacDonald, H. R. Notch Signaling in the Immune System. *Immunity* **32**, 14–27 (2010).

78. Roh, K.-H. & Roy, K. Engineering approaches for regeneration of T lymphopoiesis. *Biomater. Res.* **20**, (2016).

79. Chung, B. *et al.* Engineering the human thymic microenvironment to support thymopoiesis in vivo. *Stem Cells* **32**, 2386–2396 (2014).

80. Liu, C., Lan, Y., Liu, B., Zhang, H. & Hu, H. T Cell Development: Old Tales Retold By Single-Cell RNA Sequencing. *Trends Immunol.* **42**, 165–175 (2021).

81. Mariuzza, R. A., Agnihotri, P. & Orban, J. The structural basis of T-cell receptor (TCR) activation: An enduring enigma. *J. Biol. Chem.* **295**, 914–925 (2020).

82. Laidlaw, B. J., Craft, J. E. & Kaech, S. M. The multifaceted role of CD4+ T cells in CD8+ T cell memory. *Nat. Rev. Immunol.* **16**, 102–111 (2016).

83. Kaech, S. M. & Ahmed, R. Memory CD8+ T cell differentiation: Initial antigen encounter triggers a developmental program in naïve cells. *Nat. Immunol.* **2**, 415–422 (2001).

84. Kaech, S. M. & Cui, W. Transcriptional control of effector and memory CD8+ T cell differentiation. *Nat. Rev. Immunol.* **12**, 749–761 (2012).

85. Peloso, A. *et al.* Current achievements and future perspectives in whole-organ bioengineering. *Stem Cell Res. Ther.* **6**, 107 (2015).

86. Schladt, D. P. & Israni, A. K. OPTN/SRTR 2021 Annual Data Report: Introduction. *Am. J. Transplant.* **23**, S12–S20 (2023).

87. Tapias, L. F. & Ott, H. C. Decellularized scaffolds as a platform for bioengineered organs. *Curr. Opin. Organ Transplant.* **19**, 145–152 (2014).

88. Parmaksiz, M., Dogan, A., Odabas, S., Elçin, A. E. & Elçin, Y. M. Clinical applications of decellularized extracellular matrices for tissue engineering and regenerative medicine. *Biomed. Mater.* **11**, 022003 (2016).

89. Hynes, R. O. Extracellular matrix: not just pretty fibrils. *Science (80-.).* **326**, 1216–1219 (2009).

90. Crapo, P. M., Gilbert, T. W. & Badylak, D. V. M. An overview of tissue and whole organ

decellularization processes. *Biomaterials* **32**, 3233–3243 (2011).

91. Choudhury, D., Yee, M., Sheng, Z. L. J., Amirul, A. & Naing, M. W. Decellularization systems and devices: State-of-the-art. *Acta Biomater.* **115**, 51–59 (2020).

92. Badylak, S. F., Voytik, S. L., Kraine, M. R. & Simmons, C. The use of xenogeneic small intestinal submucosa as a biomaterial for Achille's tendon repair in a dog model. *J. Biomed. Mater. Res.* **29**, 977–985 (1995).

93. Ott, H. C. *et al.* Perfusion-decellularized matrix: using nature's platform to engineer a bioartificial heart. *Nat. Med.* **14**, 213–221 (2008).

94. Guyette, J. P. *et al.* Bioengineering Human Myocardium on Native Extracellular Matrix. *Circ. Res.* **118**, 56–72 (2016).

95. Barakat, O. *et al.* Use of decellularized porcine liver for engineering humanized liver organ. *J. Surg. Res.* **173**, e11–e25 (2012).

96. Sullivan, D. C. *et al.* Decellularization methods of porcine kidneys for whole organ engineering using a high-throughput system. *Biomaterials* **33**, 7756–7764 (2012).

97. Fan, Y. *et al.* Bioengineering Thymus Organoids to Restore Thymic Function and Induce Donor-Specific Immune Tolerance to Allografts. *Mol. Ther.* **23**, 1262–77 (2015).

98. Hun, M. *et al.* Native thymic extracellular matrix improves in vivo thymic organoid T cell output, and drives in vitro thymic epithelial cell differentiation. *Biomaterials* **118**, 1–15 (2017).

99. Campinoti, S. *et al.* Reconstitution of a functional human thymus by postnatal stromal progenitor cells and natural whole-organ scaffolds. *Nat. Commun.* **11**, (2020).

100. Asnaghi, M. A. *et al.* Thymus Extracellular Matrix-Derived Scaffolds Support Graft-Resident Thymopoiesis and Long-Term In Vitro Culture of Adult Thymic Epithelial Cells. *Adv. Funct. Mater.* **31**, (2021).

101. Zeleniak, A. *et al.* De novo construction of T cell compartment in humanized mice engrafted with iPSC-derived thymus organoids. *Nat. Methods* **19**, 1306–1319 (2022).

102. Zeleniak, A. *et al.* A tissue-engineered artificial human thymus from human iPSCs to study T cell immunity. *Nat. Methods* **19**, 1191–1192 (2022).

103. Oran, B. & Shpall, E. Umbilical cord blood transplantation: a maturing technology. *Hematology* **2012**, 215–222 (2012).

104. Sideri, A. *et al.* An overview of the progress on double umbilical cord blood transplantation. *Haematologica* **96**, 1213–1220 (2011).

105. Kiernan, J. *et al.* Clinical Studies of Ex Vivo Expansion to Accelerate Engraftment After Umbilical Cord Blood Transplantation: A Systematic Review. *Transfus. Med. Rev.* **31**, 173–182 (2017).

106. Andrade, P. Z. *et al.* Ex vivo expansion of cord blood haematopoietic stem/progenitor cells under physiological oxygen tensions: clear-cut effects on cell proliferation, differentiation and metabolism. *J. Tissue Eng. Regen. Med.* **9**, 1172–1181 (2015).

107. Branco, A. *et al.* Tailored Cytokine Optimization for ex vivo Culture Platforms Targeting the Expansion of Human Hematopoietic Stem/Progenitor Cells. *Front. Bioeng. Biotechnol.* **8**, 1–21 (2020).

108. Galipeau, J. & Sensébé, L. Mesenchymal Stromal Cells: Clinical Challenges and Therapeutic Opportunities. *Cell Stem Cell* **22**, 824–833 (2018).

109. Brown, C. *et al.* Mesenchymal stem cells: Cell therapy and regeneration potential. *J. Tissue Eng. Regen. Med.* **13**, 1738–1755 (2019).

110. Bunnell, B. A., Flaat, M., Gagliardi, C., Patel, B. & Ripoll, C. Adipose-derived stem cells: Isolation, expansion and differentiation. *Methods* **45**, 115–120 (2008).

111. Han, J. *et al.* Adipose tissue is an extramedullary reservoir for functional hematopoietic stem and progenitor cells. *Blood* **115**, 957–964 (2010).

112. Kilroy, G. E. *et al.* Cytokine profile of human adipose-derived stem cells: Expression of angiogenic, hematopoietic, and pro-inflammatory factors. *J. Cell. Physiol.* **212**, 702–709 (2007).

113. Andreeva, E. R. *et al.* Human adipose-tissue derived stromal cells in combination with hypoxia effectively support ex vivo expansion of cord blood haematopoietic progenitors. *PLoS One* **10**, 1–14 (2015).

114. Andreeva, E. *et al.* Adipose tissue-derived stromal cells retain immunosuppressive and angiogenic activity after coculture with cord blood hematopoietic precursors. *Eur. J. Cell Biol.* **99**, 151069 (2020).

115. Simões, I. N. *et al.* Human mesenchymal stem cells from the umbilical cord matrix: Successful isolation and ex vivo expansion using serum-/xeno-free culture media. *Biotechnol. J.* **8**, 448–458 (2013).

116. Zhao, D. *et al.* Hypoxia with Wharton's jelly mesenchymal stem cell coculture maintains stemness of umbilical cord blood-derived CD34 + cells. *Stem Cell Res. Ther.* **9**, 1–11 (2018).

117. Kern, S., Eichler, H., Stoeve, J., Klüter, H. & Bieback, K. Comparative Analysis of Mesenchymal Stem Cells from Bone Marrow, Umbilical Cord Blood, or Adipose Tissue. *Stem Cells* **24**, 1294–1301 (2006).

118. Jin, H. J. *et al.* Comparative analysis of human mesenchymal stem cells from bone marrow, adipose tissue, and umbilical cord blood as sources of cell therapy. *Int. J. Mol. Sci.* **14**, 17986–18001 (2013).

119. Hemeda, H., Giebel, B. & Wagner, W. Evaluation of human platelet lysate versus fetal bovine serum for culture of mesenchymal stromal cells. *Cytotherapy* **16**, 170–180 (2014).

120. Dos Santos, F. *et al.* Ex vivo expansion of human mesenchymal stem cells: A more effective cell proliferation kinetics and metabolism under hypoxia. *J. Cell. Physiol.* **223**, 27–35 (2010).

121. Pinto, D. S. *et al.* Modulation of the in vitro angiogenic potential of human mesenchymal stromal cells from different tissue sources. *J. Cell. Physiol.* **235**, 7224–7238 (2020).

122. Serra, J. *et al.* Minicircle-based expression of vascular endothelial growth factor in mesenchymal stromal cells from diverse human tissues. *J. Gene Med.* 1–12 (2021). doi:10.1002/jgm.3342

123. Loeuillet, C. *et al.* Distinct hematopoietic support by two human stromal cell lines. *Exp. Hematol.* **29**, 736–745 (2001).

124. Wang, H. X. *et al.* Comparative analysis of different feeder layers with 3T3 fibroblasts for culturing rabbits limbal stem cells. *Int. J. Ophthalmol.* **10**, 1021–1027 (2017).

125. Denning-Kendall, P., Singha, S., Bradley, B. & Hows, J. Cobblestone Area-Forming Cells in Human Cord Blood Are Heterogeneous and Differ from Long-Term Culture-Initiating Cells. *Stem Cells* **21**, 694–701 (2003).

126. Stolzing, A., Jones, E., McGonagle, D. & Scutt, A. Age-related changes in human bone marrow-derived mesenchymal stem cells: Consequences for cell therapies. *Mech. Ageing Dev.* **129**, 163–173 (2008).

127. Grégoire, C. *et al.* Comparison of mesenchymal stromal cells from different origins for the treatment of graft-vs.-host-disease in a humanized mouse model. *Front. Immunol.* **10**, 1–16 (2019).

128. Ribeiro, A. *et al.* Mesenchymal stem cells from umbilical cord matrix, adipose tissue and bone marrow exhibit different capability to suppress peripheral blood B, natural killer and T cells. *Stem Cell Res. Ther.* **4**, (2013).

129. Radtke, S. *et al.* Purification of Human CD34+CD90+ HSCs Reduces Target Cell Population and Improves Lentiviral Transduction for Gene Therapy. *Mol. Ther. - Methods Clin. Dev.* **18**, 679–691 (2020).

130. Ploemacher, R., van der Sluijs, J., Voerman, J. & Brons, N. An in vitro limiting-dilution assay of long-term repopulating hematopoietic stem cells in the mouse. *Blood* **74**, 2755–2763 (1989).

131. Singh, J. *et al.* Generation and function of progenitor t cells from stemregenin-1-expanded CD34+ human hematopoietic progenitor cells. *Blood Adv.* **3**, 2934–2948 (2019).

132. Awong, G. *et al.* Characterization in vitro and engraftment potential in vivo of human progenitor T cells generated from hematopoietic stem cells. *Blood* **114**, 972–982 (2009).

133. Szabolcs, P. T lymphocyte Recovery and Function After Cord Blood Transplantation. *Immunol. Res.* **49**, 56–69 (2011).

134. Singh, J. & Zúñiga-Pflücker, J. C. Producing proT cells to promote immunotherapies. *Int. Immunol.* **30**, 541–550 (2018).

135. Frias, A. M. *et al.* Generation of functional natural killer and dendritic cells in a human stromal-based serum-free culture system designed for cord blood expansion. *Exp. Hematol.* **36**, 61–68 (2008).

136. Kim, H. S. *et al.* Human umbilical cord blood mesenchymal stem cells reduce colitis in mice by activating NOD2 signaling to COX2. *Gastroenterology* **145**, 1392-1403.e8 (2013).

137. Li, C. Y. *et al.* Comparative analysis of human mesenchymal stem cells from bone marrow and adipose tissue under xeno-free conditions for cell therapy. *Stem Cell Res. Ther.* **6**, (2015).

138. Petrenko, Y. *et al.* A Comparative Analysis of Multipotent Mesenchymal Stromal Cells derived from Different Sources, with a Focus on Neuroregenerative Potential. *Sci. Rep.* **10**, 1–15 (2020).

139. Ding, D. C. *et al.* Human umbilical cord mesenchymal stem cells support nontumorigenic expansion of human embryonic stem cells. *Cell Transplant.* **21**, 1515–1527 (2012).

140. Zou, Q. *et al.* Development of a xeno-free feeder-layer system from human umbilical cord mesenchymal stem cells for prolonged expansion of human induced pluripotent stem cells in culture. *PLoS One* **11**, 1–18 (2016).

141. Fong, C. Y. *et al.* Human umbilical cord Wharton's jelly stem cells and its conditioned medium support hematopoietic stem cell expansion ex vivo. *J. Cell. Biochem.* **113**, 658–668 (2012).

142. Lin, H. D., Fong, C. Y., Biswas, A. & Bongso, A. Allogeneic human umbilical cord Wharton's jelly stem cells increase several-fold the expansion of human cord blood CD34+ cells both in vitro and in vivo. *Stem Cell Res. Ther.* **11**, 1–18 (2020).

143. Ponchio, L. *et al.* Mitomycin C as an alternative to irradiation to inhibit the feeder layer growth in long-term culture assays. *Cytotherapy* **2**, 281–286 (2000).

144. Kadekar, D., Kale, V. & Limaye, L. Differential ability of MSCs isolated from placenta and cord as feeders for supporting ex vivo expansion of umbilical cord blood derived CD34+ cells. *Stem Cell Res. Ther.* **6**, 201 (2015).

145. Klein, C. *et al.* Ex Vivo expansion of hematopoietic stem-and progenitor cells from cord blood in coculture with mesenchymal stroma cells from amnion, chorion, wharton's jelly, amniotic fluid, cord blood, and bone marrow. *Tissue Eng. - Part A* **19**, 2577–2585 (2013).

146. Introna, M. *et al.* Treatment of graft versus host disease with mesenchymal stromal cells: A phase I study on 40 adult and pediatric patients. *Biol. Blood Marrow Transplant.* **20**, 375–381 (2014).

147. Dhere, T. *et al.* The safety of autologous and metabolically fit bone marrow mesenchymal stromal cells in medically refractory Crohn's disease – a phase 1 trial with three doses.

Aliment. Pharmacol. Ther. **44**, 471–481 (2016).

148. Burnouf, T., Strunk, D., Koh, M. B. C. & Schallmoser, K. Human platelet lysate: Replacing fetal bovine serum as a gold standard for human cell propagation? *Biomaterials* **76**, 371–387 (2016).

149. Abdelrazik, H., Spaggiari, G. M., Chiossone, L. & Moretta, L. Mesenchymal stem cells expanded in human platelet lysate display a decreased inhibitory capacity on T- and NK-cell proliferation and function. *Eur. J. Immunol.* **41**, 3281–3290 (2011).

150. Oikonomopoulos, A. *et al.* Optimization of human mesenchymal stem cell manufacturing: The effects of animal/xeno-free media. *Sci. Rep.* **5**, 1–11 (2015).

151. Copland, I. B., Garcia, M. A., Waller, E. K., Roback, J. D. & Galipeau, J. The effect of platelet lysate fibrinogen on the functionality of MSCs in immunotherapy. *Biomaterials* **34**, 7840–7850 (2013).

152. Nakao, N. *et al.* Adipose tissue-derived mesenchymal stem cells facilitate hematopoiesis in vitro and in vivo: Advantages over bone marrow-derived mesenchymal stem cells. *Am. J. Pathol.* **177**, 547–554 (2010).

153. Nishiwaki, S. *et al.* Efficacy and safety of human adipose tissue-derived mesenchymal stem cells for supporting hematopoiesis. *Int. J. Hematol.* **96**, 295–300 (2012).

154. Lee, R. H. *et al.* Characterization and expression analysis of mesenchymal stem cells from human bone marrow and adipose tissue. *Cell. Physiol. Biochem.* **14**, 311–324 (2004).

155. Sotnezova, E. V., Andreeva, E. R., Grigoriev, A. I. & Buravkova, L. B. Ex vivo expansion of hematopoietic stem and progenitor cells from umbilical cord blood. *Acta Naturae* **8**, 6–16 (2016).

156. Li, Q. *et al.* Wharton's jelly mesenchymal stem cell-based or umbilical vein endothelial cell-based serum-free coculture with cytokines supports the ex vivo expansion/maintenance of cord blood hematopoietic stem/progenitor cells. *Stem Cell Res. Ther.* **10**, 1–9 (2019).

157. Fajardo-Orduña, G. R., Mayani, H. & Montesinos, J. J. Hematopoietic Support Capacity of Mesenchymal Stem Cells: Biology and Clinical Potential. *Arch. Med. Res.* **46**, 589–596 (2015).

158. Parmar, S. *et al.* Ex vivo expanded umbilical cord blood T cells maintain naive phenotype and TCR diversity. *Cytotherapy* **8**, 149–157 (2006).

159. Mohtashami, M. & Zúñiga-Pflücker, J. C. Cutting Edge: Three-Dimensional Architecture of the Thymus Is Required to Maintain Delta-Like Expression Necessary for Inducing T Cell Development. *J. Immunol.* **176**, 730–734 (2006).

160. Owen, J. J. T. & Ritter, M. A. Tissue interaction in the development of thymus lymphocytes. *J. Exp. Med.* **129**, 431–442 (1969).

161. Jenkinson, E. J., Franchi, L. L., Kingston, R. & Owen, J. J. T. Effect of deoxyguanosine on

lymphopoiesis in the developing thymus rudiment in vitro: Application in the production of chimeric thymus rudiments. *Eur. J. Immunol.* **12**, 583–587 (1982).

162. Jenkinson, E. J., Anderson, G. & Owen, J. J. T. Studies on T cell maturation on defined thymic stromal cell populations in vitro. *J. Exp. Med.* **176**, 845–853 (1992).

163. Schmitt, T. M. & Zúñiga-Pflücker, J. C. Induction of T cell development from hematopoietic progenitor cells by delta-like-1 in vitro. *Immunity* **17**, 749–756 (2002).

164. Awong, G., Herer, E., La Motte-Mohs, R. N. & Zúñiga-Pflücker, J. C. Human CD8 T cells generated in vitro from hematopoietic stem cells are functionally mature. *BMC Immunol.* **12**, 22 (2011).

165. Seet, C. S. *et al.* Generation of mature T cells from human hematopoietic stem and progenitor cells in artificial thymic organoids. *Nat. Methods* **14**, 521–530 (2017).

166. Montel-Hagen, A. *et al.* Organoid-Induced Differentiation of Conventional T Cells from Human Pluripotent Stem Cells. *Cell Stem Cell* 1–14 (2019). doi:10.1016/j.stem.2018.12.011

167. Okas, M. *et al.* Clinical Expansion of Cord Blood-derived T Cells for Use as Donor Lymphocyte Infusion After Cord Blood Transplantation. *J Immunother* **33**, 96–105 (2010).

168. Berglund, S., Gertow, J., Uhlin, M. & Mattsson, J. Expanded umbilical cord blood T cells used as donor lymphocyte infusions after umbilical cord blood transplantation. *Cytotherapy* **16**, 1528–1536 (2014).

169. La Motte-Mohs, R. N., Herer, E. & Zúñiga-Pflücker, J. C. Induction of T-cell development from human cord blood hematopoietic stem cells by Delta-like 1 in vitro. *Blood* **105**, 1431–1439 (2005).

170. Awong, G., La Motte-Mohs, R. N. & Zúñiga-Pflücker, J. C. In vitro human T cell development directed by notch-ligand interactions. *Methods Mol. Biol.* **430**, 135–142 (2007).

171. Holmes, R. & Zuñiga-Pflücker, J. C. The OP9-DL1 system: Generation of T-lymphocytes from embryonic or hematopoietic stem cells in vitro. *Cold Spring Harb. Protoc.* **4**, 1–13 (2009).

172. Van Coppernolle, S. *et al.* Functionally Mature CD4 and CD8 TCR**αβ** Cells Are Generated in OP9-DL1 Cultures from Human CD34+ Hematopoietic Cells. *J. Immunol.* **183**, 4859–4870 (2009).

173. Costa, M. H. G. *et al.* Three-dimensional co-culture of human hematopoietic stem/progenitor cells and mesenchymal stem/stromal cells in a biomimetic hematopoietic niche microenvironment. *Methods Mol. Biol.* **2002**, 101–119 (2019).

174. Locatelli, F. Improving cord blood transplantation in children. *Br. J. Haematol.* **147**, 217–226 (2009).

175. Liao, Y., Geyer, M. B., Yang, A. J. & Cairo, M. S. Cord blood transplantation and stem cell

regenerative potential. *Exp. Hematol.* **39**, 393–412 (2011).

176. Brauer, P. M., Singh, J., Xhiku, S. & Zúñiga-Pflücker, J. C. T Cell Genesis: In Vitro Veritas Est? *Trends Immunol.* **37**, 889–901 (2016).

177. Varnum-Finney, B. *et al.* Immobilization of Notch ligand, Delta-1, is required for induction of Notch signaling. *J. Cell Sci.* **113**, 4313–4318 (2000).

178. Reimann, C. *et al.* Human T-lymphoid progenitors generated in a feeder-cell-free delta-like-4 culture system promote T-cell reconstitution in NOD/SCID/γc-/- mice. *Stem Cells* **30**, 1771–1780 (2012).

179. Fernandez, Irina; Ooi, Tracy P; Roy, K. Generation of Functional, Antigen-Specific CD8+ Human T Cells from Cord-Blood Stem Cells using Exogenous Notch and Tetramer-TcR Signaling. *Stem Cells* **32**, 93–104 (2014).

180. Taqvi, S., Dixit, L. & Roy, K. Biomaterial-based notch signaling for the differentiation of hematopoietic stem cells into T cells. *J. Biomed. Mater. Res. Part A* **79A**, 689–697 (2006).

181. Trotman-Grant, A. C. *et al.* DL4-μbeads induce T cell lineage differentiation from stem cells in a stromal cell-free system. *Nat. Commun.* **12**, 1–11 (2021).

182. Lewis, A. *et al.* Organ donation in the US and Europe: The supply vs demand imbalance. *Transplant. Rev.* **35**, 100585 (2021).

183. Rana, D., Zreiqat, H., Benkirane-Jessel, N., Ramakrishna, S. & Ramalingam, M. Development of decellularized scaffolds for stem cell-driven tissue engineering. *J. Tissue Eng. Regen. Med.* **11**, 942–965 (2017).

184. Gilpin, A. & Yang, Y. Decellularization Strategies for Regenerative Medicine: From Processing Techniques to Applications. *Biomed Res. Int.* **2017**, (2017).

185. Heath, D. E. A Review of Decellularized Extracellular Matrix Biomaterials for Regenerative Engineering Applications. *Regen. Eng. Transl. Med.* **5**, 155–166 (2019).

186. Anderson, G. & Takahama, Y. Thymic epithelial cells: Working class heroes for T cell development and repertoire selection. *Trends Immunol.* **33**, 256–263 (2012).

187. *Thymus Gland Pathology*. (Springer Milano, 2008). doi:10.1007/978-88-470-0828-1

188. Boehm, T. Thymus development and function. *Curr. Opin. Immunol.* **20**, 178–184 (2008).

189. Poznansky, M. C. *et al.* Efficient generation of human T cells from a tissue-engineered thymic organoid. *Nat. Biotechnol.* **18**, 729–734 (2000).

190. Kont, V. *et al.* Modulation of Aire regulates the expression of tissue-restricted antigens. *Mol. Immunol.* **45**, 25–33 (2008).

191. Silva, A. C. *et al.* Three-dimensional scaffolds of fetal decellularized hearts exhibit enhanced potential to support cardiac cells in comparison to the adult. *Biomaterials* **104**, 52–64 (2016).

192. Cavalcanti, N. V., Palmeira, P., Jatene, M. B., de Barros Dorna, M. & Carneiro-Sampaio, M. Early Thymectomy Is Associated With Long-Term Impairment of the Immune System: A Systematic Review. *Front. Immunol.* **12**, 1–13 (2021).

193. Catalano, M. A., Mullan, C. W., Rich, B. S. & Glick, R. D. Pediatric thymectomy: a study of national trends in demographics, short-term outcomes, and cost. *Pediatr. Surg. Int.* **35**, 749–757 (2019).

194. Guyette, J. P. *et al.* Perfusion decellularization of whole organs. *Nat. Protoc.* **9**, 1451–1468 (2014).

195. Kornmuller, A., Brown, C. F. C., Yu, C. & Flynn, L. E. Fabrication of extracellular matrix-derived foams and microcarriers as tissue-specific cell culture and delivery platforms. *J. Vis. Exp.* **2017**, 1–11 (2017).

196. Štefanić, G., Krehula, S. & Štefanić, I. Phase development during high-energy ball-milling of zinc oxide and iron-the impact of grain size on the source and the degree of contamination. *Dalt. Trans.* **44**, 18870–18881 (2015).

197. Seach, N., Wong, K., Hammett, M., Boyd, R. L. & Chidgey, A. P. Purified enzymes improve isolation and characterization of the adult thymic epithelium. *J. Immunol. Methods* **385**, 23–34 (2012).

198. Damasceno, P. K. F. *et al.* Genetic Engineering as a Strategy to Improve the Therapeutic Efficacy of Mesenchymal Stem/Stromal Cells in Regenerative Medicine. *Front. Cell Dev. Biol.* **8**, 1–24 (2020).

199. Edgar, L. *et al.* Utility of extracellular matrix powders in tissue engineering. *Organogenesis* **14**, 172–186 (2018).

200. Xing, Q. *et al.* Natural Extracellular Matrix for Cellular and Tissue Biomanufacturing. *ACS Biomater. Sci. Eng.* **3**, 1462–1476 (2017).

201. Silva, C. S. *et al.* Fibronectin-Functionalized Fibrous Meshes as a Substrate to Support Cultures of Thymic Epithelial Cells. *Biomacromolecules* **21**, 4771–4780 (2020).

202. Silva, C. S., Cerqueira, M. T., Reis, R. L., Martins, A. & Neves, N. M. Laminin-2 immobilized on a 3D fibrous structure impacts cortical thymic epithelial cells behaviour and their interaction with thymocytes. *Int. J. Biol. Macromol.* **222**, 3168–3177 (2022).

203. Verhulsel, M. *et al.* A review of microfabrication and hydrogel engineering for micro-organs on chips. *Biomaterials* **35**, 1816–1832 (2014).

204. Kratzer, D., Ludwig-Husemann, A., Junges, K., Geckle, U. & Lee-Thedieck, C. Nanostructured bifunctional hydrogels as potential instructing platform for hematopoietic stem cell differentiation. *Front. Mater.* **5**, 1–16 (2019).

205. Jain, P., Kathuria, H. & Dubey, N. Advances in 3D bioprinting of tissues/organs for regenerative medicine and in-vitro models. *Biomaterials* **287**, 121639 (2022).

VIII. Appendix

VIII.1. Decellularization of human thymic tissue: a platform for T cell differentiation *in vitro* (supplementary information of Chapter IV)

VIII.1.1. Preparation of the decellularization solutions

Hypotonic wash buffer (10 mM Tris)

Dissolve 0.61 g of Tris (Cat. #154563, Sigma-Aldrich, USA) into 450 mL of deionized water. Correct pH to 7.8 with HCl or NaOH. Add the necessary volume of deionized water to reach a final volume of 500 mL. Confirm that the pH is 7.8, filter and store the solution at room temperature (RT).

Observation: If desired, a higher volume of hypotonic wash buffer can be made and used for the preparation of hypotonic buffer and 0.2% sodium dodecyl sulfate *(SDS) solution. Otherwise, both solutions can be completely prepared individually.*

Hypotonic buffer (10 mM Tris, 3.42 mM ethylenediamine tetraacetic acid (EDTA))

Dissolve 0.61 g of Tris into 450 mL of deionized water and add 3.42 mL of 0.5 M EDTA (Cat. #03690-100mL, Sigma-Aldrich). Correct pH to 7.8 with HCl or NaOH. Add the necessary volume of deionized water to reach a final volume of 500 mL. Confirm that the pH is 7.8, filter and store the solution at RT.

0.2% (w/v) SDS solution (0.2% SDS, 10 mM Tris)

Dissolve 0.5 g of SDS (Cat. #L3771, Sigma-Aldrich) and 0.3 g of Tris into 200 mL of deionized water. Stir at 60°C until complete SDS dissolution. Let the solution cool down to RT and correct pH to 7.8 with HCl or NaOH. Add the necessary volume of deionized water to reach a final volume of 250 mL. Confirm that the pH is 7.8 and filter the solution.

Observation: To assure decellularization efficiency, freshly prepared SDS solution should be used. Additionally, complete SDS dissolution should be assured, otherwise solution concentration can be compromised.

DNase treatment solution (20 mM Tris, 2 mM $MgCl_2$, 50 U/mL DNase I)

Dissolve 1.21 g of Tris into 450 mL of deionized water and add 1 mL of 1 M $MgCl_2$ (Cat. #M-0250, Sigma-Aldrich). Correct pH to 7.8 with HCl or NaOH. Add the necessary volume of deionized water to reach a final volume of 500 mL. Confirm that the pH is 7.8, filter and store the solution at RT. DNase I should only be added prior to use, at a final concentration of 50 U/mL.

DNase I stock solution: Dissolve the lyophilized DNase (Cat. #A3778,0050, AppliChem, USA) in a DNase buffer containing 50% (w/v) glycerol (Cat. #56-81-5, Thermo Fisher Scientific, USA), 20 mM Tris (pH 7.5) and 1 mM $MgCl_2$. For stability reasons, concentration should be at least 1 mg/mL (maximum solubility is 10%). After complete dissolution, filter the solution and prepare aliquots to be stored at -20°C.